

University of Windsor

## Scholarship at UWindor

---

Electronic Theses and Dissertations

Theses, Dissertations, and Major Papers

---

7-7-2020

# Elimination of Selected Heteroaromatics from Wastewater Using Soybean Peroxidase

Negin Ziayee Bideh  
*University of Windsor*

Follow this and additional works at: <https://scholar.uwindsor.ca/etd>

---

### Recommended Citation

Ziayee Bideh, Negin, "Elimination of Selected Heteroaromatics from Wastewater Using Soybean Peroxidase" (2020). *Electronic Theses and Dissertations*. 8411.  
<https://scholar.uwindsor.ca/etd/8411>

This online database contains the full-text of PhD dissertations and Masters' theses of University of Windsor students from 1954 forward. These documents are made available for personal study and research purposes only, in accordance with the Canadian Copyright Act and the Creative Commons license—CC BY-NC-ND (Attribution, Non-Commercial, No Derivative Works). Under this license, works must always be attributed to the copyright holder (original author), cannot be used for any commercial purposes, and may not be altered. Any other use would require the permission of the copyright holder. Students may inquire about withdrawing their dissertation and/or thesis from this database. For additional inquiries, please contact the repository administrator via email ([scholarship@uwindsor.ca](mailto:scholarship@uwindsor.ca)) or by telephone at 519-253-3000ext. 3208.

**Elimination of Selected Heteroaromatics from Wastewater Using Soybean Peroxidase**

By

**Negin Ziyee Bideh**

A Thesis  
Submitted to the Faculty of Graduate Studies  
through the Department of Civil and Environmental Engineering  
in Partial Fulfillment of the Requirements for  
the Degree of Master of Applied Science  
at the University of Windsor

Windsor, Ontario, Canada

2020

© 2020 Negin Ziyee Bideh

**Elimination of Selected Heteroaromatics from Wastewater Using Soybean  
Peroxidase**

by

**Negin Ziayee Bideh**

APPROVED BY:

---

A. Edrisy  
Department of Mechanical, Automotive and Materials Engineering

---

R. Seth  
Department of Civil and Environmental Engineering

---

N. Biswas, Co-Advisor  
Department of Civil and Environmental Engineering

---

K. E. Taylor, Co-Advisor  
Department of Chemistry and Biochemistry

April 22, 2020

## DECLARATION OF ORIGINALITY

I hereby certify that I am the sole author of this thesis and that no part of this thesis has been published or submitted for publication.

I certify that, to the best of my knowledge, my thesis does not infringe upon anyone's copyright nor violate any proprietary rights and that any ideas, techniques, quotations, or any other material from the work of other people included in my thesis, published or otherwise, are fully acknowledged in accordance with the standard referencing practices. Furthermore, to the extent that I have included copyrighted material that surpasses the bounds of fair dealing within the meaning of the Canada Copyright Act, I certify that I have obtained a written permission from the copyright owner(s) to include such material(s) in my thesis and have included copies of such copyright clearances to my appendix.

I declare that this is a true copy of my thesis, including any final revisions, as approved by my thesis committee and the Graduate Studies office, and that this thesis has not been submitted for a higher degree to any other University or Institution.

## ABSTRACT

Various heterocyclic aromatic compounds (HACs), widely used in pharmaceuticals, personal care products, household products and different industries have been detected in concentrations from ng/L to  $\mu\text{g/L}$  in surface and groundwater, soil and sediments as well as influent and effluent (treated wastewater and sludge) of municipal or industrial wastewater treatment plants (WWTPs) around the world. The persistence of these so-called emerging contaminants (ECs) and their metabolites can cause toxicological and ecotoxicological effects, even at very low concentrations. A feasibility study of soybean peroxidase-catalyzed oxidation process, as environmentally-friendly and cost effective alternative method for transformation of three selected HACs was the first aim of the present study. Soybean peroxidase (SBP) is extracted from the seed coats (hulls) which are a by-product of crushing operations and are used in animal feed. Secondly, the most important operational parameters, pH,  $\text{H}_2\text{O}_2$  concentration and enzyme activity were optimized for the two compounds that were substrates for SBP. Thirdly, time course study was conducted under optimized conditions to determine the initial first-order rate constant and half-life of each substrate. Finally, possible oligomerization products of enzymatic treatment were characterized by mass spectrometric analysis and showed formation of dimers and trimers for the two substrates.

## DEDICATION

This thesis is dedicated to my beloved parents, Ali Ziayee and Parvin Abed and my husband, Ali Taherian. Also, I would like to dedicate it to my best friends, Zahra Naghibi and Mohammad Abbaspour, the victims of airplane crash, Ukraine Flight-752, who had lots of hopes and plans for their future, that never came to reality. May they rest in peace.

## ACKNOWLEDGEMENTS

I would like to express my deep appreciation to my co-advisors, Dr. Nihar Biswas and Dr. Keith E. Taylor, for their patience, continuous motivations and strong support during this journey. I have been really lucky to be a member of this research group and get their shared immense knowledge and encouragement that made this research possible. I would like to thank my committee members, Dr. Rajesh Seth and Dr. Afsaneh Edrisy for their time, valuable suggestions and providing insightful comments.

I am truly grateful to Dr. Neda Mashhadi, for her guidance and assistance provided throughout the HPLC method development and sharing her valuable technical knowledge. Also, sincere thanks to Mr. Bill Middleton for all his efforts and technical trainings for the laboratory instruments and provided technical helps during this work, to Mr. Joe Lichaa for his technical support. I would like to extend my gratitude to Dr. Janeen Auld for the MS analysis and her guidance and suggestions. I would like to thank my lab colleagues, Baturh Yarkwan, Amanpreet Kaur, Maxim Gilbert, Anju Tiwari, Lily Xu and Kiana Mokrian. Also, special thanks to my friend, Xiaoyang Zhang, for all her support and enjoyable times and fun we have had throughout these years. To the volunteer student, Zina Sibaei, your help is greatly appreciated and thanks for all those fun conversations.

Thanks to the Natural Sciences and Engineering Research Council of Canada (NSERC) and University of Windsor Master Entrance Scholarship for providing financial supports.

## TABLE OF CONTENTS

DECLARATION OF ORIGINALITY .....	iii
ABSTRACT .....	iv
DEDICATION .....	v
ACKNOWLEDGEMENTS .....	vi
LIST OF TABLES .....	x
LIST OF FIGURES .....	xi
LIST OF ABBREVIATIONS/SYMBOLS .....	xiii
CHAPTER 1 INTRODUCTION .....	1
1.1. Background .....	1
1.2. Objectives .....	6
1.3. Scope .....	6
CHAPTER 2 LITERATURE REVIEW .....	8
2.1. Heterocyclic aromatic compounds .....	8
2.2. Selected heterocyclic aromatics .....	9
2.2.1. 3-Hydroxycoumarin .....	9
2.2.2. 2-Aminobenzoxazole .....	10
2.2.3. 3-Amino-5-methylisoxazole .....	11
2.3. Enzymatic treatment of water and wastewater .....	12
2.3.1. Oxidoreductase enzymes .....	13
2.4. Peroxidase mechanism .....	17
2.4.1. Peroxidase inactivation .....	20
2.5. Cost and availability of soybean peroxidase .....	21
2.6. Soybean peroxidase extraction .....	22
CHAPTER 3 MATERIALS AND METHODS .....	23
3.1. Materials .....	23



3.1.1. Enzymes.....	23
3.1.2. Aromatic compounds .....	23
3.1.3. Buffers and solvents .....	23
3.1.4. Other chemicals .....	24
3.1.5. Chromatography solvents, columns and filters.....	24
3.2. Analytical methods.....	24
3.2.1. Buffer preparation .....	24
3.2.2. Enzyme stock solution preparation .....	25
3.2.3. Enzyme activity assay .....	25
3.2.4. Residual enzyme activity assay .....	26
3.2.5. Residual hydrogen peroxide assay.....	27
3.3. Analytical equipment .....	27
3.3.1. UV-Vis spectrometry.....	27
3.3.2. High performance liquid chromatography (HPLC) analysis .....	27
3.3.3. Mass spectrometry .....	29
3.3.4. Other instruments.....	30
3.4. Experimental protocols .....	30
3.4.1. Enzymatic oxidation of substrate with SBP and feasibility of treatment of target aromatics .....	30
3.4.2. Optimization of important enzymatic reaction parameters .....	31
3.4.3. Stepwise addition of H <sub>2</sub> O <sub>2</sub> .....	32
3.4.4. Preliminary determination of enzymatic treatment products using mass spectrometry.....	32
3.5. Sources of error .....	33
CHAPTER 4 RESULTS AND DISCUSSION.....	34
4.1. Parameter optimization of SBP-catalyzed treatment.....	34
4.1.1. pH Optimization.....	34
4.1.2. SBP Optimization.....	38
4.1.3. Hydrogen peroxide optimization.....	41
4.2. Time course of reactions .....	43
4.3. Mass spectrometry (MS) results.....	47
4.3.1. 3-Hydroxycoumarin .....	48

4.3.2. 2-Aminobenzoxazole .....	55
CHAPTER 5 SUMMARY AND CONCLUSIONS .....	63
5.1. Summary .....	63
5.2. Conclusions.....	65
CHAPTER 6 FUTURE WORK.....	66
BIBLIOGRAPHY.....	67
APPENDICES .....	79
Appendix A. Preparation of SBP and catalase stock solutions.....	79
Appendix B. SBP activity assay .....	79
Appendix C. Residual SBP activity assay .....	80
Appendix D. Residual hydrogen peroxide assay.....	81
Appendix E. HPLC Calibration curves.....	83
Appendix F. Electron delocalization of 3-HC.....	91
Appendix G. Electron delocalization of 2-ABO .....	93
VITA AUCTORIS .....	94

## LIST OF TABLES

Table 1-1, Name, formula and molecular structure of the chemicals studied .....	7
Table 2-1, Removal efficiency and optimal parameters of enzymatic treatment of previously studied HACs .....	17
Table 3-1, HPLC analysis conditions for 3-HC under gradient elution.....	28
Table 3-2, HPLC analysis conditions for 2-ABO under gradient elution.....	29
Table 4-1, Half-lives and normalized half-lives of various SBP substrates.....	46
Table 5-1, Optimized conditions for SBP-catalyzed removal of 3-HC and 2-ABO and initial first-order kinetics.....	64
Table 5-2, Summary of MS results for standard and identified products of SBP-catalyzed process for 3-HC and 2-ABO.....	64

## LIST OF FIGURES

Figure 2-1, Some common heterocyclic compounds.....	8
Figure 2-2, Oxidative polymerization of phenol through C-C and C-O coupling.....	20
Figure 2-3, Global soybean production 2019 according to USDA (2020).....	22
Figure 3-1, Oxidative coupling of phenol and 4-AAP in the presence of H <sub>2</sub> O <sub>2</sub> and SBP...	25
Figure 4-1, pH optimization for 3-HC.....	37
Figure 4-2, pH optimization for 2-ABO.....	38
Figure 4-3, SBP optimization for 3-HC.....	39
Figure 4-4, SBP optimization for 2-ABO.....	40
Figure 4-5, Hydrogen peroxide optimization for 3-HC.....	42
Figure 4-6, Hydrogen peroxide optimization for 2-ABO.....	42
Figure 4-7, Time course experiment for 3-HC.....	45
Figure 4-8, Time course experiment for 2-ABO.....	45
Figure 4-9, Expanded ASAP-MS spectrum of 3-HC standard, from m/z 100 to 200.....	49
Figure 4-10, Expanded ASAP-MS spectrum of 3-HC standard, from m/z 161.94 to m/z 162.18.....	49
Figure 4-11, Some possible structures of oligomers formed during enzymatic treatment of 3-HC.....	51
Figure 4-12, Full-scan ASAP-MS spectrum of 3-HC reaction mixture.....	52
Figure 4-13, Expanded ASAP-MS spectrum of 3-HC reaction mixture from m/z 320 to 323.....	53
Figure 4-14, Expanded ASAP-MS spectrum of 3-HC reaction mixture from m/z 323 to 326.....	53
Figure 4-15, Expanded ASAP-MS spectrum of 3-HC reaction mixture from m/z 479 to 485.....	54
Figure 4-16, ASAP-MS spectrum of 2-ABO standard, from m/z 120 to 150.....	55
Figure 4-17, Expanded ASAP-MS spectrum of 2-ABO standard, from m/z 134.03 to 134.065.....	56
Figure 4-18, Some possible structures of oligomers formed during enzymatic treatment of 2-ABO.....	57
Figure 4-19, Full-scan ASAP-MS spectrum of 2-ABO reaction mixture.....	58

Figure 4-20, Expanded-scale ASAP-MS spectrum of 2-ABO reaction mixture from m/z 267 to 267.2.....	59
Figure 4-21, Expanded-scale ESI-MS spectrum of 2-ABO reaction mixture from m/z 266.8 to 268.....	59
Figure 4-22, Expanded-scale ESI-MS spectrum of 2-ABO reaction mixture from m/z 399.04 to 399.240.....	60
Figure 4-23, Expanded-scale preliminary ASAP-MS spectrum of 2-ABO reaction mixture from m/z 263 to 274.....	61
Figure 4-24, Expanded-scale preliminary ASAP-MS spectrum of 2-ABO reaction mixture from m/z 264.94 to 265.14.....	61
Figure 4-25, Expanded-scale preliminary ASAP-MS spectrum of 2-ABO reaction mixture from m/z 398.90 to 399.20.....	62

## LIST OF ABBREVIATIONS/SYMBOLS

### **Abbreviations**

HAC, Heterocyclic aromatic compound

SBP, Soybean peroxidase

EC, Emerging contaminant

ED, Endocrine disruptor

HRP, Horseradish peroxidase

TP, Turnip peroxidase

BGP, Bitter gourd peroxidase

CPO, Chloroperoxidase

MnP, Manganese peroxidase

3-HC, 3-Hydroxycoumarin

2-ABO, 2-Aminobenzoxazole

3A-5MI, 3-Amino-5methylisoxazole

MS, Mass spectrometry

ASAP, Atmospheric solids analysis probe

ESI, Electrospray ionization

UV-Vis, Ultraviolet-Visible

WWTP, Wastewater treatment plant

MP, Micropollutant

4-AAP, 4-Amino-antipyrine

ACN, Acetonitrile

HPLC, High-performance liquid chromatography

U.S. FDA, The United States Food and Drug Administration

CGW, Coal gasification wastewater

PAHs, Polycyclic aromatic compounds

AOP, Advanced oxidation process

SMX, Sulphamethoxazole

MBT, Mercaptobenzothiazole

MMT, Million metric tons

USDA, The United States Department of Agriculture

ARP, *Arthromyces ramosus* peroxidase

PES, Polyethersulfone

Tof, Time-of-flight

ABTS, 2,2'-azino-bis (3-ethylbenzothiazoline-6-sulphonic acid)

NMR, Nuclear magnetic resonance

FTIR, Fourier transform infrared

IPA: Isopropyl alcohol

## **Symbols**

$\lambda_{\max}$ , Maximum wavelength

m/z, Mass-to-charge ratio

mDa, Millidalton

pK<sub>a</sub>, -log<sub>10</sub> K<sub>a</sub>, where K<sub>a</sub> is acid dissociation constant

k<sub>cat</sub>/K<sub>M</sub>, Specificity constant or, catalytic efficiency, where K<sub>M</sub> is Michaelis constant

and k<sub>cat</sub> is turnover number

Arg-38, Arginine-38

His-42, Histidine-42

k, First-order kinetic rate constant

$t_{\frac{1}{2}}$ , Half-life



## CHAPTER 1

### INTRODUCTION

Heterocyclic aromatic compounds along with many other organic contaminants have been detected in influent and effluent of wastewater treatment plants and cannot be removed efficiently by conventional treatment methods. Hence, they have found their way to the water sources and been detected in concentrations ranging from ng/L to  $\mu\text{g/L}$ . Many of these compounds have been reported to show acute toxicity, cytotoxicity, carcinogenicity and mutagenicity (Brack and Schirmer, 2003). Accordingly, developing an environmentally friendly, economical and efficient alternative for treatment of HACs is essential.

#### *1.1. Background*

Heterocyclic aromatic compounds (HACs) are defined as cyclic compounds having ring member atoms of at least two different elements (McNaught and Wilkinson, 2014). In addition to carbon, the most frequent substitutes involved as the heteroatoms are typically oxygen, sulfur or nitrogen. Heterocyclic aromatics including coumarin, oxazole, indole, pyrrole, quinoline, etc. and their derivatives have widespread applications in medicinal chemistry, agricultural pesticides, personal care and household products and various industries.

HACs are considered as the backbone of many pharmaceutical fragments and are used in drug synthesis, pharmaceutical intermediates and medicinal chemistry research. These compounds have received significant attention due to their important biological properties such as anticancer potential, antimicrobial, antifungal, anxiolytic, antipsychotic,

anti-inflammatory, antiviral and diverse activities (Chikhale et al., 2017; Martins et al., 2015). Among HACs, nitrogen heterocyclic aromatics (N-heterocycles) are considered as the typical structural units of many pharmaceuticals such that nearly 60% of small-molecule drugs approved by the U.S. FDA (Food and Drug Administration) contain an N-heterocycle with 3- to 8-membered rings, bridged bicyclic or macrocyclic nitrogen heterocycles (Vitaku et al., 2014). HACs also have extensive applications in agricultural pesticides and particularly, some N-heterocyclic aromatic compounds like pyridine, quinolone and their derivatives often exist in the structure of these substances (Padoley et al., 2008). Furthermore, HACs and their derivatives have been widely used in various industries such as corrosion inhibitors, rubber additives and many personal care products such as cosmetics, disinfectants and household products (Asimakopoulos et al., 2013; Chen and Ying, 2015; Leyva et al., 2008; Padoley et al., 2008; Wang et al., 2015).

Extensive occurrence of HACs with concentrations ranging from ng/L to µg/L has been reported in surface and groundwater, soil and sediments as well as influent and effluent (treated wastes and sludge) of municipal or industrial wastewater treatment plants (WWTPs) around the world (Asimakopoulos et al., 2013; Chen and Ying, 2015; Kosjek et al., 2012; Liu et al., 2012; Siemers et al., 2017; Stasinakis et al., 2013; Lei Wang et al., 2016). Coal gasification wastewater (CGW) is another source of HACs and several other organic pollutants. N-heterocycles such as quinoline, pyridine and indole make up 60% of the persistent compounds in CGW which has negative health and environmental impacts (Shi et al., 2019).

In Canada, the presence of heterocyclic aromatics like quinolone and quinoxaline dioxide in the effluent of eight WWTPs has been reported (Miao et al., 2004).

Also, in northern Alberta, Canada, over 100 polycyclic aromatic compounds (PAHs), HACs and their derivatives were discovered in the ambient air of the oil sands region which are the result of incomplete combustion and mining activities (Hsu et al., 2015). HACs were also observed in extracts from petroleum coke in lakes, sediments and snow in the same region. Although the concentration of heterocyclic aromatics decreased with the distance from the oil sand source, some were detected at a large distance in snow and lake sediments suggesting that heterocyclic aromatics pollutant from petroleum coke can travel and be a potential source of the environment (Manzano et al., 2017).

It is worth mentioning that analysis of parent HACs may cause underestimating their real effects, toxicity and overall concentrations, since some heterocyclic aromatic metabolites have been reported in much higher concentration than their parent compounds. For example, N-heterocyclic aromatics like quinoline and isoquinoline as well as their hydroxylated and hydrogenated metabolites were discovered in groundwater of a tar contaminated site. Further analysis showed that the concentration of the hydroxylated quinoline, 2(1H)-quinolinone and 1(2H)-isoquinolinone, were much higher than their parent compounds in groundwater (Reineke et al., 2007). Also, compared to PAHs, HACs, due to their lower octanol-water partition coefficient, have shown higher solubility in water leading to more bioavailability, though the concentration of HACs are less than the PAHs in the environment (Feldmannova et al., 2006).

Although HACs, particularly heterocycles containing nitrogen, oxygen and/or sulfur, are ubiquitous in the environment, insufficient attention has been paid to their toxicological and ecotoxicological effects and they are considered as emerging contaminants (ECs). ECs, also called micropollutants (MPs), refers to putative organic

pollutants that have been commonly found in the environment in concentrations of ng/L to µg/L, but are not regulated yet and can have actual or potential adverse effects on the environment and human body (Noguera-Oviedo and Aga, 2016). HACs exhibit a large range of ecotoxic effects such as acute (short-term) and chronic (long-term) toxicity, genotoxicity, mutagenicity, carcinogenicity, estrogenic activities and bioaccumulation (Brinkmann et al., 2014; Salam et al., 2017; Wang et al., 2015).

Primary control at the source of pollutant discharge into the environment through recycling or raw material substitution is one of the effective ways of reducing pollution load, although it is not always possible (Padoley et al., 2008). Consequently, there is a substantial interest in finding an efficient and cost-effective treatment method for eliminating HACs, including the group of emerging contaminants, from water. Various conventional treatment techniques such as physical, chemical and biological, which are widely known and employed for removal of ECs are inefficient and unable to completely remove these compounds and ECs have been detected in the effluent of many WWTPs (Behera et al., 2011; Rivera-Utrilla et al., 2013; Stasinakis et al., 2013).

More effective and targeted treatment methods are essential to eliminate ECs from water and wastewater. Hence, some advanced treatment technologies including advanced oxidation processes (AOPs), adsorption on activated carbon, membrane filtration, photo-oxidation and electrooxidation have been introduced to improve water and wastewater treatment efficiency for removal of ECs. However, these technologies have some disadvantages and suffer from low efficiency, production of toxic by-products, high cost and/or long processing time (Lafi et al., 2009; Rivera-Utrilla et al., 2013).

Consequently, a feasibility study of enzymatic treatment of selected HACs as an environmentally-friendly and cost-effective alternative method was one of the aims of the present study. Enzymatic treatment using a biological catalyst for chemical reaction, combines aspects of physico-chemical and biological processes. Similar to AOPs, which are based on the generation of free radicals such as hydroxyl ( $\text{OH}^\cdot$ ) that can attack the organic molecules, peroxidase, as an oxidoreductase enzyme originating from living organisms like plants, catalyzes the transformation of pollutants to free radicals in the presence of hydrogen peroxide as an oxidant. Free radicals can form oligomers by coupling non-enzymatically, which then can be removed by filtration or sedimentation (Cordova Villegas et al., 2016). Enzymatic treatment can be applied either as a primary treatment or in combination with a biological process to improve the removal efficiency (Steevensz et al., 2014 a). Some of the advantages of enzymatic treatment are its effectiveness over a broad range of pH, salinity and temperature, applicable for the substances that are toxic to microorganisms, short contact time, no limitation due to the shock loading or accumulation of biomass (Al-Ansari et al., 2011). Like any other treatment method, enzymatic treatment may suffer from some drawbacks including inactivation of enzyme, its cost and availability (Steevensz et al., 2014 a; Steevensz et al., 2014 b).

## ***1.2. Objectives***

The objectives of the present research were as follows:

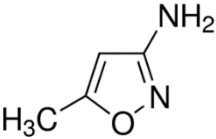
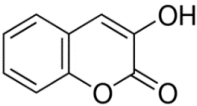
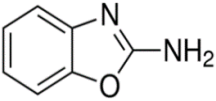
1. To determine the feasibility of enzyme-catalyzed treatment of three selected heterocyclic aromatics, 3-amino-5-methylisoxazole, 3-hydroxycoumarin and 2-aminobenzoxazole from synthetic wastewater; structures and chemical formulae are given in Table 1-1.
2. To optimize the catalyzed removal of the heterocyclic aromatics using soybean peroxidase (SBP);
3. To identify the possible transformation products of enzymatic reaction using mass spectrometry (MS).

## ***1.3. Scope***

1. Investigate the feasibility of SBP treatment of mM concentrations of 3-amino-5-methylisoxazole, 3-hydroxycoumarin and 2-aminobenzoxazole;
2. Optimize the most important operational parameters, pH, hydrogen peroxide ( $\text{H}_2\text{O}_2$ ) concentration and SBP activity for removal of the above compounds using SBP;
3. Employ high-performance liquid chromatography (HPLC) detection methods for the substrates to evaluate the removal efficiency of enzymatic treatment;
4. Study the effect of step-wise addition of  $\text{H}_2\text{O}_2$  on the removal efficiency of the substrate;

5. Determine the initial first-order rate constants and half-lives of the substrates by monitoring the time course of substrate consumption;
6. Identify the possible formation of oligomers as the result of enzymatic treatment using high resolution mass spectrometry (MS).

Table 1-1, Name, formula and molecular structure of the chemicals studied

Chemical	Formula	Molecular structure
3-Amino-5-methylisoxazole	$C_4H_6N_2O$	
3-Hydroxycoumarin	$C_9H_6O_3$	
2-Aminobenzoxazole	$C_7H_6N_2O$	

## CHAPTER 2

### LITERATURE REVIEW

#### 2.1. *Heterocyclic aromatic compounds*

Heterocyclic aromatic compounds (HACs), defined as cyclic compounds having ring member atoms of at least two different elements, are classified according to the heteroatom(s) present in the structure. In each class, compounds are categorized based on the size of the ring built by the total number of atoms. Physicochemical properties of the HACs strongly depend on the size of the ring and type of heteroatom(s) present in the structure (Broughton and Watson, 2005; Gomtsyan, 2012; Martins et al., 2015). Benzene fused to the different heterocyclic structures results in heterocycles such as benzoxazole, coumarin, quinoline, indole and benzofuran. Some of the more common HACs are shown in Figure 2-1.

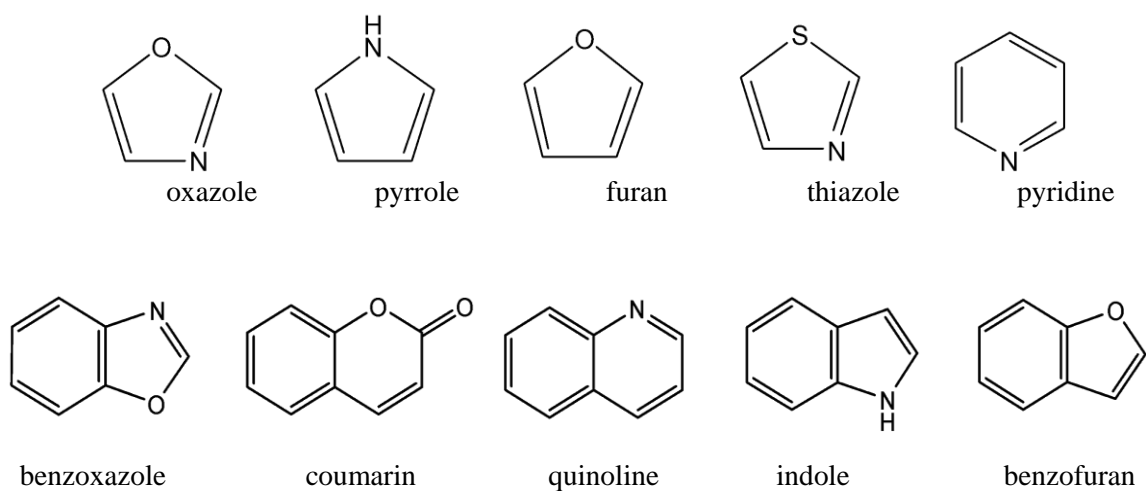


Figure 2-1, Some common heterocyclic compounds



## **2.2. *Selected heterocyclic aromatics***

As discussed in Section 1-1, HACs have extensive applications in drug synthesis, pharmaceutical intermediates, medical chemistry research and are considered as the backbone of many pharmaceutical fragments. Many HACs were discovered in the effluent of conventional wastewater treatment plants and find their way to the water resources. Hence, occurrence of these compounds or their derivatives as emerging contaminants have been reported in concentrations ranging from ng/L to  $\mu\text{g/L}$  in water, having possible adverse effects on the environment and human body. The feasibility of SBP-catalyzed treatment of many HACs has been studied previously (Mashhadi, 2019) while selected compounds mentioned below are the HACs, not yet studied for the feasibility of SBP-catalyzed removal.

### **2.2.1. *3-Hydroxycoumarin***

Coumarin and its derivatives constitute a large class of substances as metabolites from plants, bacteria, and fungi (Detsi et al., 2017). Numerous derivatives of coumarin have been used as antimicrobial, antibacterial, antitumor, anti-HIV, anticancer, antioxidant and also anticoagulant agents due to their similarity with the structure of vitamin K (Amin et al., 2011; Belluti et al., 2010; Chang et al., 2015; Detsi et al., 2017; Gacche & Jadhav, 2012; Shen et al., 2010). Specifically, some coumarin derivatives such as warfarin and dicoumarol (an anticoagulant) and novobiocin (an antibiotic) were found to be applicable in drug synthesis. Hydroxycoumarin derivatives have been shown to suppress many oxidation/inflammation-related degenerative diseases, including cancer, neurodegenerative diseases and chronic kidney disease. (Alavi et al., 2018; Chang et al.,

2015) and found to be potent antioxidant compounds comparable to quercetin or vitamin C (Bailly et al., 2004).

Coumarin and 3-hydroxycoumarin (3-HC) are a promising class of prospective drugs with photo-protective properties based on the research done by Cássio et al. (2015) in sea urchin gametes and zygotes exposed to ultraviolet radiation B. Also, improving tyrosinase activity by 3-HC has been demonstrated. Tyrosinase is an enzyme for which defects in its activity can lead to some skin disorders such as hyperpigmentation of the skin, melasma and age spots (Schlich et al., 2018). The 3-HC has been reported to be able to inhibit the fungus *Moniliophthora perniciosa*, which is the causal agent of witches' broom, a destructive pathogen disease in cocoa plants (*Theobroma cacao* L.) (de Andrade Gonçalves et al., 2019). It was used as one of the components to synthesize dihydropyrano[2,3-c] chromene derivatives which are widely employed in pharmaceuticals, cosmetics and agrochemicals (Paul et al., 2011). In addition, 3-HC has application as a matrix for matrix-assisted laser desorption/ionization time-of-flight mass spectrometry of DNA and has been reported having considerable improvement in resolution, spot-to-spot and sample-to-sample reproducibility compared to conventional matrices for mass spectrometric analysis DNA segments (Zhang et al., 2006).

### **2.2.2. 2-Aminobenzoxazole**

Benzoxazole and its derivatives are currently the most significant scaffolds in pharmacologically active compounds (Šlachťova and Brulíková, 2018). As a consequence, benzoxazole heterocycles and their properties have been reviewed by many researchers (Demmer and Bunch, 2015; Maruthamuthu et al., 2016; Singh et al., 2015; Šlachťova and Brulíková, 2018; Šlachťová et al., 2019). Substituted benzoxazoles are associated with an

extensive range of biological activities including antitumor, antifungal, antibacterial and anticancer (Balaswamy et al., 2012; Jyothi and Merugu, 2013; Kamal et al., 2010; Seenaiiah et al., 2017; Sommer et al., 2008). Several marketed drugs including caboxamycin (an antibiotic), flunaproxen and benoxaprofen (anti-inflammatory drugs) are the result of the synthesis of variety of benzoxazole derivatives (Dunwell et al., 1975; Hohmann et al., 2009; Šlachtova and Brulíková, 2018).

The 2-Aminobenzoxazoles and their substituted analogues have been described as potential drug candidates for HIV and inflammatory disease (Khatik et al., 2011) and various enzyme inhibitors including those for proteases, chymase, butyrylcholinesterase and topoisomerase II (Chikhale et al., 2018; Harmange et al., 2008; Potashman et al., 2007). 2-Aminobenzoxazole derivatives have shown potential activity against tuberculosis which is an infectious disease caused predominantly by the bacillus *Mycobacterium tuberculosis* (Šlachtova and Brulíková, 2018). In addition, aminobenzoxazoles serve as positron emission tomography probes for imaging of Alzheimer's disease (Cui et al., 2012).

### **2.2.3. 3-Amino-5-methylisoxazole**

Isoxazole and its substituted analogues display a broad spectrum of pharmaceutical properties and biological activities such as antibacterial, anticancer, anti-inflammatory, anti-HIV or anti-diabetic properties and have been extensively used as key components for valuable molecules of medicinal interest (Bakr et al., 2016; Sysak and Obmińska-Mrukowics, 2017).

3-Amino-5-methylisoxazole (3A-5MI) is a recalcitrant by-product resulting from biological degradation of sulphamethoxazole (SMX) which is a heterocyclic compound extensively used in humans and livestock as an effective and cheap antibiotic, thus, its

occurrence in water and the effluent of wastewater treatment plants raises environmental concerns (Kim et al., 2017; Martini et al., 2018; Mulla et al., 2018; Souza et al., 2017; Wang et al., 2016).

### ***2.3. Enzymatic treatment of water and wastewater***

Various physical, chemical and advanced treatment techniques are extensively used for removal of emerging contaminants (ECs). However, they have potential limitations, such as low removal efficiency, high cost and/or long processing time, high sludge production and/or formation of toxic by-products (Behera et al., 2011; Rivera-Utrilla et al., 2013; Stasinakis et al., 2013). Biodegradation processes have been employed successfully for removal of ECs from wastewater (Al-Maqdi et al., 2017; Morsi et al., 2020). Compared to physicochemical techniques, biodegradation processes as environmentally friendly alternatives have many advantages such as lower cost, lower energy consumption, less disruptive and/or applicable to low pollutant concentrations (Al-Maqdi et al., 2017; Morsi et al., 2020; Padoley et al., 2008). Major drawbacks of biological treatment are that microorganisms may not be able to grow under harsh environmental conditions and are unable to treat high concentrations of pollutants and may require longer time (Behera et al., 2011; Cordova Villegas et al., 2016; Morsi et al., 2020; Rivera-Utrilla et al., 2013; Rosal et al., 2010; Stasinakis et al., 2013).

Biocatalytic remediation of contaminated water and wastewater using enzyme-based treatments has many advantages such as effectiveness over a broad ranges of pH, salinity and temperature, lower energy input, reduced sludge volume, no limitations due to shock loading or accumulation of biomass and can be employed for a wide range of pollutants with high and low concentrations (Al-Ansari et al., 2011; Karam and Nicell,

1997; Morsi et al., 2020; Steevensz et al., 2014 b). Like any other treatment methods, enzymatic treatment may have some drawbacks and may suffer from enzyme inactivation (discussed later), enzyme cost and availability on a large scale (which can be mitigated by advanced technology and new resources) or the possibility of forming hazardous by-products (Steevensz et al., 2014 a; Steevensz et al., 2014 b).

### ***2.3.1. Oxidoreductase enzymes***

Oxidoreductase enzymes (include oxidases, peroxidases, dehydrogenases and oxygenases) catalyze the oxidation-reduction of a wide variety of pollutants including phenols, anilines, synthetic dyes, pharmaceuticals, personal care products and many others (Bilal et al., 2018; Bilal et al., 2019; Mashhadi et al., 2019 b; Steevensz et al., 2014 b). Laccases and peroxidases are the most commonly used oxidoreductases for the degradation of organic pollutants and emerging contaminants from water and wastewater (Alneyadi et al., 2018; Bilal et al., 2018, Bilal et al., 2019; Ćirić-Marjanović et al., 2017; Morsi et al., 2020). In 1979, Bollag and co-workers polymerized 2,6-dimethoxyphenol using laccase (Bollag et al., 1979). A year later, polymerization of phenols and anilines present in industrial wastewater was conducted by Klibanov et al., (1980) using horseradish peroxidase (HRP).

#### ***2.3.1.1. Laccases***

Laccases are a class of multi-copper oxidases that catalyze single-electron oxidation of a substrate along with reduction of oxygen to water. A wide range of ECs and HACs have been reported to be enzymatically transformed by laccases (Barrios-Estrada et al., 2018; Bilal et al., 2019; Morsi et al., 2020). For instance, many kinds of sulfonamide

antibiotics such as sulfadiazine, sulfathiazole, sulfapyridine, sulfamethazine, sulfamethoxazole have been transformed by laccase so quantitative removal of each antibiotic reached (Ding et al., 2016). Another study by Naghdi et al. (2018) revealed efficient enzymatic removal of carbamazepine, as one of the most commonly used pharmaceuticals, from synthetic wastewater catalyzed by laccase in the presence of redox mediators. Another study reported the enzymatic polymerization of 8-hydroxyquinoline, by laccase from the white rot fungus *Trametes pubescens* (Ncanana and Burton, 2007). Oxidative coupling of three coumarin derivatives, 4-methyl-7,8-dihydroxycoumarin, 7,8-dihydroxy-4-phenylcoumarin and 7,8-dihydroxycoumarin, using laccase was also reported (Wang et al., 2019). Also, the degradation of 5 mg/L of diclofenac, trimethoprim, carbamazepine and sulfamethoxazole by laccase from *Trametes versicolor* was investigated by Alharbi et al. (2019). Several studies using laccases from many different sources for the *in-vitro* treatment of endocrine disruptors (EDs) and ECs were comprehensively reviewed by Barrios et al. (2018). In another study, biocatalytic elimination of 30 trace organic contaminants including pharmaceuticals such as carbamazepine and parimidone, steroid hormones such as estriol and estrone and personal care products were investigated in an enzymatic membrane reactor equipped with an ultrafiltration membrane (Nguyen et al., 2015). Also, laccase-catalyzed degradation of the endocrine disrupting chemicals nonylphenol and Bisphenol A and the personal care product ingredient, Triclosan by laccase from the white rot fungus *Coriolopsis polyzona* was studied (Cabana et al., 2007). Furthermore, the breakdown potential of a mixture of 18 endocrine disruptors, pharmaceuticals and personal care products with concentrations

ranging from ng/L to µg/L by a fungal laccase in a model solution and real wastewater collected from a municipal wastewater treatment plant was carried out (Spina et al., 2015).

### **2.3.1.2. Peroxidases**

Peroxidases have seen widespread biotechnological application and been used in remediation of environmental contaminants from wastewater due to their ability to catalyze the oxidation-reduction reaction of wide range of phenolic and aniline substrates, aromatic compounds, dyes and non-phenolic aromatics in the presence of hydrogen peroxide (Mashhadi, 2019; Mukherjee et al., 2018; Cordova Villegas et al., 2018; Jun et al., 2019). The feasibility of treatment of twenty-one different ECs including antibiotics such as norfloxacin, trimethoprim and sulfamethoxazole, fungicides, herbicides, nonsteroidal anti-inflammatory drugs has been studied by Almaqdi et al., (2019) using 5 different peroxidases with or without 1- hydroxybenzotriazole as a redox mediator. Compared with soybean peroxidase (SBP), HRP which has been much studied in the last four decades, suffers from difficulty of extraction and purification in large quantity at an appropriate price (Al-Ansari et al., 2009), lower thermal stability (inactivated at temperature above 65 °C) than SBP with inactivation temperature of 90.5 °C and its activity is limited to narrower ranges of pH (4.0-8.0) compared with SBP ( pH 2.0-10.0) (Flock et al., 1999; Henriksen et al., 2001; Ryan et al., 2006).

### **2.3.1.3. Soybean peroxidase**

SBP is receiving a lot of attention because of its appealing biological features (Al-Ansari et al., 2009). SBP has shown to be a more potent peroxidase estimated by its Michaelis-Menten parameter, specificity constant ( $k_{cat}/K_M$ ), less susceptibility to

irreversible inactivation by  $\text{H}_2\text{O}_2$ , lower potential price, greater availability and higher thermal and conformational stabilities than HRP (Al-Ansari et al., 2009; Steevensz et al., 2014 b). SBP has catalytic ability for oxidation of a wide range of HACs. Treatment of 2-mercaptobenzothiazole (MBT), a regulated toxic heterocycle produced in various industries, has been conducted by Al-Ansari et al., (2010) and 95% removal of 1.0 mM MBT was obtained under optimum pH range, 6.0-9.0,  $\text{H}_2\text{O}_2$ :MBT ratio of 0.6 and 0.9 U/mL of SBP. Enzymatic treatment of sulfamethoxazole, a heterocyclic antimicrobial agent, along with other antimicrobials, phenolic steroids and phenolic surfactants as micropollutants has also been studied using SBP, where the removal efficiency of sulfamethoxazole was 80% under the optimal conditions (Mashhadi et al., 2019). Recently, treatment of several HACs using SBP has been done and the results are summarized in Table 2-1 (Mashhadi, 2019). In addition, the following HACs were examined and the results showed that they were not substrates of SBP: thiophene, furan, pyridine, 2-hydroxypyridine, 4-hydroxypyridine, 2-aminopyridine, 3-aminopyridine, 4-aminopyridine, thiazole, pyrazole, imidazole, indazole, quinoline, 2-hydroxyquinoline, 4-hydroxycoumarin, 2-aminooxazole, 2-hydroxybenzothiazole, benzotriazole, atrazine, amitrole, trimethoprim (Mashhadi, 2019; Mashhadi et al., 2019). In this study, three selected HACs (Section 1.3) were studied to investigate the feasibility of SBP treatment in wastewater. To our knowledge, no literature on transformation of these three HACs, with any peroxidase or laccase exists.



Table 2-1, Removal efficiency and optimal parameters of enzymatic treatment of previously studied HACs

Substrate	Substrate concentration (mM)	Optimal conditions			Removal %
		pH	SBP activity (U/mL)	H <sub>2</sub> O <sub>2</sub> (mM)	
Pyrrole	1.0	1.6	5.0	1.0	85
Indole	1.0	1.6	0.45	1.25	>95
2-Aminothiazole	1.0	6.0	4.0	2.0	84
2-Aminobenzothiazole	0.5	7.0	4.5	0.75	30
3-Hydroxyquinoline	0.5	8.6	0.1	1.0	>95
3-Aminoquinoline	1.0	5.6	4.5	2.0	89
2-Aminoimidazole	0.5	8	1.5	1.0	93
2-Aminobenzimidazole	0.5	7	3.0	0.75	77
3-Aminopyrazole	1.0	6	3.0	1.5	70
4-Aminoantipyrine	0.5	7.5	0.1	1.0	87
Hydroxybenzotriazole	1.0	3.6	0.12	1.25	>95

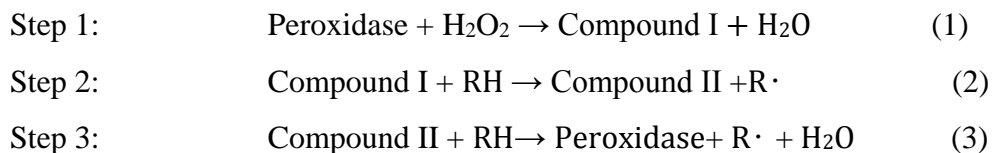
#### 2.4. Peroxidase mechanism

Peroxidases represent a large family of oxidoreductive enzymes, widely distributed in bacteria, fungi, algae, plants and animals and have been classified into heme and non-heme peroxidases (Morsi et al., 2020; Pandey et al., 2017). Heme peroxidases have been

assigned into two super-families: animal and non-animal heme peroxidases. The non-animal heme peroxidases have further been sub-divided into three classes. Class I are intracellular peroxidases; Class II includes extracellular fungal peroxidases and Class III constitutes the secretory plant peroxidases, including HRP, SBP, turnip peroxidase (TP), bitter melon peroxidase (BMP), potato pulp peroxidase and ginger peroxidase (Pandey et al., 2017; Jun et al., 2019).

Peroxidases utilize hydrogen peroxide ( $\text{H}_2\text{O}_2$ ) as a co-substrate to catalyze a wide range of organic and non-organic chemicals. Their appealing biocatalytic properties, including high substrate specificity, high thermal stability and high redox potential, enables them to degrade recalcitrant contaminants efficiently in water. (Chiong et al., 2016; Mukherjee et al., 2018; Steevensz et al., 2013). Peroxidases have been used for degradation of various emerging pollutants. Almaqdi et al. (2019) worked on degradation of a mixture of 21 emerging contaminants with concentration of 2 ppm in a synthetic wastewater, using 5 different peroxidases (SBP, chloroperoxidase (CPO), lactoperoxidase, manganese peroxidase (MnP) and HRP). In another study, enzymatic treatment of 0.5 or 1 mM of a large group of heterocyclic aromatics (most compounds were N-heterocyclic aromatics with a few sulfur- and oxygen-heterocycles) using SBP in synthetic wastewater was investigated (Mashhadi, 2019). Removal of many emerging contaminants using different peroxidases such as SBP, HRP, lignin peroxidase (LIP), MnP and CPO were reviewed by Morsi et al., (2020).

The catalytic mechanism of peroxidases for oxidation of the substrates, which is a two-electron oxidation-reduction in three steps illustrated below (Pandey et al., 2017):



Where, RH is a peroxidase substrate and  $\text{R}\cdot$  is its free-radical. In the first step, the 2-electron oxidation of the native form of enzyme by  $\text{H}_2\text{O}_2$  leads to formation of the active form of enzyme (compound I, which is a high oxidation state intermediate) and one molecule of water. In the second step, compound I oxidizes the substrate to the free radical and converts to compound II. Compound II in the next step oxidizes another molecule of substrate to the free radical and yields the native form of enzyme (Ćirić-Marjanović et al., 2017; Pandey et al., 2017). Free radicals generated, can form dimers by coupling non-enzymatically. With additional peroxidase cycles, the dimers grow until the oligomers reach their solubility limit and precipitate, to be removed by filtration or sedimentation (Cordova Villegas et al., 2016). For phenolic compounds, higher oligomers are generated from resonance-stabilized radicals through C-C and C-O coupling with *ortho*- and *para*-orientation as shown in Figure 2-2 (Steevensz et al., 2014 b). Analogous coupling of enzyme-generated anilino radicals occurs (Ćirić-Marjanović et al., 2017).

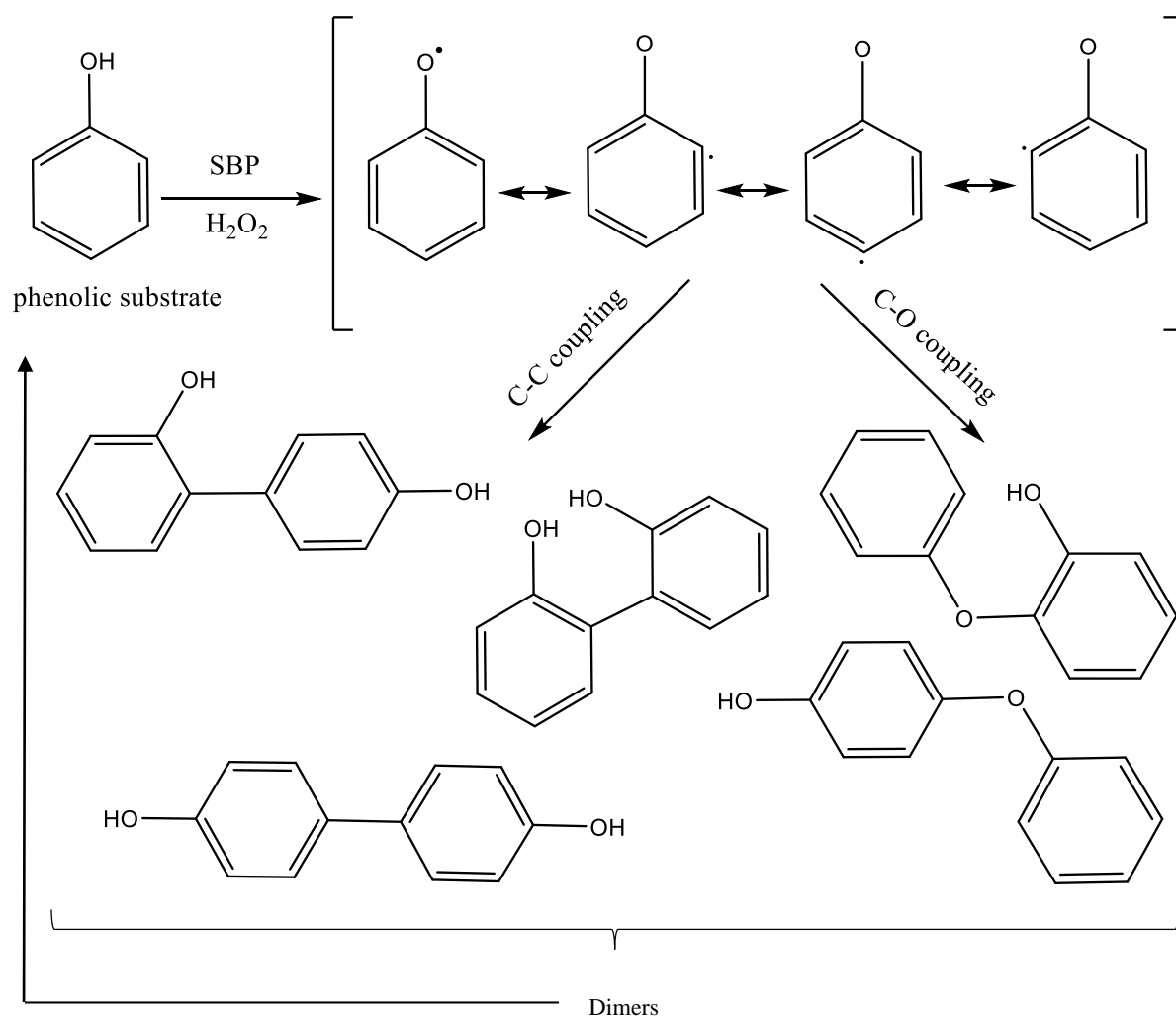


Figure 2-2, Oxidative polymerization of phenol through C-C and C-O coupling

#### 2.4.1. Peroxidase inactivation

Peroxidases can suffer from suicide inactivation pathways in the presence of excess hydrogen peroxide and low concentration of reducing substrate (Steevensz et al., 2014 b). In the first pathway, reversible formation of an intermediate (compound I- $H_2O_2$ ) can further be converted to an inactive intermediate P-670 (absorbance peak at 670 nm upon opening of the heme structure). The second pathway is the reversible accumulation of compound III (an inactive form of enzyme) in the presence of excess  $H_2O_2$  through oxidation of

compound II; although compound III can decay back to the native form of enzyme, the rate of decomposition is very low (Valderrama et al., 2002). Thirdly, adsorption of active enzyme by the solid end-product oligomers can also lead to an apparent inactivation of peroxidases as reported by Feng et al., (2013). Finally, free radicals generated from the substrate can also attach to the enzyme's active site heme (Klibanov et al., 1983).

## ***2.5. Cost and availability of soybean peroxidase***

Global production of soybeans has been reported as 337.70 million metric tons (MMT) in 2019/2020 (USDA, 2020). Soybeans are one of the major oilseed products in North and South America, Figure 2-3. According to Agriculture and Agri-Food Canada (2020), there has been a steady rise in soybean production and seeded area during last 15 years, though soybean production is estimated to have a slight drop in 2020 due to the drop in planted area and difficult growing and harvesting conditions in Western Canada. The price of soybeans is reported as \$395-425 /ton in 2020 (Agriculture and Agri-Food Canada, 2020). Soybean hulls, from which SBP can be extracted, are cheaper and estimated to be \$125/ton (Mukherjee et al., 2018). Accordingly, SBP could be a widely available and affordable source for commercial applications.

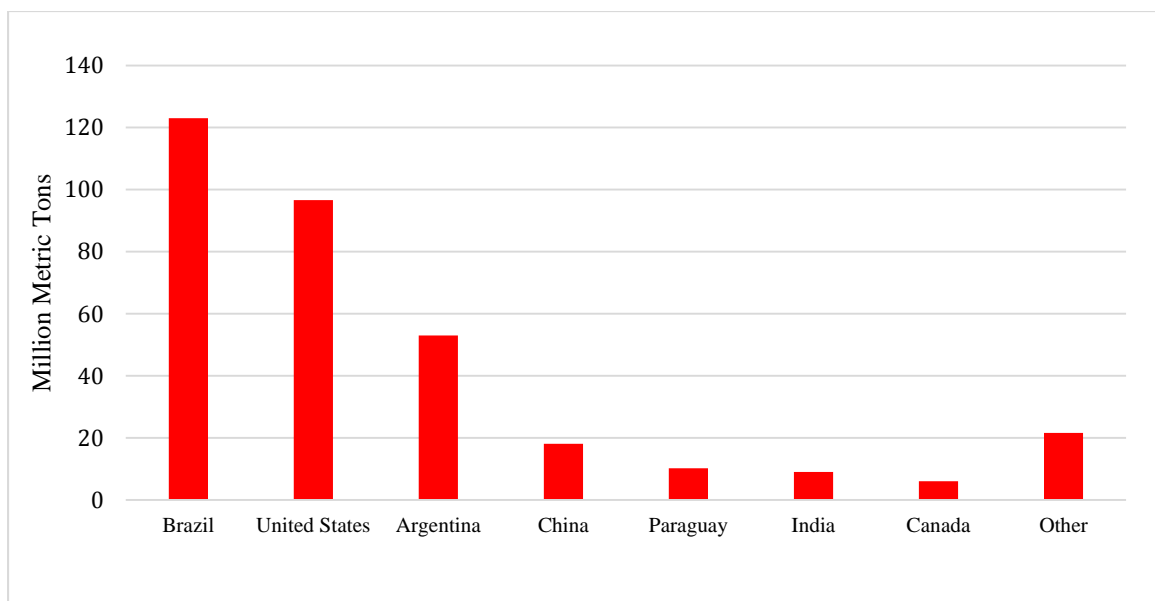


Figure 2-3, Global soybean production 2019 according to USDA (2020)

## 2.6. *Soybean peroxidase extraction*

SBP is extracted from the seed coats (hulls) which are a by-product of crushing operations and are used in animal feed. The extraction process begins with soaking the dry soybean seed in water to for 1-2 hours, so the seed coat/hull becomes softer and crumpled. Then, the hulls are washed with water and SBP can be extracted without diminishing the feed value of the hulls. Notably, it is reported that the activity of the SBP varies among the cultivars and seed coats (Steevensz et al., 2014 b).

## CHAPTER 3

### MATERIALS AND METHODS

#### **3.1. Materials**

##### **3.1.1. Enzymes**

Crude solid SBP (E.C. 1.11.7, Industrial Grade Lot No. 18541NX) was obtained from Organic Technologies (Coshocton, OH). Solid bovine liver catalase (E.C. 1.11.1.6, lot No. 120H7060) was purchased from Sigma Aldrich Chemical Company Inc. (Oakville, ON). Both enzymes were stored at -15 °C. Novo ARP (*Arthromyces ramosus* peroxidase) was donated by Novozymes Inc. (Franklinton, NC) and was kept at 4 °C.

##### **3.1.2. Aromatic compounds**

Both 3-hydroxycoumarin ( $\geq 100\%$  pure) and 2-aminobenzoxazole ( $\geq 97\%$  pure) were purchased from Sigma Aldrich (Oakville, ON). 3-Hydroxycoumarin was stored at room temperature and 2-aminobenzoxazole was stored at 4°C. 3-Amino-5-methylisoxazole ( $>97\%$ ) was obtained from TCI (Philadelphia, PA) and was kept at 4 °C.

##### **3.1.3. Buffers and solvents**

Glacial acetic acid, concentrated hydrochloric acid, sodium acetate, monobasic sodium phosphate, dibasic sodium phosphate and potassium chloride were purchased from ACP Chemicals Inc. (Montreal, QC). Tris (hydroxymethyl)-aminomethane was purchased from Sigma. Buffer standards (pH 4, 7 and 10) were obtained ACP Chemicals Inc. and buffer standard pH 1.68 was from Hanna Instruments (Newmarket, ON). Dimethyl Sulfoxide ( $\geq 100\%$  pure) was purchased from Sigma Aldrich.

#### ***3.1.4. Other chemicals***

Phenol (99% pure) was purchased from Sigma Aldrich. 4-Aminoantipyrine (4-AAP) was obtained from BDH Inc. (Toronto, ON). Hydrogen peroxide (30% w/v) was purchased from ACP Chemicals Inc. and stored at 4°C. All other chemicals used in this study were analytical grade and purchased either from Sigma Aldrich Chemical Company or BDH Inc.

#### ***3.1.5. Chromatography solvents, columns and filters***

HPLC grade methanol was obtained from ACP Chemicals Inc. HPLC-grade water was obtained from Waters Co. (Mississauga, ON). HPLC-grade acetonitrile (ACN) was obtained from Fisher Scientific Company (Ottawa, ON). Phosphoric acid and HPLC-grade 2-propanol were obtained from Sigma Aldrich. Polyethersulfone (PES) syringe filters 0.22 µm with 26 mm diameter were purchased from Sarstedt (Montreal, QC). Gemini C18 Column, 110Å, 5 µm, 4.6 mm \*100 mm was purchased from Phenomenex (Torrance, CA).

### ***3.2. Analytical methods***

#### ***3.2.1. Buffer preparation***

Various buffers for the pH range of 1-10 were prepared according to Gomori (1955). HCl-KCl buffer was prepared to be used in the range of pH 1.0-2.2. Acetic acid-sodium acetate buffer was prepared for the pH range of 3.6 -5.6. Monobasic-dibasic sodium phosphate buffer was prepared to be used in the pH range of 5.6-8.0. Tris (hydroxymethyl)-aminomethane-HCl buffer for the basic range of 7.2-9.0 was prepared.



### 3.2.2. Enzyme stock solution preparation

SBP (1.4 g) was added to 100 mL distilled water followed by mixing for 24 hours. The solution was then centrifuged at 4000 rpm for 25 minutes. The supernatant was stored at 4°C. Catalase stock solution was prepared by adding 0.5 g of solid catalase to 100 mL of distilled water followed by mixing for 4 hours and stored at 4°C. More information is provided in Appendix A.

### 3.2.3. Enzyme activity assay

A colorimetric assay was used in this study to quantify the enzyme activity (Ibrahim et al. 2001). Enzyme activity is defined in standard catalytic units (U/mL) and 1.0 unit of SBP equals to the amount of enzyme needed to convert 1.0  $\mu\text{mol}$  of hydrogen peroxide per minute under the assay condition. Enzyme activity can be measured by monitoring the initial rate of color formation of a pink chromophore at 510 nm, generated by oxidative coupling of phenol and 4-aminoantipyrine (4-AAP) in the presence of  $\text{H}_2\text{O}_2$  with SBP:

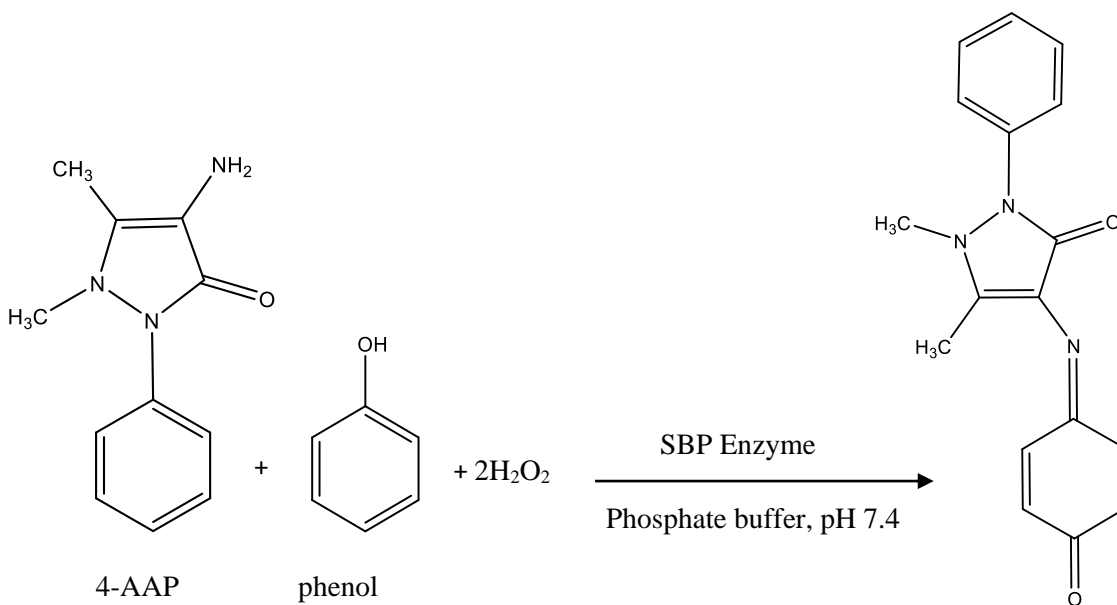


Figure 3-1, Oxidative coupling of phenol and 4-AAP in the presence of  $\text{H}_2\text{O}_2$  and SBP

The initial rate of the reaction shown in

Figure 3-1 was measured by a built-in kinetic rate calculation function in the UV-Vis spectrometer. The reagent mixture consisted of 100  $\mu\text{L}$  of 100 mM hydrogen peroxide stock solution, 0.025 g of 4-AAP, 5 mL of concentrated phenol (100 mM phenol and 0.5 mM phosphate buffer pH 7.4) and the mixture was made up to 47.5 mL in a volumetric flask. Three different dilutions of enzyme (30, 40 and 50 times diluted) were prepared and 50  $\mu\text{L}$  of each diluted solution was added to the quartz cuvette followed by addition of 950  $\mu\text{L}$  of freshly prepared reagent mixture and very quick mixing. The absorbance change was monitored immediately after adding the reagent for 30 seconds at 510 nm. The rate of the reaction was calculated by the first-order kinetics features in UV-Vis software. All reagents, ( $\text{H}_2\text{O}_2$ , 4-AAP and phenol), were present in non-limiting concentration except SBP, therefore, the initial rate of reaction is directly proportional to the concentration of the enzyme present. More information regarding this assay is provided in Appendix B.

#### ***3.2.4. Residual enzyme activity assay***

In order to measure the remaining enzyme activity after the enzymatic treatment of substrate, a residual enzyme activity test is required. The concept of the residual enzyme activity test is the same as the regular enzyme activity assay. However, for lower concentration of enzyme, after the enzymatic reaction, the reagent concentration and ratio of mixing were reformulated so that the final concentration of each component in the cuvette remained constant. More information about this assay is provided in Appendix C.

### ***3.2.5. Residual hydrogen peroxide assay***

A similar colorimetric method (Figure 3-1) was used to determine the residual hydrogen peroxide after enzymatic treatment (Caza et al. 1999). The reagent consisted of phenol and Novo ARP liquid concentrate at pH 7.4. After adding the reagent to the sample, phenolic radicals form due to the reaction with ARP and peroxide, couple with 4-AAP and generate a chromophore (same chromophore as in enzyme activity test) with maximum absorbance of 510 nm. The absorbance of the solution after this reaction (18 minutes) was measured and compared to a hydrogen peroxide calibration curve to determine the concentration of residual hydrogen peroxide. Detailed information regarding this assay is provided in Appendix D.

## ***3.3. Analytical equipment***

### ***3.3.1. UV-Vis spectrometry***

A UV-Vis spectrophotometer (model 8453, Agilent company, Mississauga, ON) with a range of 190 -1100 nm connected to a computer was used to measure the maximum absorbance ( $\lambda_{\text{max}}$ ) of each substrate. The detected  $\lambda_{\text{max}}$  of the substrate was then used in HPLC analysis. Also, the UV-Vis spectrophotometer was used for enzyme activity assay and peroxide and enzyme residual test.

### ***3.3.2. High performance liquid chromatography (HPLC) analysis***

A Waters (Oakville, ON) HPLC system with binary pumps, model 1525, dual wavelength absorbance detector, model 2489 and auto-sampler model 2707 connected to a computer and operated by Breeze 2.0 software was used to construct the curves as well as quantify the residual substrate concentration after enzymatic treatment. A gradient

method with 5  $\mu\text{L}$  injection volume was reproduced for 3-HC (Asthana et. al, 2015). The UV-detector was adjusted based on the predetermined  $\lambda_{\text{max}}$ . The mobile phase ratios, flow rate, column temperature and type of column used are given in Table 3-1. Solvent A was 0.085% phosphoric acid and 5% methanol in water(v/v). Solvent B was 0.085% phosphoric acid and 95% methanol in water (v/v). Calibration curves in different buffers can be found in Appendix E. For 2-ABO, a gradient method with 5  $\mu\text{L}$  injection was developed. The mobile phase ratios, flow rate, column temperature and type of column used are given in Table 3-2. Solvent A was 0.1 % phosphoric acid and solvent B was 40:60 IPA: ACN.

Table 3-1, HPLC analysis conditions for 3-HC under gradient elution

Substrate	Time (min)	Flow (mL/min)	Ratio of solvents (%)		$\lambda_{\text{max}}$ (nm)	Column temperature	Column type
			Pump A	Pump B			
3-HC	0	1.0	90	10	312	30 °C	Gemini C18
	10		90	10			
	20		10	90			
	23		10	90			
	23.1		90	10			
	35		90	10			

Table 3-2, HPLC analysis conditions for 2-ABO under gradient elution

Substrate	Time (min)	Flow (mL/min)	Ratio of solvents (%)		$\lambda_{\max}$ (nm)	Column temperature	Column type
			Pump A	Pump B			
2-ABO	0	1.0	98	2	237	40 °C	Gemini C18
	2		98	2			
	10		80	20			
	11		20	80			
	19		20	80			
	19.1		0	100			
	26		0	100			
	26.1		80	20			
	30		80	20			
	30.1		98	2			
	38		98	2			

### 3.3.3. Mass spectrometry

A Xevo G2-XS Time-of-Flight (ToF) mass spectrometer, equipped with Atmospheric Solids Analysis Probe (ASAP) or Electrospray Ionization (ESI) obtained from Waters was used for enzymatic products analysis. The ASAP method uses heated nitrogen gas to volatilize the sample from a disposable glass capillary tip. It is a sensitive method for ionizing low polarity compounds, which are typically not amenable to the ESI technique. The gas-phase ions then enter the mass spectrometer and are detected based on their mass-to-charge ( $m/z$ ) ratio. In ESI, the analyte is pumped to a capillary and a high

voltage is applied which makes the droplets spraying from the tip of the capillary and evaporate. The evaporation process is also supported by heat and a nebulizing gas, generally nitrogen. The gas-phase ions then enter the mass spectrometer detection. The acquisition range of probe was 50 to 1500 mass-to-charge ratio ( $m/z$ ).

#### ***3.3.4. Other instruments***

A LSE compact centrifuge was from Corning Company (New York, USA). The centrifuge conditions are defined in the respective experimental protocols. An Oakton PC 700 pH meter with range of 0.00 to 14.00 connected to a Thermo Scientific Orion pH Probe (9110DJWP, refillable/double junction/glass/semi-micro) with  $\pm 0.02$  pH accuracy was used (Vernon Hills, IL). Various magnetic stir bars in different sizes were obtained from Cole-Parmer Canada Inc. (Montreal, QC). The magnetic stirrers from VWR international Inc. (Mississauga, ON) with 0-1100 rpm and 100-1500 rpm was used for mixing. Vortex mixer model K-550-G was purchased from Scientific Industries Inc (New York, USA).

### ***3.4. Experimental protocols***

#### ***3.4.1. Enzymatic oxidation of substrate with SBP and feasibility of treatment of target aromatics***

The enzymatic reactions were conducted in 30 mL batch reactors, in triplicate and at room temperature, to obtain 95% removal (except for pH optimization). The 20 mL reaction medium in batch reactors consisted of 40 or 10 mM buffer, 0.5 or 0.1 mM of substrate, SBP and hydrogen peroxide in appropriate concentrations. Hydrogen peroxide was the last chemical added to the solution to start the reaction. After mixing the solution for 3 hours using Teflon-coated magnetic stirrer bars on magnetic stirring plates, the

reaction was stopped by adding 100  $\mu$ L catalase stock solution (0.5 g/100 mL) to quench the reaction by immediately consuming residual hydrogen peroxide. The sample was then microfiltered with pre-conditioned, 0.22  $\mu$ m PES syringe filters and the residual substrate concentration was analyzed by HPLC.

Time-course experiments were also conducted using optimized parameters to monitor the substrate conversion over time. Three big batch reactors with 200-300 mL volume were used and samples (5 mL) were taken at selected time intervals, quenched with catalase and vortexed to stop the reaction immediately. Later on, samples were filtered and analyzed by HPLC. For each set of batch reactors, different control batch reactors were also run, formulated the same as sample but without either hydrogen peroxide or SBP to monitor the effect of enzyme or hydrogen peroxide on the substrate, respectively.

In order to verify if the selected aromatic compounds are substrates for SBP, a set of preliminary experiments were conducted. Batch reactors with sufficient enzyme and hydrogen peroxide along with aromatic compound and buffer were stirred for 3 hours and the reaction was then stopped by adding catalase, microfiltered and analyzed for the residual concentration by UV-Vis and/or HPLC.

#### ***3.4.2. Optimization of important enzymatic reaction parameters***

In this study, pH and hydrogen peroxide concentration were optimized. Also, minimum effective concentration of SBP to reach 95% removal of target compound was determined. For pH optimization, initially some preliminary experiments were conducted for range finding. Then, the experiments were repeated with shorter pH intervals and smaller ranges. The reactions were conducted at different pHs using various buffers under stringent conditions (SBP was limited), therefore the effect of pH can be clearly monitored.

Later on, at optimal pH, the reactions were formulated for peroxide optimization and minimum effective concentration of SBP to reach 95% removal. If 95% removal was not obtained, residual peroxide and residual SBP tests were conducted to determine the residual amounts of peroxide and enzyme in order to reformulate the reactions to reach 95% conversion.

#### ***3.4.3. Stepwise addition of H<sub>2</sub>O<sub>2</sub>***

For a substrate with less than 95% removal efficiency, stepwise addition of hydrogen peroxide was tested because SBP is likely to be inactivated irreversibly by addition of excess hydrogen peroxide (Valderrama et al. 2002). Optimal peroxide concentration established previously was divided into 4 equal aliquots and added in intervals, every 45 minutes, to reach the same final concentration. The reaction was stirred for 3 h in total. Half of the reaction mixture was then microfiltered for hydrogen peroxide residual test and catalase was added to the other half to stop the reaction. Later on, the reaction mixture was filtered and the removal efficiency was determined using HPLC.

#### ***3.4.4. Preliminary determination of enzymatic treatment products using mass spectrometry***

For identification of plausible polymerization products of enzymatic treatment, reaction mixtures under established conditions were analyzed. The experiments were conducted in batch reactors and then, the mixtures were centrifuged for 20 minutes at 4000 rcf and the supernatant and precipitate (if any) along with the standard sample were run on the mass spectrometer with ASAP or ESI method. Since buffers produce interferences with product peaks in MS, the concentration of buffer in batch reactors was reduced to 10 mM for MS samples. MassLynx V. 4.1 software was used for data analysis.



### ***3.5. Sources of error***

There is a level of uncertainty in every analysis. The accuracy and reliability of the results are affected by inevitable systematic or random errors that can happen during the experiments. Symmetric errors caused by analytical methods and are predictable and usually constant, whereas random errors, that are always present, can show different results for the same repeated measurement. Random errors can be minimized not avoided. In order to minimize random errors, experiments were conducted in triplicates and standards were injected in the HPLC along with the samples. All Figures show the standard deviation of each triplicate data set as well as the average. For the data points with very small deviation ( $<1\%$ ), the error bars may not visible since they could be hidden by the icons. The SBP activity test using freshly prepared reagents was conducted every day prior to the experiments since the activity is affected by the temperature. Equipment such as pipets, analytical balance and pH meter were calibrated to avoid systematic errors.

## CHAPTER 4

### RESULTS AND DISCUSSION

The feasibility of SBP-catalyzed transformation of three selected HACs, 3-hydroxycoumarin, 2-aminobenzoxazole and 3-amino-5-methylisoxazole was studied initially. 3-Hydroxycoumarin and 2-aminobenzoxazole were found to be substrates for SBP, but 3-amino-5-methylisoxazole showed no conversion in SBP-catalyzed treatment. Later on, three important operational parameters: pH, H<sub>2</sub>O<sub>2</sub> concentration and minimum effective enzyme activity were optimized for each substrate to reach  $\geq 95\%$  conversion efficiency. Time-course experiments based on optimal parameters were conducted to determine the time to reach 95% conversion and to find the first-order reaction rate constants and half-lives of substrates. Finally, possible products were identified using mass spectrometric analysis.

#### ***4.1. Parameter optimization of SBP-catalyzed treatment***

##### ***4.1.1. pH Optimization***

pH of the reaction medium is one of the major biocatalytic parameters which affects the activity and stability of SBP and consequently, the efficiency of enzymatic treatment and its industrial application. This is due to the pH effects on the ionization state of specific amino acid side chains that are mainly responsible for catalytic function and conformational stability of enzyme. Two key amino acid residues, distal histidine-42 (His-42) as proton acceptor from hydrogen peroxide, and distal arginine-38 (Arg-38) as the charge stabilizer (Dunford 1999), require optimum pH that satisfies their ionization states. Also, pH affects the 3-dimensional structure of SBP and its conformational stability mainly

due to interaction of amino-acid residues with heme (Al-Ansari et al., 2011). pH-dependent activity of soybean peroxidase is mostly reversible if the enzyme is incubated in weak acidic or basic solutions and can regain its activity when shifted back to the optimum pH. But, some enzyme structural changes can be irreversible and the enzyme cannot regain its maximum activity. Furthermore, pH of the reaction medium could influence the ionization state of reducing substrate and electron transfer rate (Parsiavash et al., 2015). The catalytic activity of SBP is also dependent on pH because of the existence of more solvent-exposed heme edge in the structure (Kamal and Behere, 2003). SBP was found to be active over a broad range of pH and have its maximum activity ( $\geq 95\%$ ) at pH 5.5-6.0 for guaiacol as the reducing substrate (Geng et al., 2001). The maximum catalytic activity of SBP at 25 °C for ABTS (2,2'-azino-bis (3-ethylbenzothiazoline-6-sulphonic acid)) was observed at pH 5.5 (Kamal and Behere, 2003). Also, SBP was found to remain active between pH 3.0 and 10.0 for 3-substituted quinolines (Mashhadi et al., 2019 a).

In this work, optimum pH is considered as the pH at which the highest removal efficiency of substrate is obtained. To determine the optimum pH, the experiments were conducted under a stringent condition with insufficient amount of SBP, leading to incomplete removal of substrate, in order to clearly distinguish pH effects. Preliminary experiments were conducted over a broad pH range. Later on, the experiments were done over a narrower range of pH. Also, the experiments were repeated with less enzyme if necessary to have the stringent condition. In these experiments, hydrogen peroxide concentration was generally chosen as 1.5-2.0 times the molar concentration of the substrate, based on previous experiments performed in the lab. The substrate concentration was either 0.50 mM or 0.10 mM and experiments were run in triplicate at room temperature

( $22 \pm 3$  °C). Three control experiments were conducted: the first one without SBP, the second one without H<sub>2</sub>O<sub>2</sub>, and the third one without SBP and H<sub>2</sub>O<sub>2</sub>. The error bars on the figures demonstrate the standard deviation; error bars are not visible for the data points with very small deviation.

The effect of pH on conversion of 3-HC after 3-hour enzymatic treatment is shown in Figure 4-1. Range finding was conducted for a broader range of pH using UV-Vis (data not shown). Later on, the experiments were analyzed by HPLC with the pH range 3.6-9.0, 0.003 U/mL SBP, and 0.75 mM hydrogen peroxide. For pH 8.0, the experiments were conducted both with phosphate buffer and Tris buffer to check the possible effect of buffer species. Then, the experiments were repeated with less enzyme (0.001 U/mL) to reach stringent condition. As shown in Figure 4-1, 3-HC was best transformed around neutral pH and the optimum pH was 7.0 which showed 3% and 10% remaining with 0.003 U/mL and 0.001 U/mL SBP, respectively. Decreasing the SBP concentration by three-fold, did not show much change in remaining percentages; it presumably indicates even small amount of enzyme is capable of converting the substrate efficiently. The increase observed in the remaining percentage of the substrate on either side of the optimum pH could be because of the lower stability of the Compound I (active form of enzyme) in a neutral solution (Patapas et al., 2007). Also, the bell-shaped pH dependence indicates the variation of ionization state of catalytic residues of the enzyme and/or ionization state of substrate (Kamal and Behere, 2003). Optimum pH for 3-HC was very close to its pK<sub>a</sub> value, which is 6.95-7.0 (Nowak et al., 2016). Similar results were reported for 3-hydroxyquinoline (optimum pH range 8.0-8.6; pK<sub>a</sub> 8.0) (Mashhadi, 2019), *p*-cresidine (2-methoxy-5-methylaniline, optimal pH 4.6, pK<sub>a</sub> 4.7) (Mukherjee et al., 2018) and Bromoxynil and

Ioxynil (optimal pH 4;  $pK_a$  3.86 and 3.96 respectively) (X. Zhang, 2019). Increasingly more remaining 3-HC can be seen from pH 7.0 to 9.0, likely because of increasing in ionization of hydroxyl group to the anionic form of the substrate that is not able to participate in peroxidase cycle (Urrea et al., 2018).

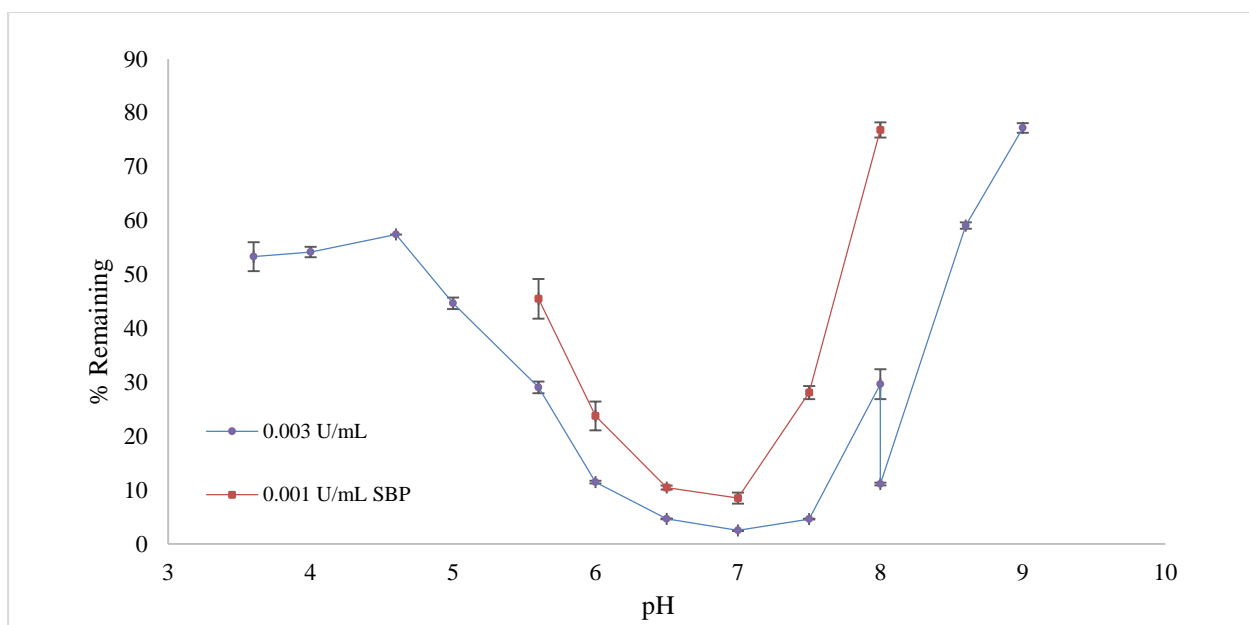


Figure 4-1, pH optimization for 3-HC.

Conditions: 0.50 mM 3-HC, 40 mM buffer, 0.001 U/mL and 0.003 U/mL SBP, 0.75 mM hydrogen peroxide, 3-h reaction.

The results of 2-ABO (0.10 mM) pH optimization using HPLC are shown in Figure 4-2. After pH range finding by UV-Vis (data not shown), the experiments were conducted in triplicate with HPLC detection, over a pH range of 4.5-7.5, with 10 mM buffer to avoid absorbance interference from buffer, 0.15 mM  $H_2O_2$ , and 0.5 U/mL SBP. 2-ABO showed a very poor conversion efficiency and the optimum pH was found to be 6.0. A similar optimum pH was reported for 2-aminothiazole and 3-aminopyrazole in a previous study (Mashhadi, 2019). Also, optimum pH for 2-ABO can be compared to the optimum value

reported in the same study, for treatment of 2-aminoquinoline (pH 5.6) and 2-aminobenzoimidazole (pH 7.0), both having some structural similarities with 2-ABO.

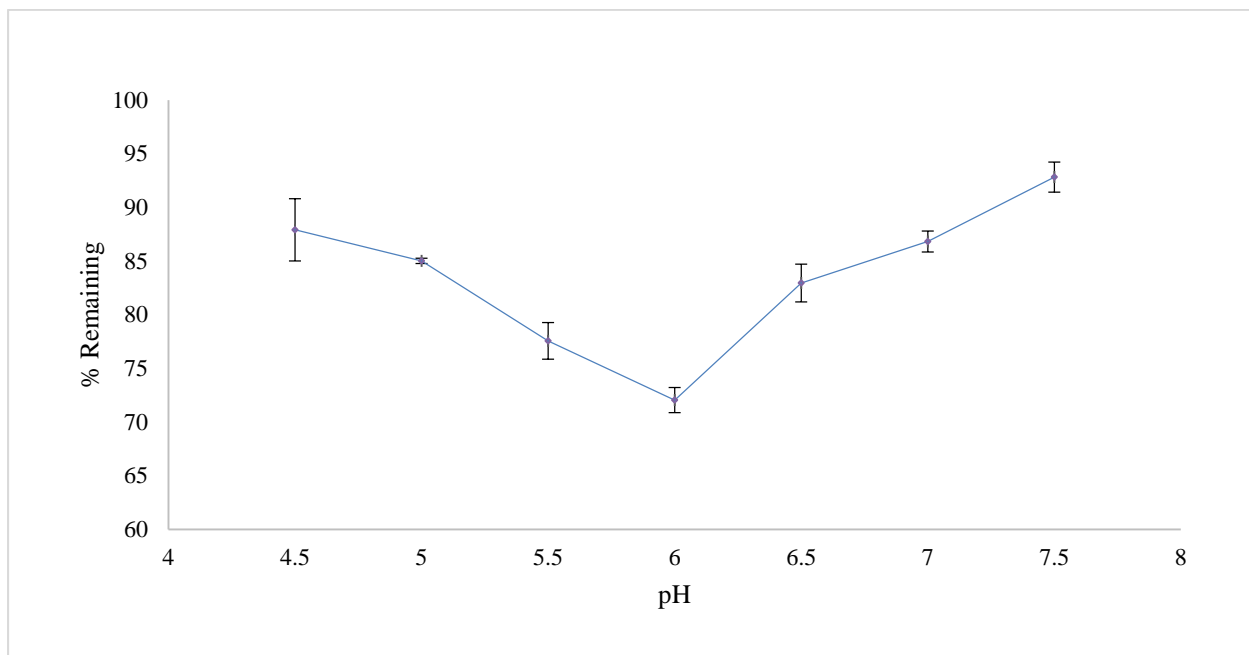


Figure 4-2, pH optimization for 2-ABO.

Conditions: 0.10 mM 2-ABO, 10 mM buffer, 0.5 U/mL SBP, 0.15 mM hydrogen peroxide, 3-h reaction.

#### ***4.1.2. SBP Optimization***

Economic feasibility of a treatment method is very important and the cost of enzyme can be one of the barriers to application of enzymatic treatment to real wastewater (Steevensz et al., 2009). Hence, determining the minimum effective amount of SBP contributes to the cost-effectiveness of the enzymatic treatment of target pollutants.

The minimum concentration of SBP needed to reach 95% removal of organic pollutant is considered as optimum enzyme. The experiments were conducted at the previously established pH optima for each substrate and the samples were analyzed by

HPLC. The  $\text{H}_2\text{O}_2$  concentration was kept at a level where it did not become limiting during the experiments. Enzyme optimization was repeated after hydrogen peroxide optimization if 95% removal was not reached. Figures 4-3 and 4-4 show the final optimization for each substrate.

For 0.50 mM 3-HC, the removal efficiency increased very slightly with increasing enzyme activity up to 0.003 U/mL and the highest removal efficiency achieved was > 97%. Minimum effective SBP was selected as 0.002 U/mL which shows 96% removal efficiency. This value may be compared to 0.43 mU/mL SBP required for conversion of 0.1 mM benzidine in synthetic wastewater (Altaf et al., 2016). Also, minimum effective SBP for 3-HC can be quantitatively compared to 0.005 U/mL SBP required for removal of 1.0 mM *p*-phenylenediamines (Al-Ansari et al., 2009).

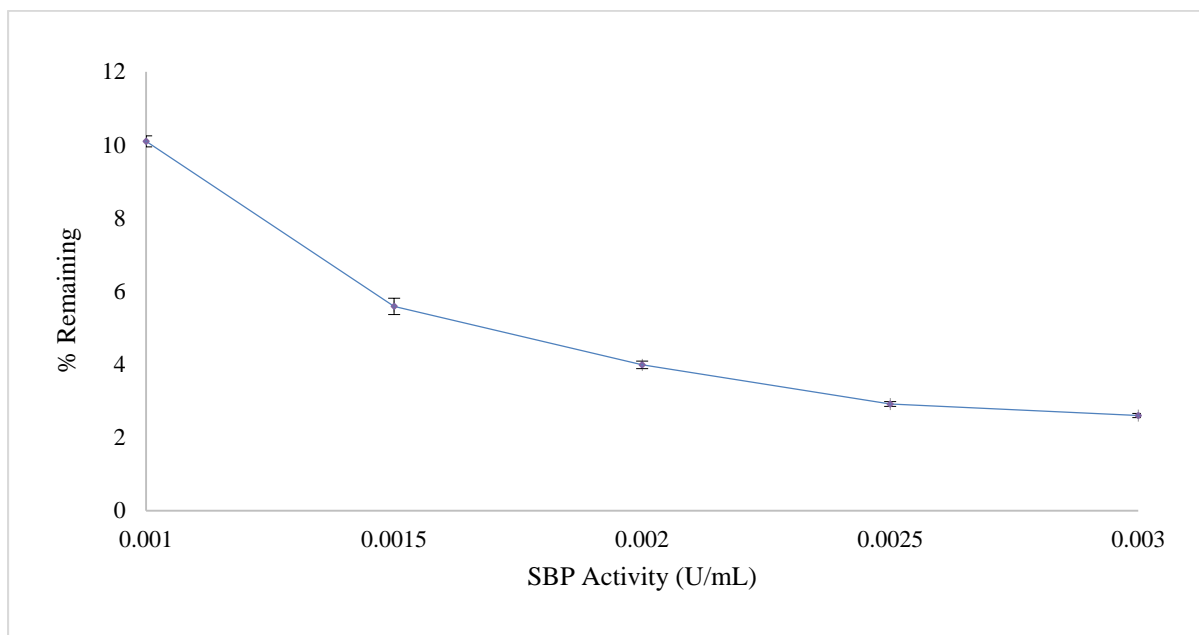


Figure 4-3, SBP optimization for 3-HC.

Conditions: 0.50 mM 3-HC, 40 mM phosphate buffer pH 7.0, 0.75 mM hydrogen peroxide, 3-h reaction.

Enzyme optimization for 2-ABO was conducted in the range of 2-5 U/mL of SBP activity, based on the fact that in the preceding experiments done for pH optimization, 0.5 U/mL enzyme activity could only contribute to ~28% conversion. Figure 4-4 is the final SBP optimization for 2-ABO (after H<sub>2</sub>O<sub>2</sub> optimization, see section 4.1.3., below) with the following conditions: 0.10 mM 2-ABO, 10 mM phosphate buffer pH 6.0 and 0.25 mM H<sub>2</sub>O<sub>2</sub>. Increasing the amount of enzyme from 0.5 to 3.5 U/mL resulted in almost 16% improvement in removal of substrate after 3 hours. However, further increase in SBP did not show a positive effect on the removal efficiency. Clearly, pH and enzyme optimization for 2-ABO have shown this substrate is not a good candidate for enzymatic treatment of wastewater.

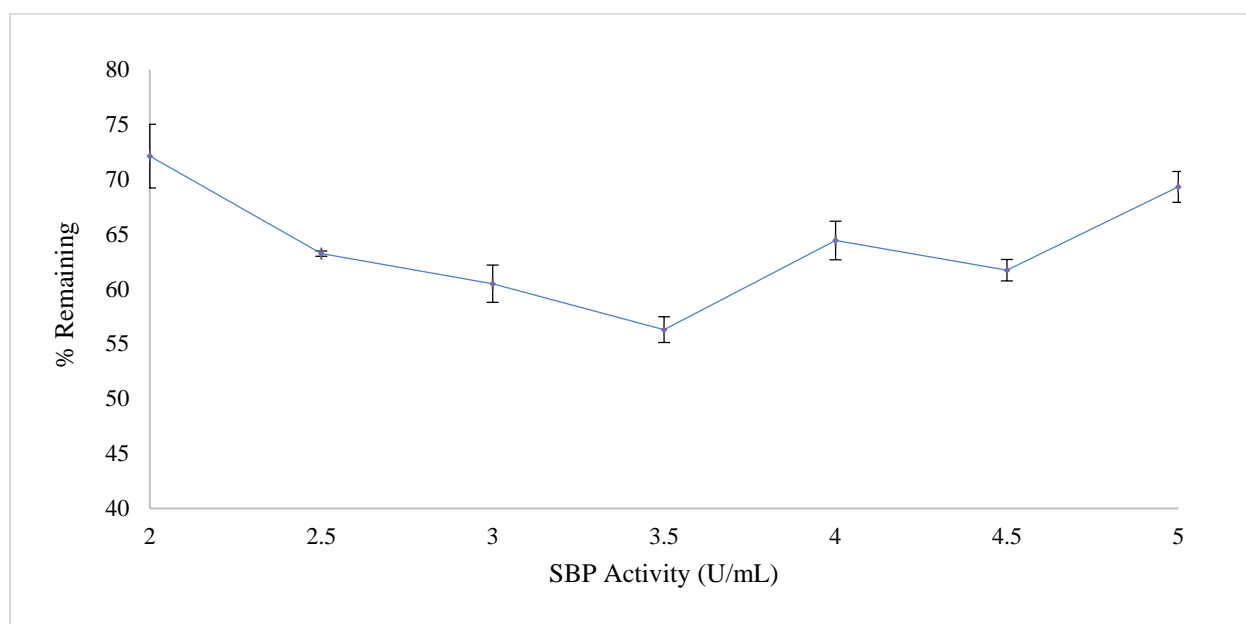


Figure 4-4, SBP optimization for 2-ABO.

Conditions: 0.10 mM 2-ABO, 10 mM phosphate buffer pH 6.0, 0.25 mM hydrogen peroxide, 3-h reaction.



#### ***4.1.3. Hydrogen peroxide optimization***

Hydrogen peroxide is one of the significant factors in enzymatic treatment and as a co-substrate, initiates the peroxidase reaction. As discussed in Section 2.4.1. if  $\text{H}_2\text{O}_2$  concentration is in excess, peroxidase inactivation will occur. On the other hand, a low concentration of  $\text{H}_2\text{O}_2$  might lead to insufficient conversion of the substrate. According to the oxidation-reduction mechanism in the peroxidase cycle, for 1 mole of  $\text{H}_2\text{O}_2$  consumed, 2 moles of the substrate would be converted to free radicals. However, this stoichiometry is subject to change depending on the catalase activity of peroxidase and subsequent enzymatic cycles generating higher oligomers from the dimers formed firstly in the peroxidase cycle (Valderrama et al., 2002).

Experiments were conducted, for optimizing hydrogen peroxide concentration with optimum amount of SBP for each substrate in a 3-h reaction period to reach  $\geq 95\%$  removal. For the substrate with  $< 95\%$  conversion, subsequent stepwise addition of peroxide was studied to increase the removal efficiency.

Hydrogen peroxide optimization of 3-HC (HPLC analysis) was carried out at 0.002 U/mL SBP. Figure 4-5 shows that increasing the concentration of  $\text{H}_2\text{O}_2$  over 0.75 mM, resulted in a lower removal efficiency. This might be because of inactivation of SBP through the formation of compound III in the presence of excess amount of  $\text{H}_2\text{O}_2$ , resulting in lower conversion. Also, 0.25 mM  $\text{H}_2\text{O}_2$  which is the theoretical molar concentration of  $\text{H}_2\text{O}_2$  needed for conversion of 0.50 mM 3-HC according to the peroxidase cycle, showed low conversion efficiency, indicating the higher peroxide demand due to the oligomer formation and/or due to catalase activity of soybean peroxidase. Accordingly, 0.75 mM

H<sub>2</sub>O<sub>2</sub> was considered as the optimum peroxide concentration for 0.5 mM 3-HC, which led to > 96% removal efficiency.

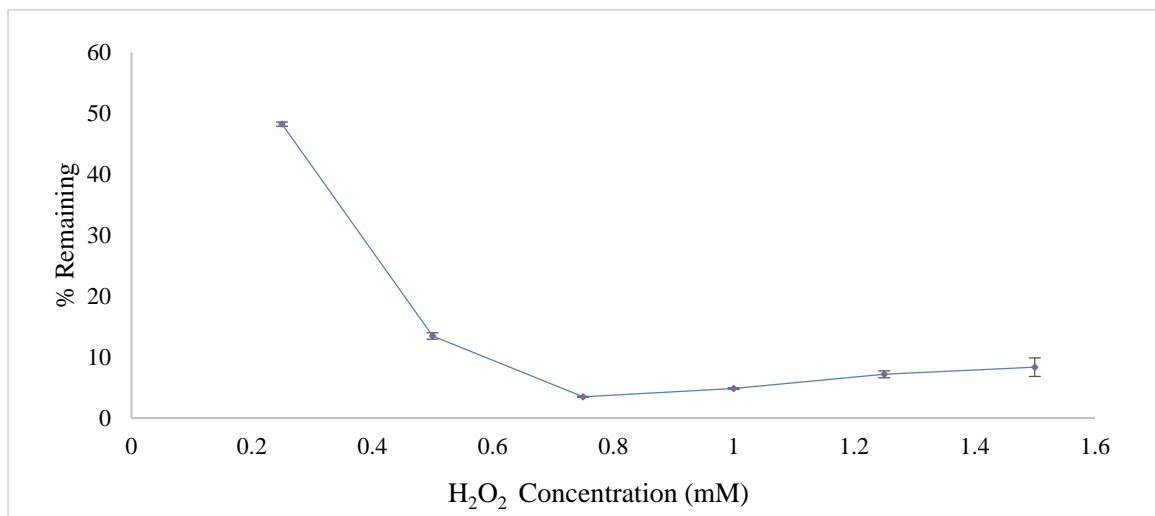


Figure 4-5, Hydrogen peroxide optimization for 3-HC.

Conditions: 0.50 mM 3-HC, 40 mM phosphate buffer pH 7.0, 0.002 U/mL SBP, 3-h reaction.

Figure 4-6 demonstrates H<sub>2</sub>O<sub>2</sub> optimization for 2-ABO (HPLC analysis). The best performance was observed at 0.25 mM H<sub>2</sub>O<sub>2</sub> with 55% remaining.

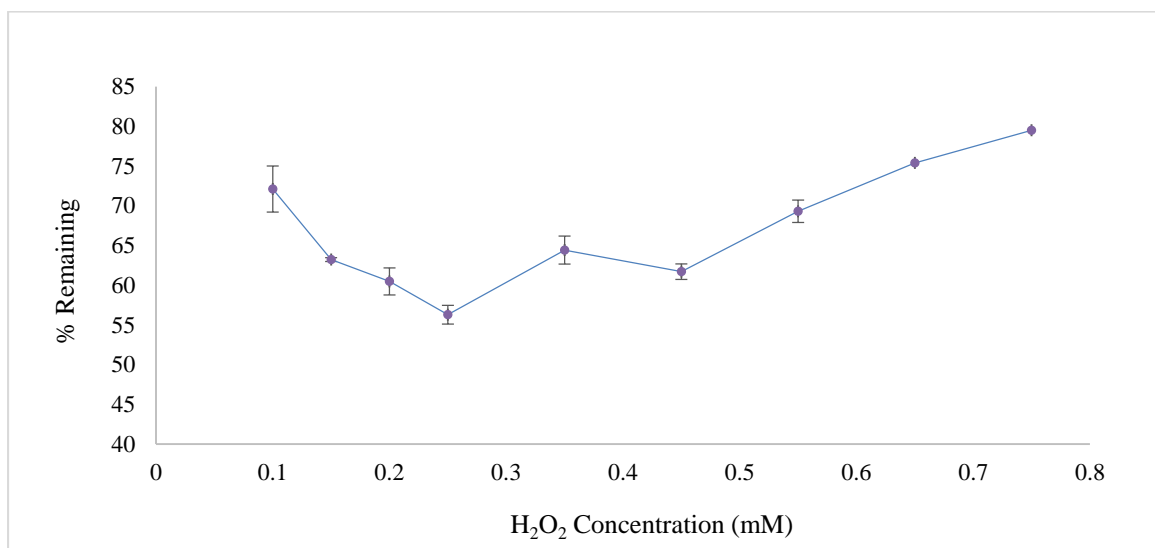


Figure 4-6, Hydrogen peroxide optimization for 2-ABO.

Conditions: 0.10 mM 2-ABO, 10 mM phosphate buffer pH 6.0, 3.0 U/mL SBP, 3-h reaction.

To increase the removal efficiency of 2-ABO, residual H<sub>2</sub>O<sub>2</sub> and SBP tests were conducted as reported in Appendix C and D, since the low removal efficiency may happen if the reaction runs out of enzyme and/or peroxide. The residual SBP and H<sub>2</sub>O<sub>2</sub> tests for 2-ABO were performed after 3-hour reaction under the optimal conditions of Figure 4-6 and showed 73% of initial enzyme activity remaining and only 5% of the initial H<sub>2</sub>O<sub>2</sub> concentration respectively. Therefore, the effect of incremental addition of H<sub>2</sub>O<sub>2</sub> was studied for possible improvement of 2-ABO removal efficiency. The optimum concentration of H<sub>2</sub>O<sub>2</sub> for 2-ABO (0.25 mM) was divided into 4 equal aliquots added to the reaction mixture every 45 minutes. Results showed 53% of the substrate remaining with stepwise addition of H<sub>2</sub>O<sub>2</sub>, thus only 2% improvement in the removal efficiency.

#### ***4.2. Time course of reactions***

Reaction time is one of the important parameters when designing a treatment plant, because it influences the reactor volume and overall cost of the plant. The reaction time chosen for the preceding experiments was 3 hours, an arbitrary choice. Therefore, it is useful to determine the minimum time needed to reach > 95% conversion of pollutants. Following parameter optimization, substrate conversion was monitored during 3 hours under optimal conditions. Aliquots taken at various time intervals were quenched with catalase and then micro-filtered and analyzed by HPLC to measure the residual substrate concentration at each time. The first-order kinetic constants  $k$  and half-lives of 3-HC and 2-ABO were derived from the plots and calculated based on equations (1):

$$C = C_0 e^{-kt}; \quad t_{\frac{1}{2}} = \frac{\ln(2)}{k} \quad (1)$$

Figures 4-7 and 4-8 correspond to the time course of catalytic oxidation of the two compounds, and the red lines are the fitted first-order exponential lines for the initial reaction stage (best-fit equations and related  $R^2$  are shown in the Figures). Not surprisingly, the reaction does not stay first-order for the entire period, since the rate constant is changing due to the enzyme activity reduction and  $H_2O_2$  consumption (loss of pseudo-first-order behavior). Thus, the initial stages of the reaction have been used for reaction half-life calculation. As can be seen, there is a slowing reaction rate likely due to the enzyme inactivation by reactive radicals and/or end-product adsorption of active enzyme (Al-Ansari et al., 2009; Feng et al., 2013).

As shown in Figure 4-7, 95% conversion of 3-HC occurred within the first 52 minutes and the rate constant was  $0.056 \pm 0.002 \text{ (min}^{-1}\text{)}$ . The corresponding half-life for 3-HC under given conditions was  $12.4 \pm 0.5 \text{ min}$ . The rate constant for 2-ABO was estimated as  $0.0054 \pm 0.0002 \text{ (min}^{-1}\text{)}$  and the corresponding half-life obtained was  $129 \pm 4 \text{ min}$  (Figure 4-8). Also, for comparison, normalized half-lives were calculated by multiplying half-life of each substrate by its SBP concentration (This gives the half-life at 1.0 U/mL SBP). Thus, normalized half-lives of 3-HC and 2-ABO were calculated as  $0.026 \pm 0.001$  and  $452 \pm 15$ , respectively; SBP-catalyzed reaction of 3-HC progressed much faster than 2-ABO.

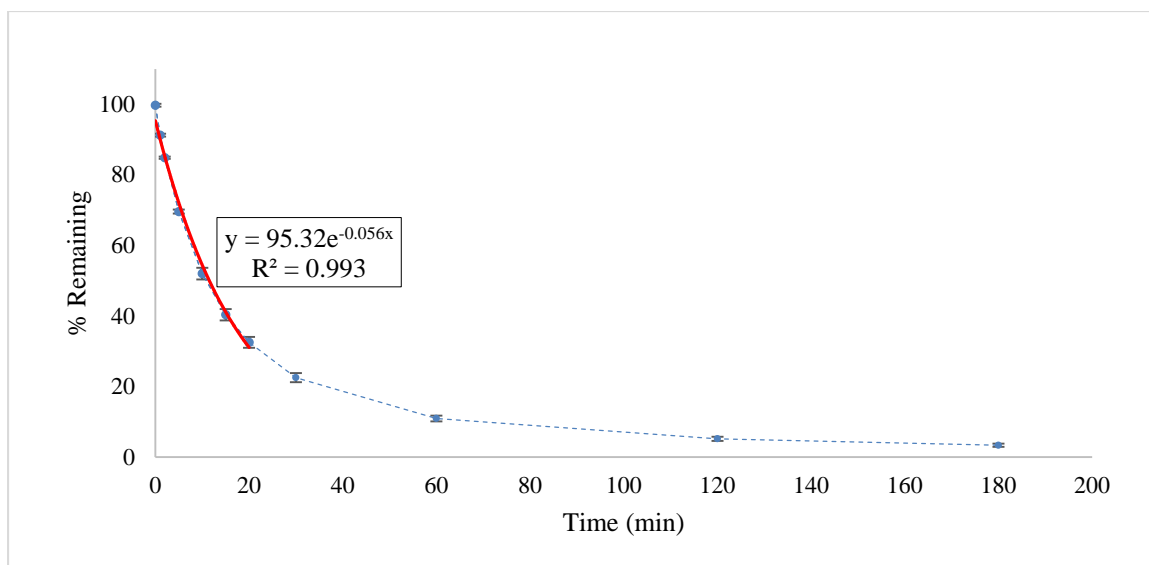


Figure 4-7, Time course experiment for 3-HC.

Conditions: 0.50 mM 3-HC, 40 mM phosphate buffer pH 7.0, 0.002 U/mL SBP, 0.75 mM H<sub>2</sub>O<sub>2</sub>, 3-h reaction

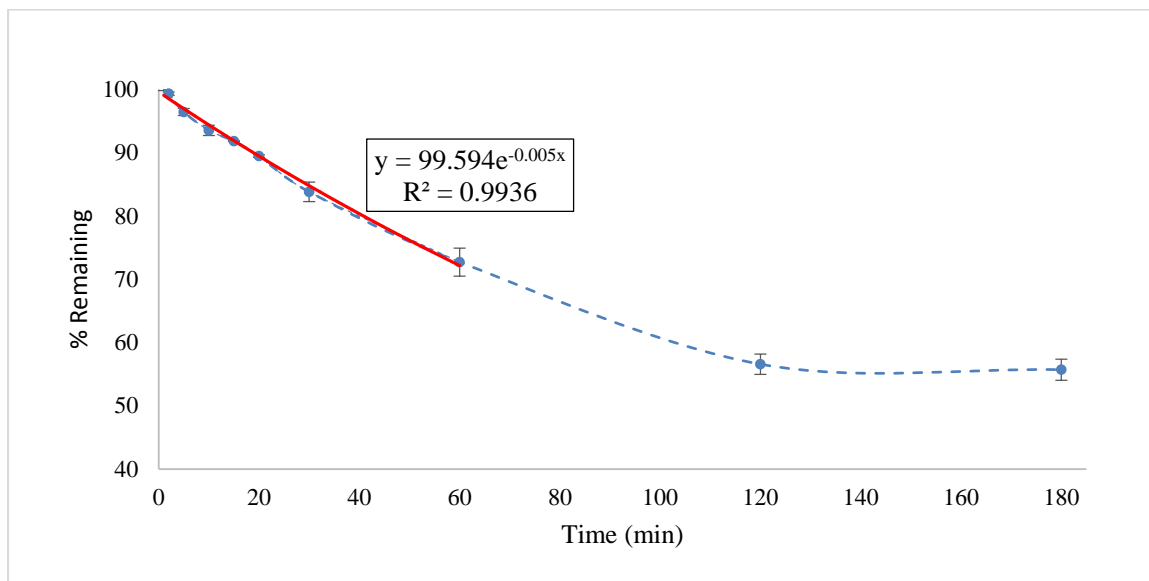


Figure 4-8, Time course experiment for 2-ABO.

Conditions: 0.10 mM 2-ABO, 10 mM phosphate buffer pH 6.0, 3.5 U/mL SBP, 0.25 mM H<sub>2</sub>O<sub>2</sub>, 3-h reaction

Table 4-1 summarizes normalized half-lives of various SBP substrates studied in this group with respect to the optimum enzyme concentration. Comparing the half-lives of different substrates, the normalized half-life of 3-HC,  $0.026 \pm 0.001$  min, shows it to be the fastest substrate in SBP-catalyzed reactions amongst the studied compounds.

Table 4-1, Half-lives and normalized half-lives of various SBP substrates

	Substrate	Half-life (min)	Normalized half-life (min)
HACs (Mashhadi, 2019)	Pyrrole	$49.2 \pm 3$	$246 \pm 15$
	Indole	$25.2 \pm 1.2$	$11.3 \pm 0.5$
	2-Aminothiazole	$33.0 \pm 0.6$	$132 \pm 2$
	2-Aminobenzothiazole	$720 \pm 0.01$	$3240 \pm 0.0$
	3-Hydroxyquinoline	$11.9 \pm 0.59$	$1.19 \pm 0.06$
	3-Aminoquinoline	$14.99 \pm 0.6$	$67.5 \pm 2.7$
	2-Aminoimidazole	$5.1 \pm 0.2$	$7.7 \pm 0.3$
	2-Aminobenzimidazole	$29.4 \pm 0.6$	$88.2 \pm 1.8$
	3-Aminopyrazole	$36 \pm 1.2$	$108 \pm 4$
	4-Aminoantipyrine	$60.6 \pm 1.2$	$6.06 \pm 0.12$
	Hydroxybenzotriazole	$41.4 \pm 1.8$	$4.97 \pm 0.22$
Arylamines (Mukherjee, 2019)	<i>p</i> -Cresidine	$12.4 \pm 0.0$	$0.124 \pm 0.0$
	4-Chloro- <i>o</i> -toluidine	$11.5 \pm 0.0$	$0.104 \pm 0.0$
	4,4'-Oxydianiline	$1.80 \pm 0.02$	$0.072 \pm 0.001$
	4,4'-Methylenedianiline	$0.58 \pm 0.10$	$0.40 \pm 0.07$
	4,4'-Thiodianiline	$0.513 \pm 0.007$	$0.0770 \pm 0.0011$
	4,4'-Methylenebis (2-chlororaniline)	$4.08 \pm 0.02$	$0.408 \pm 0.002$
Pesticides (X. Zhang, 2019)	Bromoxynil	$3.00 \pm 0.13$	$2.7 \pm 0.02$
	Ioxynil	$0.51 \pm 0.018$	$0.18 \pm 0.01$

Azo-dyes (Cordova Villegas, 2017)	Acid Blue 113	$8.76 \pm 0.60$	$13.2 \pm 0.9$
	Direct Black 38	$2.1 \pm 0.2$	$6.4 \pm 0.6$
Present study	3-hydroxycoumarin	$12.4 \pm 0.5$	$0.0257 \pm 0.0010$
	2-Aminobenzoxazole	$129 \pm 4.44$	$452 \pm 15$

#### 4.3. Mass spectrometry (MS) results

Free radicals generated in the peroxidase catalytic cycle couple non-enzymatically as discussed in Section 2-4. Various coupling positions such as C-C, C-O, O-O (O-O coupling is not stable), N-N and N-C are expected due to the presence of different resonance-stabilized radical structures, leading to formation of several isomeric coupling products. The peroxidase cycle continues until the oligomers grow to reach their solubility limit and precipitate (Cordova Villegas et al., 2016). MS analysis helps to identify the nature of generated products which can lead to a better understanding of plausible toxicity of these compounds. Based on the molecular weight of oligomers obtained from MS data, possible reaction product structures have been assigned. Notably, MS analysis can only offer preliminary insights into the possible products and cannot discriminate among isomeric structures. MS analysis was conducted using the ASAP ionization technique and ESI method in this study (both in positive-ion mode; thus protonated forms of the products were frequently detected). After enzymatic treatment of the substrates under optimal conditions, the unfiltered reaction mixture (in order to prevent losing possible products) and the standards were analyzed using a high-resolution Waters Xevo®-G2-XS TOF. Based on the molecular weight of generated oligomers (mass to charge ratio ( $m/z$ )) derived from mass spectrometry data and analyzed by MassLynx software within  $\pm 3$  mDa and  $\pm 5$  ppm, possible structures and formulae have been assigned. During the analysis, the isotope

abundance was considered for corroboration of the assigned formulae. The following symbols have been used for the obtained structures: M, standard; MH, protonated standard;  $^{13}\text{C}$ -MH, protonated natural abundance  $^{13}\text{C}$ -isomer of standard,  $\text{M}_2\text{H}-2$ , protonated oxidative dimer;  $\text{M}_2\text{H}-4$ , protonated oxidized oxidative dimer,  $\text{M}_3\text{H}-4$ , protonated oxidative trimer,  $\text{M}_3\text{H}-6$ , protonated oxidized oxidative trimer.

To the best of our knowledge, there is no published literature available on polymerization products of 3-HC and 2-ABO using any peroxidase. However, formation of various polymerization products of variety of HACs by SBP-catalyzed reaction has been studied by others (Mashhadi, 2019; Mashhadi et al., 2019).

#### ***4.3.1. 3-Hydroxycoumarin***

Figure 4-9 shows the expanded-scale mass spectrum of 3-HC standard (not treated, powder) from  $m/z$  100 to 200. Based on its formula  $[\text{C}_9\text{H}_6\text{O}_3]$ , the exact mass of 162.031 is expected for the standard radical cation ( $[\text{C}_9\text{H}_6\text{O}_3]$ ); the observed base peak with  $m/z$  163.0393 can be assigned to the protonated standard (MH) peak, with the formula of  $[\text{C}_9\text{H}_7\text{O}_3]$  with its  $^{13}\text{C}$ -isotope at  $m/z$  164.0427. Also, with further scale-expansion of the spectrum, a peak at  $m/z$  162.0313 was observed and shown in Figure 4-10, matches with standard radical cation ( $\text{M}^+$ ) and its  $^{13}\text{C}$  was observed at  $m/z$  163.0393 that is not visible without scale-expansion of the spectrum.



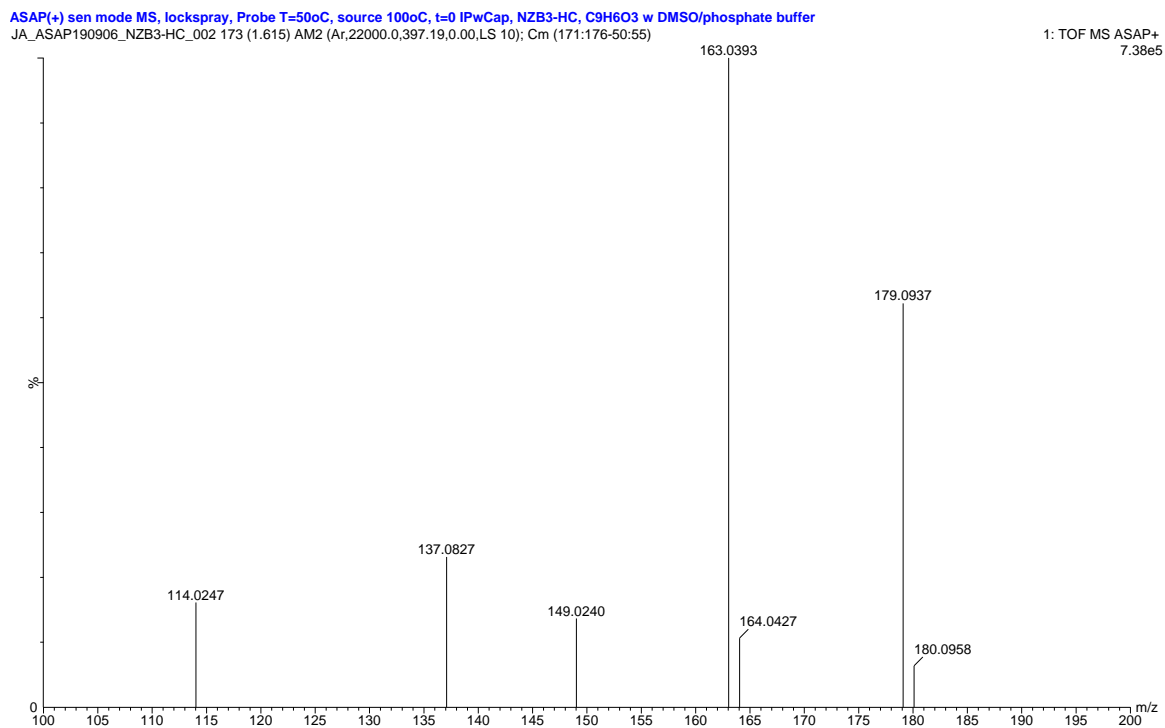


Figure 4-9, Expanded ASAP-MS spectrum of 3-HC standard, from m/z 100 to 200

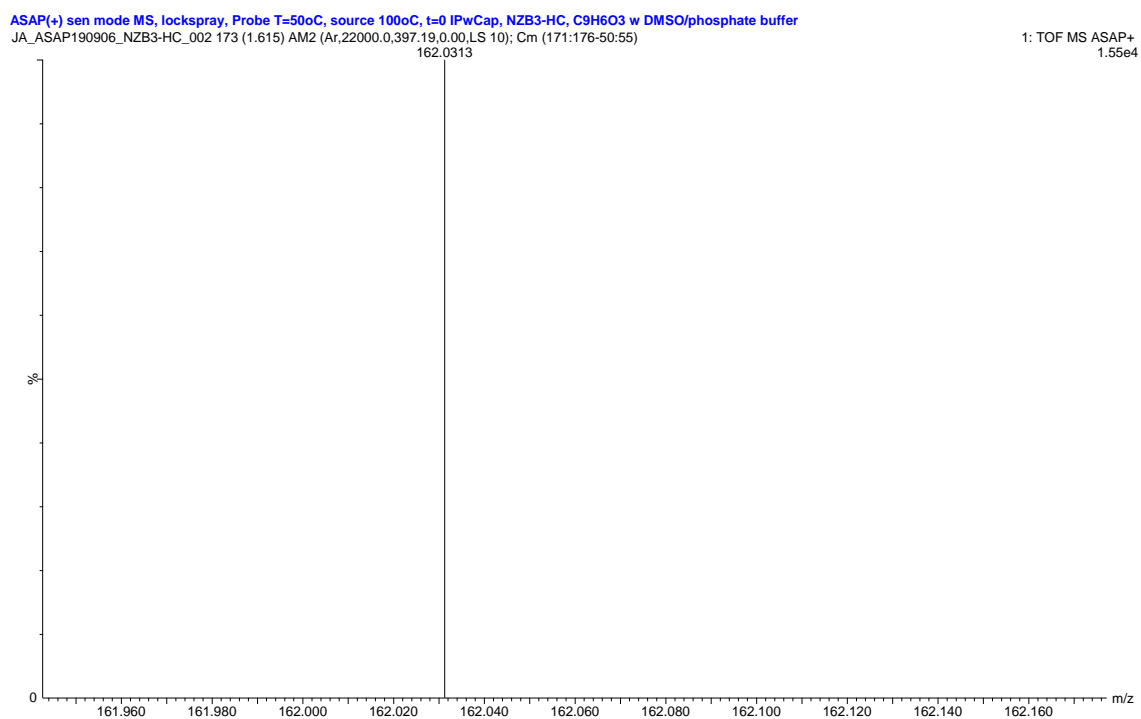


Figure 4-10, Expanded ASAP-MS spectrum of 3-HC standard, from m/z 161.94 to m/z 162.18

Electron de-localization of 3-HC radical has resonance-contributors shown in Appendix F. Coupling through C-C and C-O leads to formation of different dimers, Figure 4-11 (a, b) that could re-enter the oxidation-reduction reaction and form higher oligomer, Figure 4-11 (c, d).

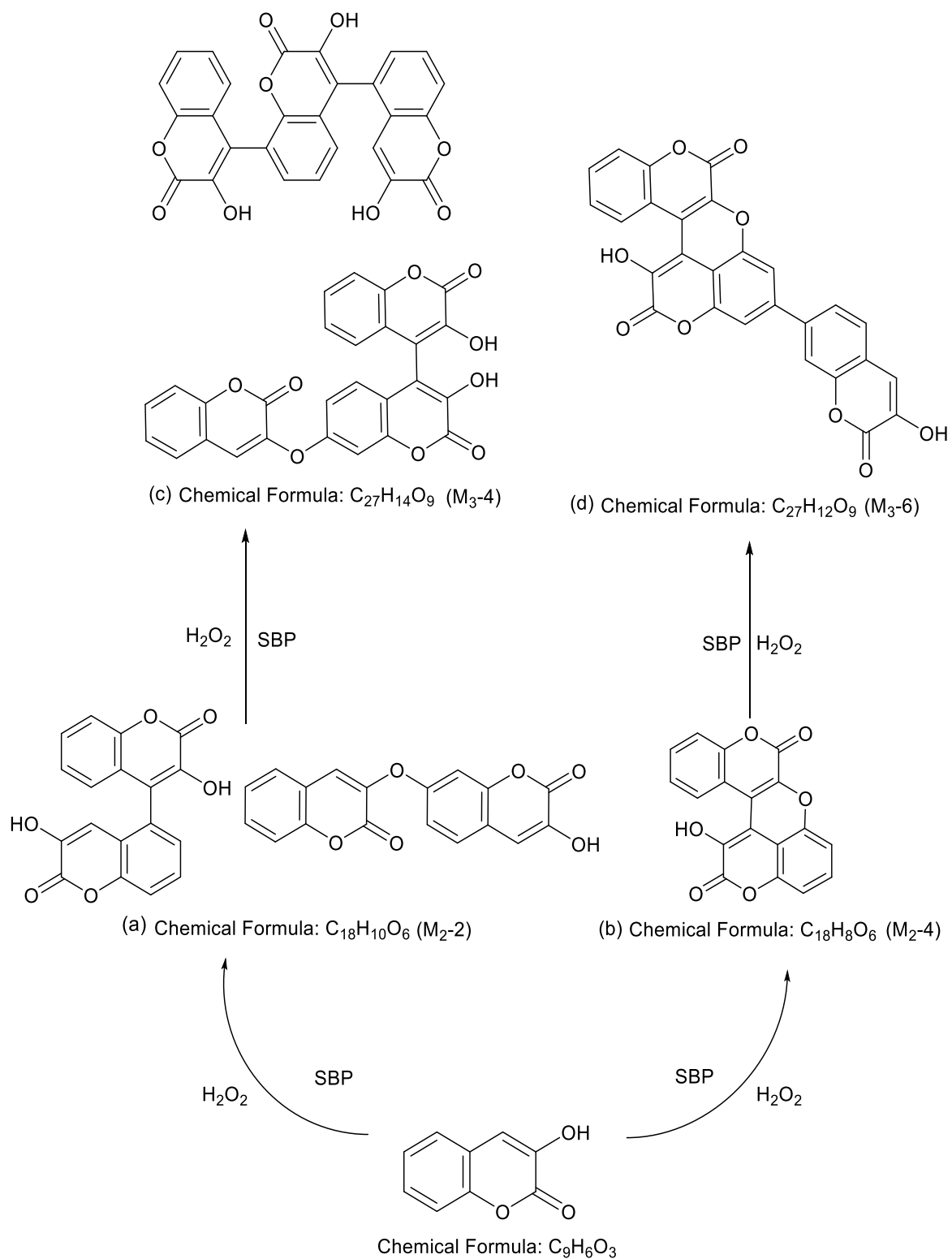


Figure 4-11, Some possible structures of oligomers formed during enzymatic treatment of 3-HC

The mass spectrum of the product mixture after 3-hour of enzymatic reaction of 3-HC under optimum conditions (95% removal efficiency) is shown in Figure 4-12. The base peak at  $m/z$  321.0400 was observed for ( $M_2H-4$ ) and was attributed to the protonated cyclic dimer (Figure 4-11 (b)) with formula of  $[C_{18}H_9O_6]$ , formed through C-C and C-O coupling of 3-HC resonance-stabilized radicals. Also, a peak at  $m/z$  as 322.0434 was observed with scale-expansion of the spectrum (Figure 4-13) and could be assigned to  $^{13}C$ -isotope of this dimer. A lower intensity peak at  $m/z$  323.0545 shown in Figure 4-12 might suggest the presence of the protonated form of oxidative dimer with ( $M_2H-2$ ) structure, shown in Figure 4-11 (a) and molecular formula of  $[C_{18}H_{11}O_6]$ . Also, the  $^{13}C$ -isotope of this dimer at  $m/z$  324.0583 is shown in Figure 4-14.

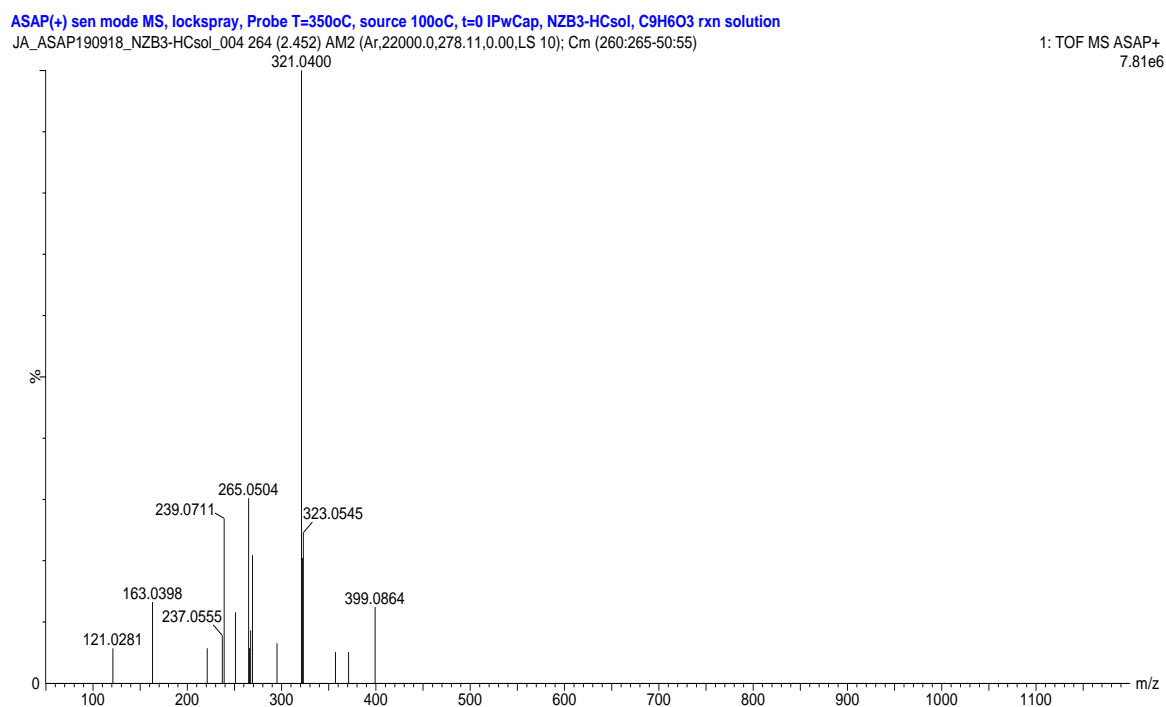


Figure 4-12, Full-scan ASAP-MS spectrum of 3-HC reaction mixture.

Conditions: 0.50 mM 3-HC, 10 mM phosphate buffer pH 7.0, 0.002 U/mL SBP, 0.75 mM  $H_2O_2$ , 3-h reaction

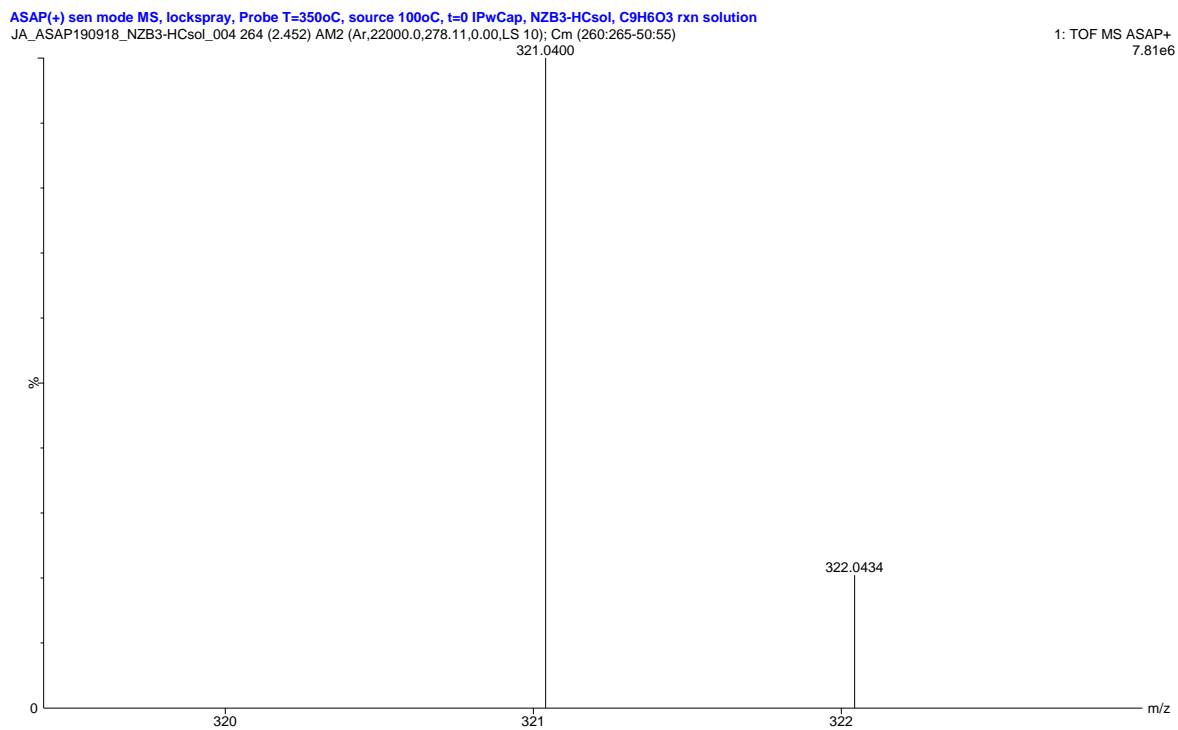


Figure 4-13, Expanded ASAP-MS spectrum of 3-HC reaction mixture from m/z 320 to 323

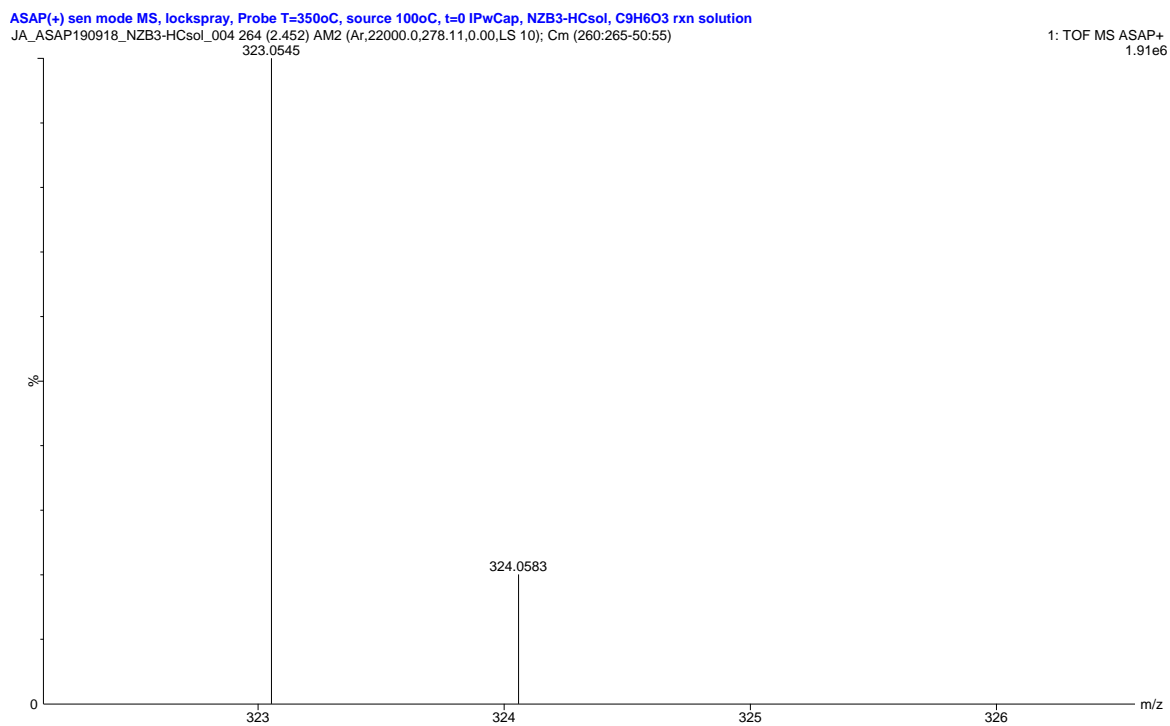


Figure 4-14, Expanded ASAP-MS spectrum of 3-HC reaction mixture from m/z 323 to 326

In addition to dimers, higher oligomeric peaks were observed in the optimal reaction mixture, which correspond to the trimers originating from coupling of dimers and monomers as shown in Figure 4-11 (c) and (d). Figure 4-15 displays the expanded spectrum of optimal reaction mixture and observed peaks that matches with the protonated oxidized oxidative trimer ( $M_3H-6$ ) with molecular formula of  $[C_{27}H_{13}O_9]$  at  $m/z$  481.0552, plus its  $^{13}C$ -isotope at  $m/z$  482.0590 and can be assigned to the protonated trimer of structure shown in Figure 4-11(d). Also, the base peak at  $m/z$  483.0715 corresponded to the protonated oxidative trimer ( $M_3H-4$ ) with the molecular formula of  $[C_{27}H_{15}O_9]$  with plausible structures shown in Figure 4-11 (c). Its  $^{13}C$  at  $m/z$  484.0755 was also observed and is shown in the spectrum.

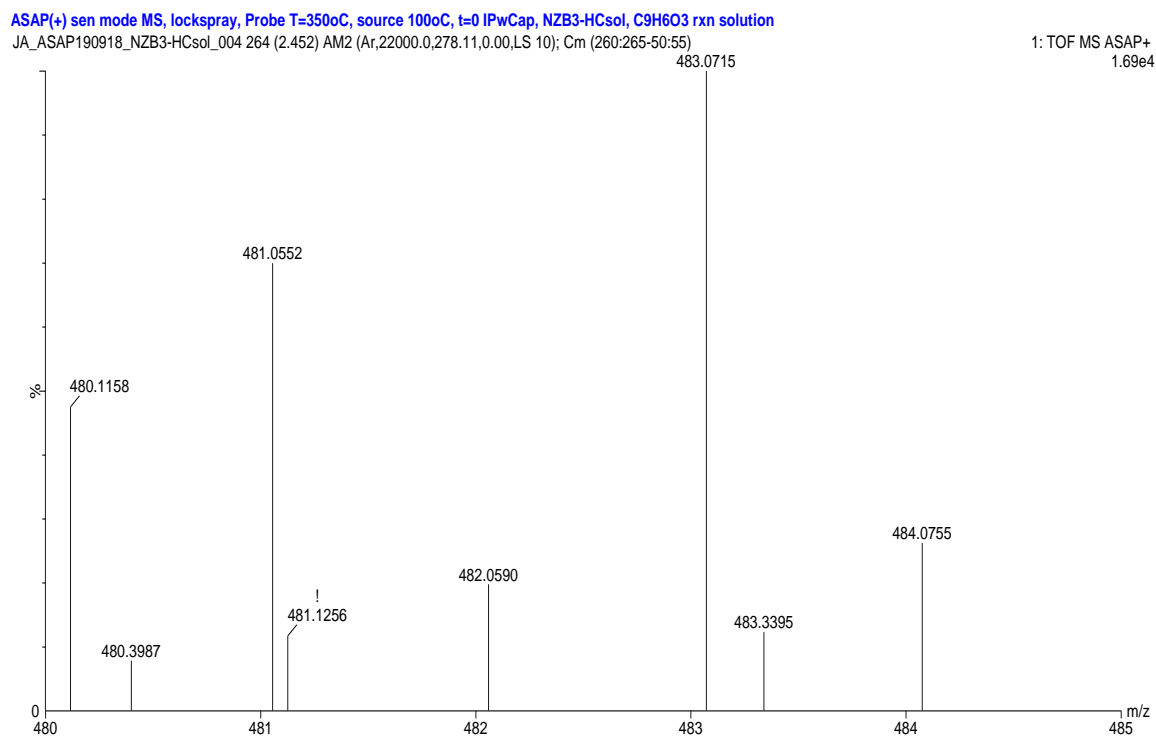


Figure 4-15, Expanded ASAP-MS spectrum of 3-HC reaction mixture from  $m/z$  479 to 485

#### 4.3.2. 2-Aminobenzoxazole

Figure 4-16 shows the mass spectrum of 2-ABO standard (not treated, powder) from  $m/z$  120 to 150. Based on its formula  $[C_7H_6N_2O]$ , the exact mass of 134.048 is expected for the standard radical cation and 135.056 for the protonated standard. The base peak in Figure 4-16 at  $m/z$  135.0557 matches with the protonated standard peak (MH) with the formula of  $[C_7H_7N_2O]$  with its  $^{13}C$ -isotope at  $m/z$  136.0583. Also, the un-protonated standard radical cation with formula of  $[C_7H_6N_2O]$  at  $m/z$  134.0477 was observed with scale-expansion of the spectrum and shown in Figure 4-17.

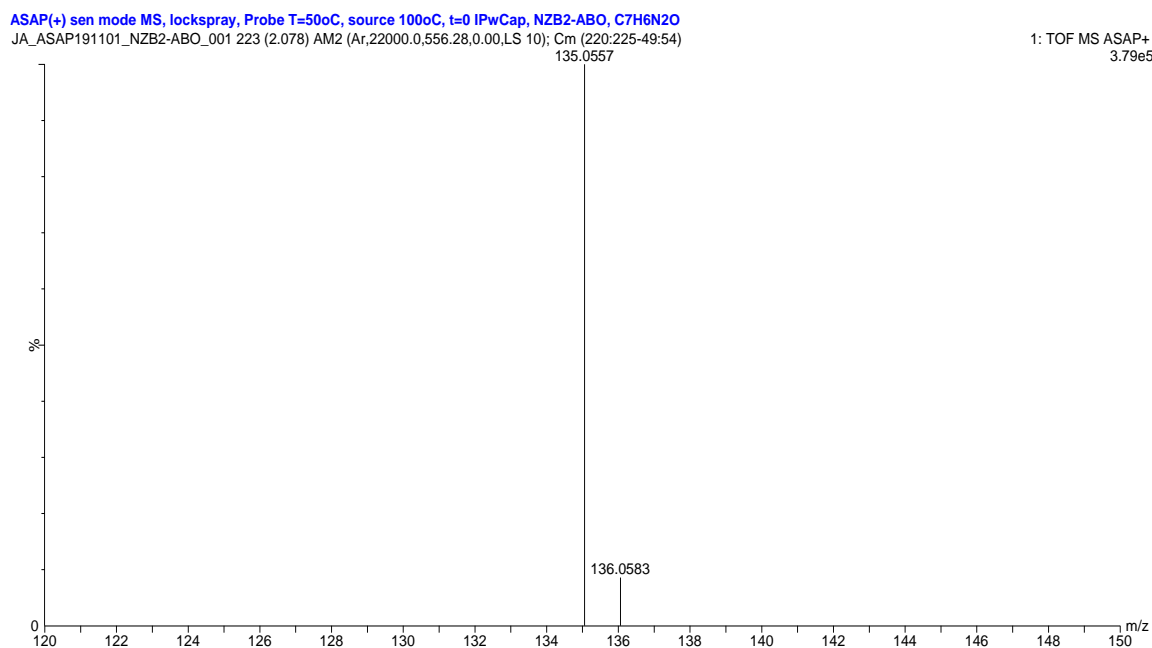


Figure 4-16, ASAP-MS spectrum of 2-ABO standard, from  $m/z$  120 to 150

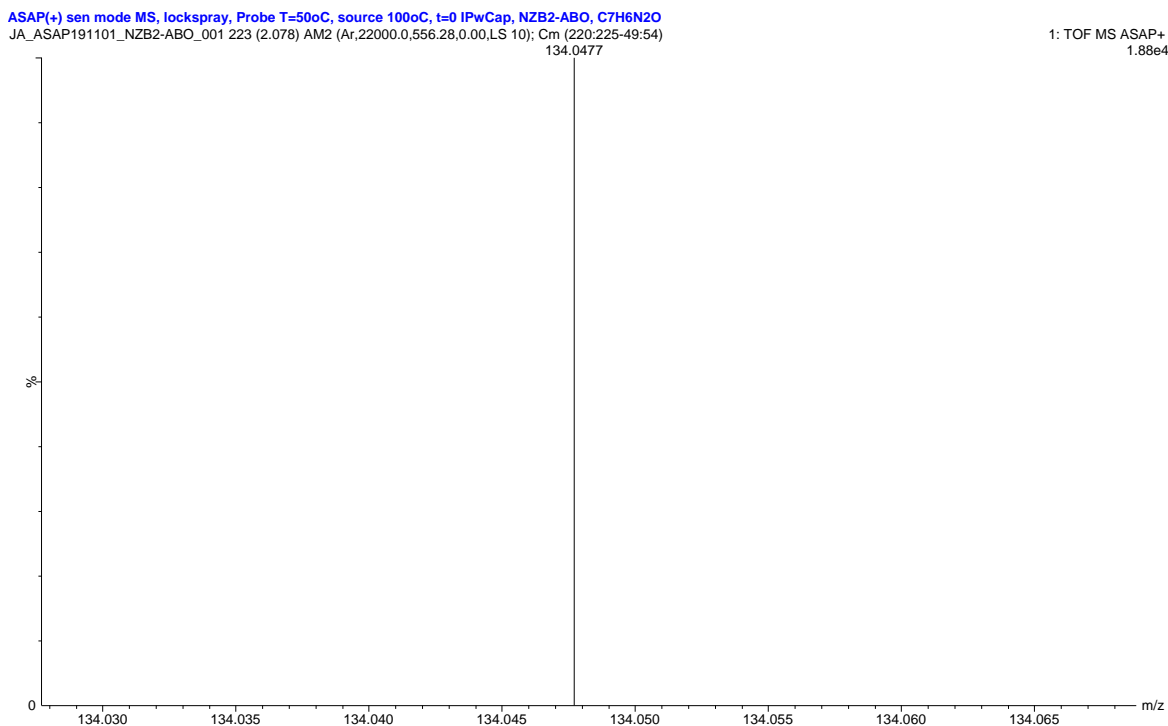


Figure 4-17, Expanded ASAP-MS spectrum of 2-ABO standard, from m/z 134.03 to 134.065

Figure 4-18 displays some of the plausible oligomers formed from resonance-contributors of 2-ABO radical shown in Appendix G. Different coupling positions such as C-C, N-N and N-C are expected which leads to the generation of different polymerization products. Notably, some of these oligomers could re-enter the SBP catalytic cycle hence contribute to the formation of higher oligomers.



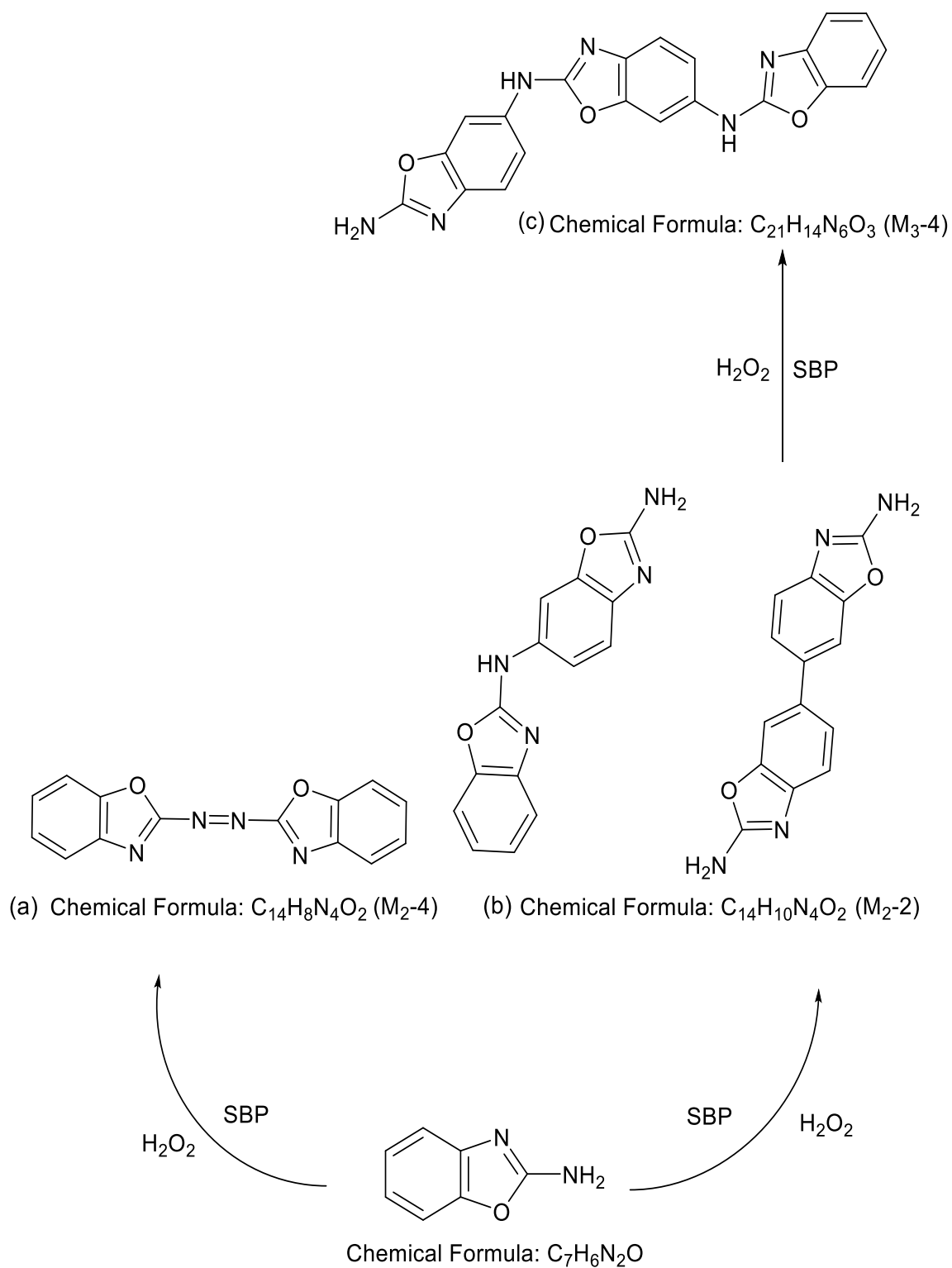


Figure 4-18, Some possible structures of oligomers formed during enzymatic treatment of 2-ABO

Mass spectral analysis of the product mixture after 3-hour enzymatic reaction of 2-ABO under optimum conditions (45% removal efficiency, analyzed by HPLC) was conducted. Figure 4-19 displays a full-scan spectrum of 2-ABO reaction mixture. With scan-expansion of spectrum, a base peak at  $m/z$  267.0893 which represents a protonated dimer with formula of  $[C_{14}H_{11}N_4O_2]$  ( $M_2H-2$ ), structure shown in Figure 4-18 (b), was observed as shown in Figure 4-20. Due to the low sensitivity and presence of other strong peaks near its  $^{13}C$ -isotope peak position, the isotope peak was not observed in the spectrum. Using the ESI method for mass spectral analysis of the reaction mixture, a peak at  $m/z$  267.0887 matches with protonated dimer with formula of  $[C_{14}H_{11}N_4O_2]$  was observed (shown in Figure 4-21) along with its  $^{13}C$ -isotope at  $m/z$  268.0916.

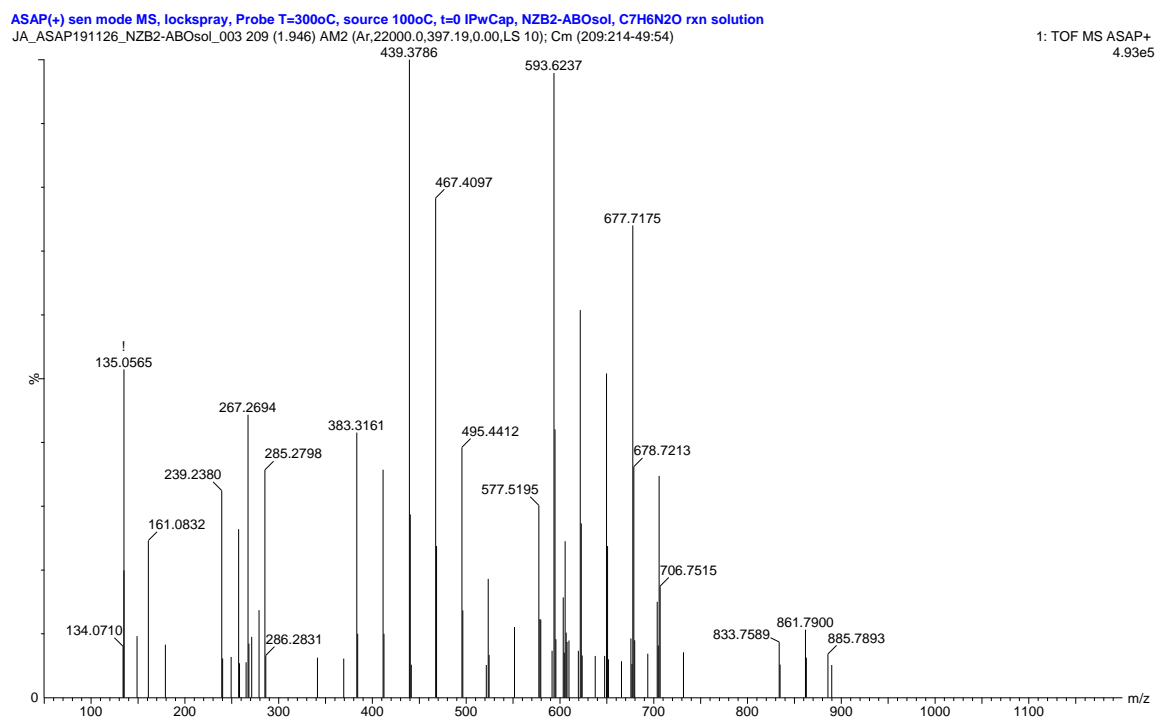


Figure 4-19, Full-scan ASAP-MS spectrum of 2-ABO reaction mixture.

Conditions: 0.10 mM 2-ABO, 10 mM phosphate buffer pH 6.0, 3.5 U/mL SBP, 0.25 mM  $H_2O_2$ , 3-h reaction

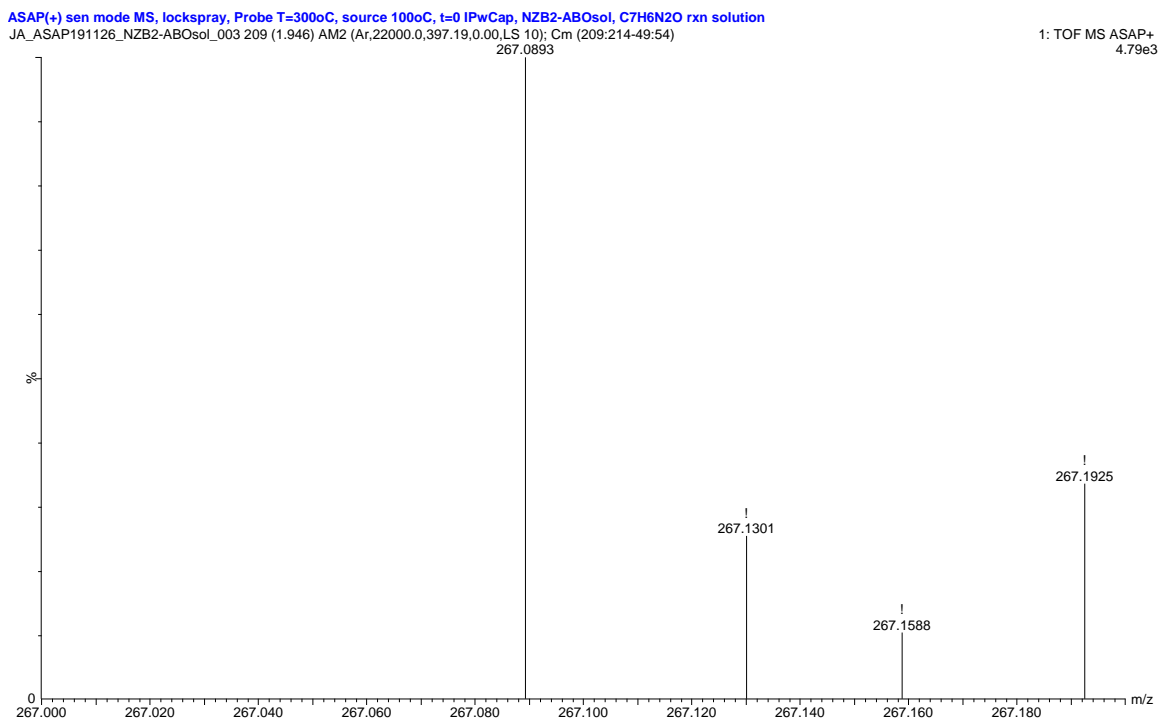


Figure 4-20, Expanded-scale ASAP-MS spectrum of 2-ABO reaction mixture from m/z 267 to 267.2

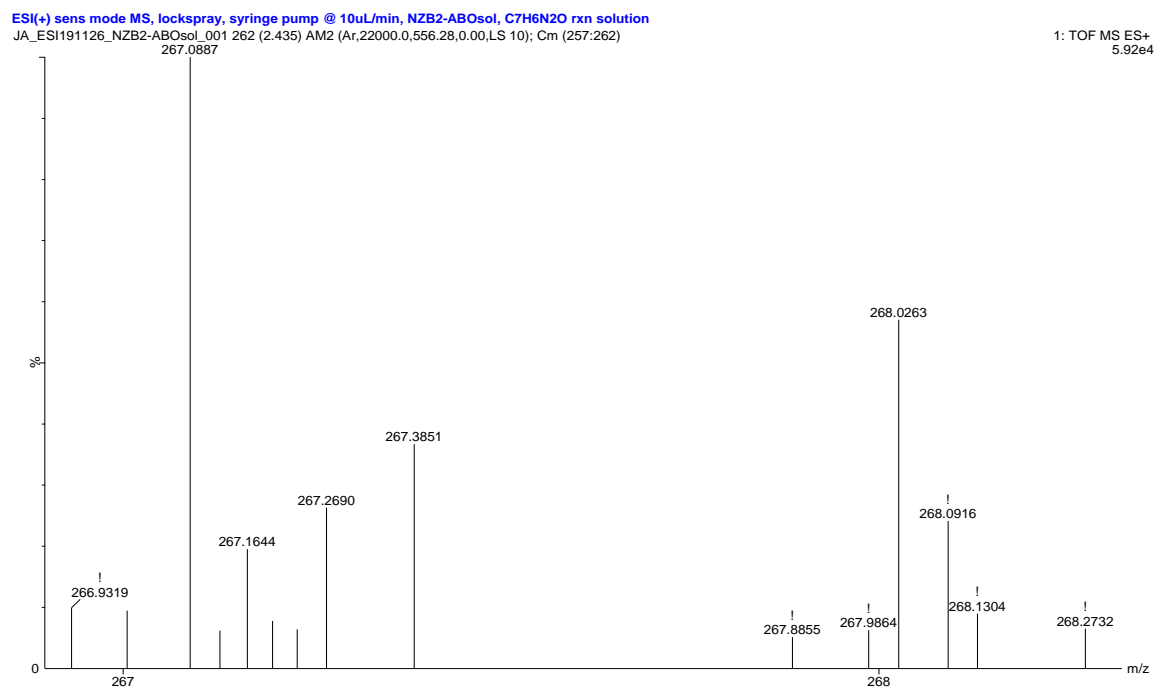


Figure 4-21, Expanded-scale ESI-MS spectrum of 2-ABO reaction mixture from m/z 266.8 to 268

In addition to dimers, a peak at m/z 399.1227 was observed in the ESI mass spectrum of optimal reaction mixture, shown in Figure 4-22, corresponded to the

protonated trimer with formula of  $[C_{21}H_{15}N_6O_3]$  ( $M_3H-4$ ) and probable structure shown in Figure 4-18 (c).

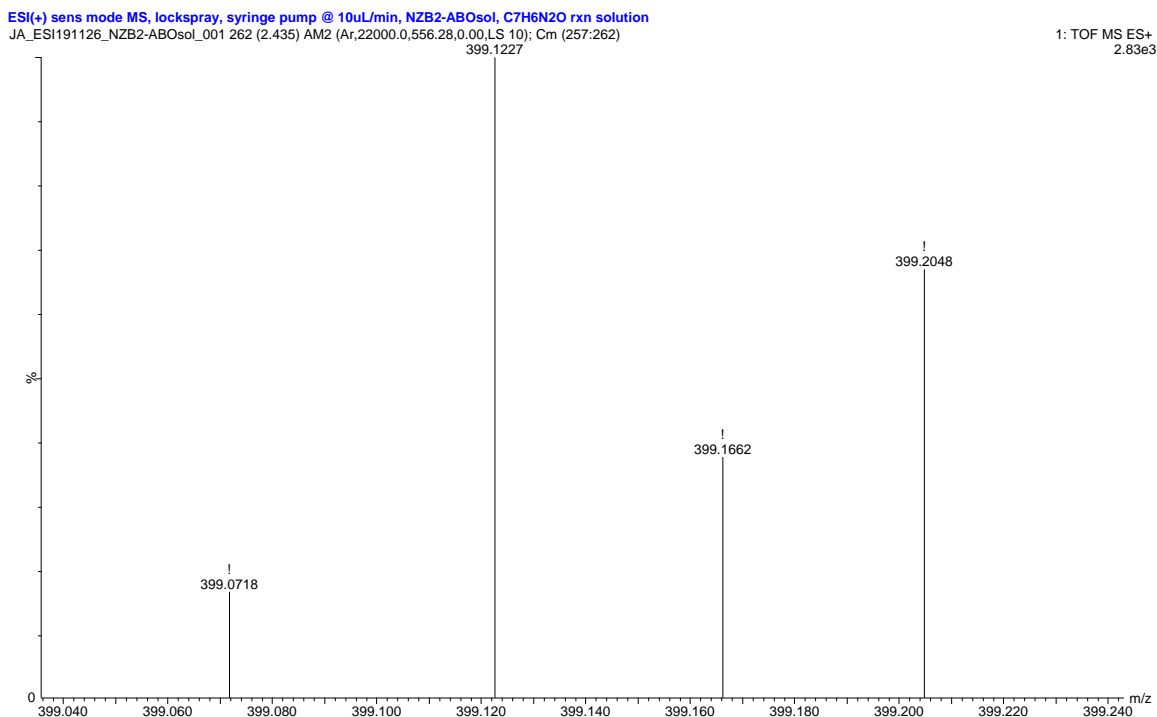


Figure 4-22, Expanded-scale ESI-MS spectrum of 2-ABO reaction mixture from m/z 399.04 to 399.240

Preliminary ASAP-MS analysis was conducted in un-optimized conditions (with respect to the reaction) but at higher temperature (350 °C) (un-published by Dherbecourt, Taylor and Biswas, 2019) and two different peaks with the exact masses matches with the dimers shown in Figure 4-18 (a) and (b) were observed. Figure 4-23 shows a base peak at m/z 267.0885 which represents a protonated oxidative dimer with formula of  $[C_{14}H_{11}N_4O_2]$  ( $M_2H-2$ ), Figure 4-18 (b) and its un-protonated dimer at m/z 266.0812. Also, Figure 4-24 displays a base peak at m/z 265.0727 matches with protonated oxidized oxidative dimer  $[C_{14}H_9N_4O_2]$  ( $M_2H-4$ ), Figure 4-18 (a). The fact this azo-dimer exists, implies N-N radical coupling to form the hydrazine which was subsequently oxidized under the reaction conditions (Mashhadi, 2019; Mukherjee, 2019). In addition to the dimers, a peak at m/z

399.1201 was observed (Figure 4-25), corresponded to the protonated trimer with formula of  $[C_{21}H_{15}N_6O_3]$  (M<sub>3</sub>H-4) and probable structure shown in Figure 4-18 (c).

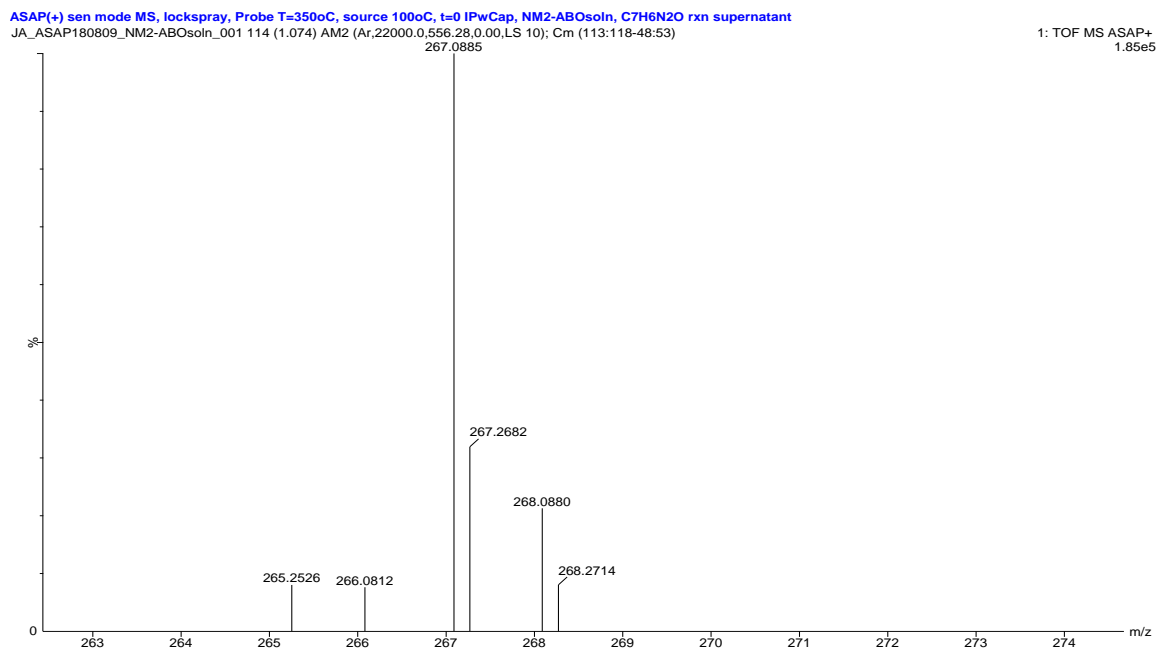


Figure 4-23, Expanded-scale preliminary ASAP-MS spectrum of 2-ABO reaction mixture from m/z 263 to 274; un-published data from Dherbecourt, Taylor and Biswas, 2019.

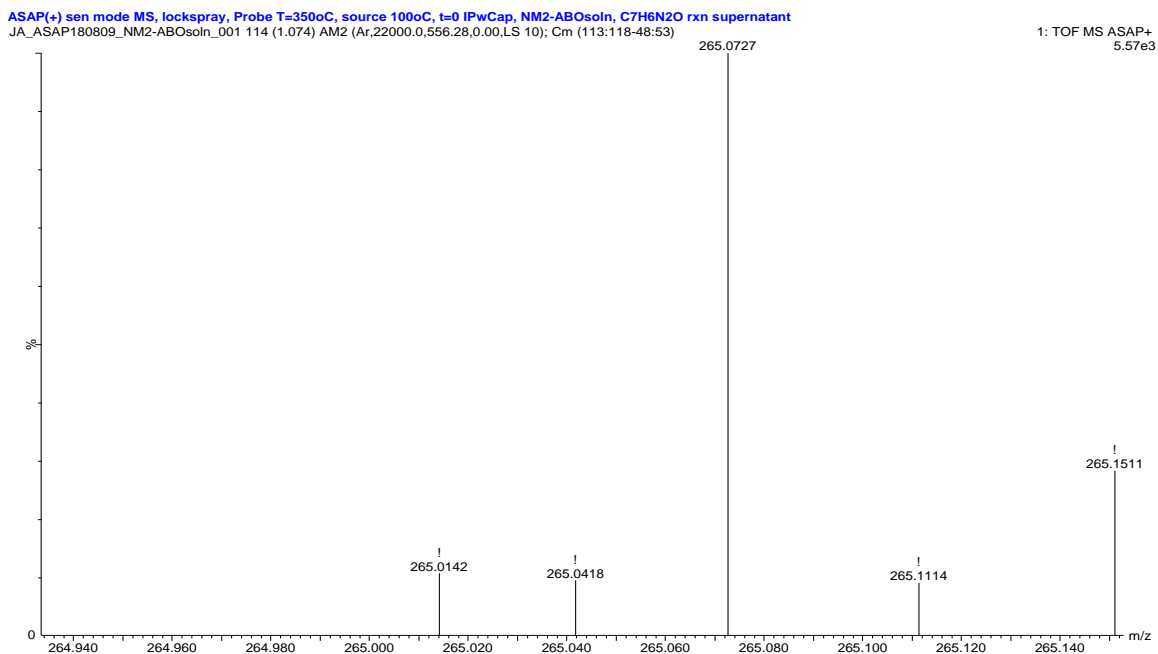


Figure 4-24, Expanded-scale preliminary ASAP-MS spectrum of 2-ABO reaction mixture from m/z 264.94 to 265.14; un-published data from Dherbecourt, Taylor and Biswas, 2019.

ASAP(+) sen mode MS, lockspray, Probe T=350oC, source 100oC, t=0 IPwCap, NM2-ABOsoln, C7H6N2O rxn supernatant  
JA\_ASAP180809\_NM2-ABOsoln\_002 109 (1.031) AM2 (Ar,22000.0,556.28,0.00,LS 10); Crn (107:112-49:54)

1: TOF MS ASAP+  
1.25e3

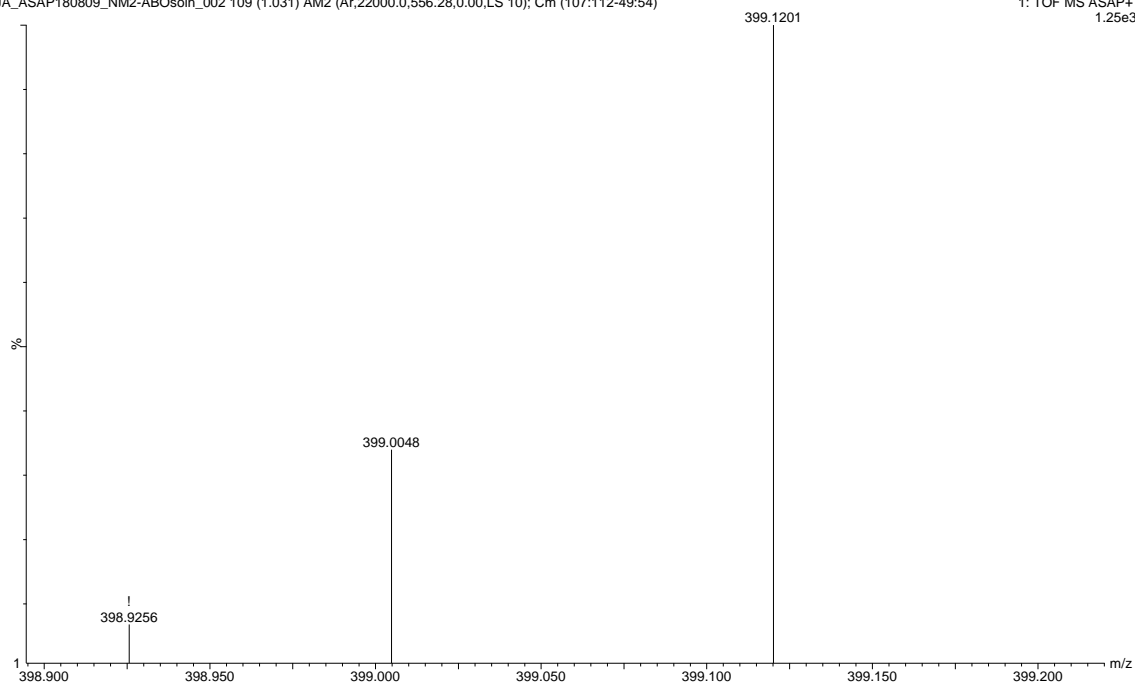


Figure 4-25, Expanded-scale preliminary ASAP-MS spectrum of 2-ABO reaction mixture from m/z 398.90 to 399.20; un-published data from Dherbecourt, Taylor and Biswas, 2019.

## CHAPTER 5

### SUMMARY AND CONCLUSIONS

#### *5.1. Summary*

In this thesis as the first objective, feasibility of treating selected heterocyclic aromatic compounds with soybean peroxidase in synthetic wastewater was studied. Preliminary experiments showed that 3-hydroxyxoumarin and 2-aminobenzoxazole are substrates for soybean peroxidase, while 3-amino-5-methylisoxazole is not. Secondly, the most important operation parameters (pH, SBP activity and  $\text{H}_2\text{O}_2$  concentration) were optimized with the goal of reaching >95% removal (only met for 3-HC) of the two compounds, Table 5-1. The pH optima were in neutral range, close to the operating pH range of wastewater (6.5 to 8.5) and close to the  $\text{pK}_a$  value for 3-HC. The minimum effective SBP activities were dramatically different, 8750-fold less for 3-HC than 2-ABO on a per mM basis. Both compounds showed an optimum  $\text{H}_2\text{O}_2$ -to-substrate molar ratio well in excess of the theoretical value (0.5) for radical formation, possibly due to the peroxide demand of higher oligomer formation and/or endogenous catalase activity of soybean peroxidase (the greater for 2-ABO which required so much SBP). Poor removal efficiency of 2-ABO was not improved by stepwise addition of  $\text{H}_2\text{O}_2$ . Thirdly, time course experiments under optimized conditions and fitting the initial stage of each progress curve to a first-order model (also in Table 5-1) yielded half-lives, 10-fold shorter for 3-HC as measured and 18,000-fold shorter once normalized for minimum effective enzyme activity.

Table 5-1, Optimized conditions for SBP-catalyzed removal for 3-HC and 2-ABO and initial first-order kinetics

Parameters	3-Hydroxycoumarin (0.5 mM)	2-Aminobenzoxazole (0.1 mM)
pH	7.0	6.0
SBP activity (U/mL)	0.002	3.5
H <sub>2</sub> O <sub>2</sub> concentration (mM)	0.75	0.25
Removal (%)	95	45
Rate constant, k (min <sup>-1</sup> )	0.056 ± 0.002	0.0054 ± 0.0002
Half-life (min)	12.4 ± 0.5	129 ± 4
Normalized half-life (min)	0.026 ± 0.0010	450 ± 15

Finally, enzymatic transformation products were analyzed by mass spectrometry after 3-h SBP-catalyzed treatment under optimized conditions. MS results are summarized in Table 5-2. For both compounds, the data show evidence of oxidative dimers and trimers, which would have formed by direct radical coupling. In addition, the Table shows evidence for subsequent oxidation (under the reaction conditions) of the dimers and trimers of 3-HC and the dimer of 2-ABO.

Table 5-2, Summary of MS results for standard and identified products of SBP-catalyzed process of 3-HC and 2-ABO

Compound		Symbols	Molecular formula	m/z*
3-HC	Standard	MH	C <sub>9</sub> H <sub>7</sub> O <sub>3</sub>	163.0393
		M	C <sub>9</sub> H <sub>6</sub> O <sub>3</sub>	162.0313
	Identified products	M <sub>2</sub> H-4	C <sub>18</sub> H <sub>9</sub> O <sub>6</sub>	321.0400
		M <sub>2</sub> H-2	C <sub>18</sub> H <sub>11</sub> O <sub>6</sub>	323.0545
		M <sub>3</sub> H-6	C <sub>27</sub> H <sub>13</sub> O <sub>9</sub>	481.0552
		M <sub>3</sub> H-4	C <sub>27</sub> H <sub>15</sub> O <sub>9</sub>	483.0715
2-ABO	Standard	MH	C <sub>7</sub> H <sub>7</sub> N <sub>2</sub> O	135.0557
		M	C <sub>7</sub> H <sub>6</sub> N <sub>2</sub> O	134.0477***



	M <sub>2</sub> H-2	C <sub>14</sub> H <sub>11</sub> N <sub>4</sub> O <sub>2</sub>	267.0887** and 267.0893***
Identified	M <sub>2</sub> -2	C <sub>14</sub> H <sub>10</sub> N <sub>4</sub> O <sub>2</sub>	266.0812***
products	M <sub>2</sub> H-4	C <sub>14</sub> H <sub>9</sub> N <sub>4</sub> O <sub>2</sub>	265.0727***
	M <sub>3</sub> H-4	C <sub>21</sub> H <sub>15</sub> N <sub>6</sub> O <sub>3</sub>	399.1227** and 399.1201***

\* All peaks, unless noted, were accompanied by a <sup>13</sup>C-isotopic peak one mass unit larger and of consistent relative height.

\*\*Data obtained using ESI method, including <sup>13</sup>C-isotope, all others by ASAP.

\*\*\* <sup>13</sup>C-isotopic peak obscured by other large peak nearby.

## 5.2. Conclusions

In conclusion, enzyme-catalyzed transformation of 3-HC, as a hypothetically emerging contaminant, using SBP extracted from soybean hulls can be a cost-effective and efficient alternative to conventional treatment methods for removal from wastewater. By contrast, 2-ABO had no more than 45% removal efficiency and then only with 8750-fold more SBP and enzymatic treatment would not be efficient for the removal of this compound. The only products detected were dimers and trimers, which provides valuable insights into the mechanism of product formation.

## CHAPTER 6

### FUTURE WORK

The results of this research confirm the potential of SBP to catalyze the removal of some heterocyclic aromatic compounds. Further studies are required before the implementation of this treatment in real wastewater.

1. A detailed study on the transformation products of these enzymatic treatments using other analytical techniques such as NMR and FTIR, to determine the structures of end-products more accurately.
2. Environmental fate and toxicity studies for the transformation products formed after the enzymatic treatment, hence, avoiding further possible contamination.
3. Additional research on sedimentation or filtration systems for the oligomers generated in the enzyme-catalyzed reactions, determining the settling characteristics and possible flocculants requirement.
4. Feasibility of enzymatic treatment of the studied heterocyclic aromatics in real wastewater, considering the matrix effect of wastewater and competition of other contaminants and multiple substrates in SBP-catalyzed reactions.
5. More study on the kinetic modeling of the enzyme-catalyzed reaction in order to estimate the reactor size and operation parameters.
6. Cost-benefit analysis of SBP-catalyzed treatment combined with a wastewater treatment plant to estimate cost of a full-scale application.

## BIBLIOGRAPHY

- Agriculture and Agri-Food Canada, (2020). Outlook for principle corps. Weblink: <http://www.agr.gc.ca/eng/crops/reports-and-statistics-data-for-canadian-principal-field-crops/canada-outlook-for-principal-field-crops-2019-19/?id=1577189965774#a3>. Accessed: Janurary 2020. Accessed: Janurary 2020.
- Al-Ansari, M. M., Saha, B., Mazloun, S., Taylor, K. E., Bewtra, J. K., & Biswas, N. (2011). Soybean peroxidase applications in wastewater treatment. In *Soybeans: Cultivation, Uses and Nutrition* (pp. 189–221). Hauppauge, N.Y.: Nova Science Publishers, Inc.
- Al-Ansari, M. M., Taylor, K. E., Bewtra, J. K., & Biswas, N. (2009). Soybean peroxidase-catalyzed removal of phenylenediamines and benzenediols from water. *Enzyme Microb. Technol.*, 45, 253–260. <https://doi.org/10.1016/j.enzmictec.2009.07.004>
- Al-maqdi, K. A., Hisaindee, S. M., Rauf, M. A., & Ashraf, S. S. (2017). Comparative degradation of a thiazole pollutant by an advanced oxidation process and an enzymatic approach. *Biomolecules*, 7(3), 64. <https://doi.org/10.3390/biom7030064>
- Almaqdi, K. A., Morsi, R., Alhayuti, B., Alharthi, F., & Ashraf, S. S. (2019). LC-MSMS based screening of emerging pollutant degradation by different peroxidases. *BMC Biotechnology*, 19(83), 1–16. <https://doi.org/https://doi.org/10.1186/s12896-019-0574-y>
- Alavi, S. J., Sadeghian, H., Seyedi, S. M., Salimi, A., & Eshghi, H. (2018). A novel class of human 15-LOX-1 inhibitors based on 3-hydroxycoumarin. *Chem. Biol. Drug Des.*, 91, 1125–1132. <https://doi.org/10.1111/cbdd.13174>
- Alharbi, S. K., Nghiem, L. D., Merwe, J. P. Van De, Frederic, D. L., Asif, M. B., Hai, F. I., & Price, W. E. (2019). Degradation of diclofenac, trimethoprim, carbamazepine, and sulfamethoxazole by laccase from *Trametes versicolor*: Transformation products and toxicity of treated effluent products and toxicity of treated effluent. *Biocatal. Biotransform.*, 37(6), 399–408. <https://doi.org/10.1080/10242422.2019.1580268>
- Alneyadi, A. H., Rauf, M. A., & Ashraf, S. S. (2018). Oxidoreductases for the remediation of organic pollutants in water – a critical review. *Crit. Rev. Biotechnol.*, 38(7), 971–988. <https://doi.org/10.1080/07388551.2017.1423275>
- Altahir, B. M., Feng, W., Jasim, H. H., Taylor, K. E., Biswas, N., Brwtra, J. K., & Jassim, S. A. A. (2016). Soybean peroxidase-catalysed removal of benzidines from water. *J. Environ. Eng. Sci.*, 10(JS4), 73–80. <https://doi.org/https://doi.org/10.1680/jenes.15.00018>
- Amin, K. M., Awadalla, F. M., Eissa, A. A. M., Abou-seri, S. M., & Hassan, G. S. (2011). Design, synthesis and vasorelaxant evaluation of novel coumarin –

- pyrimidine hybrids. *Bioorg. Med. Chem.*, 19(20), 6087–6097.  
<https://doi.org/10.1016/j.bmc.2011.08.037>
- Asimakopoulos, A. G., Ajibola, A., Kannan, K., & Thomaidis, N. S. (2013). Occurrence and removal efficiencies of benzotriazoles and benzothiazoles in a wastewater treatment plant in Greece. *Sci. Total Environ.*, 452–453, 163–171.  
<https://doi.org/10.1016/j.scitotenv.2013.02.041>
- Bailly, F., Maurin, C., Teissier, E., Vezin, H., & Cotellet, P. (2004). Antioxidant properties of 3-hydroxycoumarin derivatives. *Bioorg. Med. Chem.*, 12, 5611–5618.  
<https://doi.org/10.1016/j.bmc.2004.07.066>
- Bakr, S. M. A., El-Karim, S. S. A., Said, M. M., & Youns, M. M. (2016). Synthesis and anticancer evaluation of novel isoxazole / pyrazole derivatives. *Res. Chem. Intermed.*, 42(2), 1375–1387. <https://doi.org/10.1007/s11164-015-2091-5>
- Balaswamy, G., Srinivas, K., Pradeep, P., & Sarangapani, M. (2012). Synthesis, characterization and anti-microbial activity of novel substituted benzoxazole derivatives. *Int. J. Chem. Sci.*, 10(2), 619–626.
- Barrios-Estrada, C., Rostro-alanis, M. D. J., Muñoz-gutiérrez, B. D., Iqbal, M. N., Kannan, S., & Parra-saldívar, R. (2018). Emergent contaminants: Endocrine disruptors and their laccase-assisted degradation – A review. *Sci. Total Environ.*, 612, 1516–1531. <https://doi.org/10.1016/j.scitotenv.2017.09.013>
- Behera, S. K., Kim, H. W., Oh, J. E., & Park, H. S. (2011). Occurrence and removal of antibiotics, hormones and several other pharmaceuticals in wastewater treatment plants of the largest industrial city of Korea. *Sci. Total Environ.*, 409(20), 4351–4360. <https://doi.org/10.1016/j.scitotenv.2011.07.015>
- Belluti, F., Fontana, G., Dal, L., Carenini, N., Giommarelli, C., & Zunino, F. (2010). Design, synthesis and anticancer activities of stilbene-coumarin hybrid compounds: Identification of novel proapoptotic agents. *Bioorg. Med. Chem.*, 18(10), 3543–3550. <https://doi.org/10.1016/j.bmc.2010.03.069>
- Bilal, M., Rasheed, T., Iqbal, M. N., & Yan, Y. (2018). Peroxidases-assisted removal of environmentally-related hazardous pollutants with reference to the reaction mechanisms of industrial dyes. *Sci. Total Environ.*, 644, 1–13.  
<https://doi.org/10.1016/j.scitotenv.2018.06.274>
- Bilal, M., Rasheed, T., Nabeel, F., Iqbal, M. N., & Zhao, Y. (2019). Hazardous contaminants in the environment and their laccase-assisted degradation – A review. *J. Environ. Manage.*, 234, 253–264. <https://doi.org/10.1016/j.jenvman.2019.01.001>
- Bollag, J., Liu, S., & Minard, R. D. (1979). Asymmetric Diphenol Formation by a Fungal Laccase. *Appl. Environ. Microbiol.*, 38(1), 90–92.
- Brack, W., & Schirmer, K. (2003). Effect-directed identification of oxygen and sulfur heterocycles as major polycyclic aromatic cytochrome P4501A-inducers in a

- contaminated sediment. *Environ. Sci. Technol.*, 37(14), 3062–3070.  
<https://doi.org/10.1021/es020248j>
- Brinkmann, M., Blenkle, H., Salowsky, H., Bluhm, K., Schiwy, S., Tiehm, A., & Hollert, H. (2014). Genotoxicity of heterocyclic PAHs in the micronucleus assay with the fish liver cell line RTL-W1. *PLoS ONE*, 9(1).  
<https://doi.org/10.1371/journal.pone.0085692>
- Broughton, H. B., & Watson, I. A. (2005). Selection of heterocycles for drug design. *J. Mol. Graph. Model.*, 23, 51–58. <https://doi.org/10.1016/j.jmgm.2004.03.016>
- Cabana, H., Jiwan, J. H., Rozenberg, R., Elisashvili, V., Penninckx, M., Agathos, S. N., & Jones, J. P. (2007). Elimination of endocrine disrupting chemicals nonylphenol and bisphenol A and personal care product ingredient triclosan using enzyme preparation from the white rot fungus *Coriolopsis polyzona*. *Chemosphere*, 67, 770–778. <https://doi.org/10.1016/j.chemosphere.2006.10.037>
- Chang, K., Chen, H., Wang, T., Chen, I., Chen, Y., Yang, S., Chen, Y., Chang, H., Huang, C., Chang, J., Shih, C., Kuo, C., Tzeng, C. (2015). Novel oxime-bearing coumarin derivatives act as potent Nrf2 / ARE activators in vitro and in mouse model. *Eur. J. Med. Chem.*, 106, 60–74.  
<https://doi.org/10.1016/j.ejmech.2015.10.029>
- Chen, Z. F., & Ying, G. G. (2015). Occurrence, fate and ecological risk of five typical azole fungicides as therapeutic and personal care products in the environment: A review. *Environ. Int.*, 84, 142–153. <https://doi.org/10.1016/j.envint.2015.07.022>
- Chikhale, R., Thorat, S., Kumar, R., Gadewal, N., & Khedekar, P. (2018). Design, synthesis and anticancer studies of novel aminobenzazoly pyrimidines as tyrosine kinase inhibitors. *Bioorg. Chem.*, 77, 84–100.  
<https://doi.org/10.1016/j.bioorg.2018.01.008>
- Chikhale, R. V., Pant, A. M., Menghani, S. S., Wadibhasme, P. G., & Khedekar, P. B. (2017). Facile and efficient synthesis of benzoxazole derivatives using novel catalytic activity of PEG-SO<sub>3</sub>H. *Arab. J. Chem.*, 10(5), 715–725.  
<https://doi.org/10.1016/j.arabjc.2014.06.011>
- Chiong, T., Yon, S., Hong, Z., Yew, B., & Danquah, M. K. (2016). Enzymatic treatment of methyl orange dye in synthetic wastewater by plant-based peroxidase enzymes. *J. Environ. Chem. Eng.*, 4(2), 2500–2509. <https://doi.org/10.1016/j.jece.2016.04.030>
- Ćirić-Marjanović, G., Milojević-Rakić, M., Janošević-Ležaić, A., Luginbühl, S., & Walde, P. (2017). Enzymatic oligomerization and polymerization of arylamines : state of the art and perspectives. *Chem. Pap.* (2017), 71, 199–242.  
<https://doi.org/10.1007/s11696-016-0094-3>
- Cordova Villegas, L. G. (2017). *Enzymatic treatment of azo-dyes with soybean peroxidase*. PhD dissertation, University of Windsor, Ontario, Canada

- Cordova Villegas, L. G., Mashhadi, N., Chen, M., Mukherjee, D., Taylor, K. E., & Biswas, N. (2016). A Short review of techniques for phenol removal from wastewater. *Curr. Pollution Rep.*, 2, 157–167. <https://doi.org/10.1007/s40726-016-0035-3>
- Cordova Villegas, L. G., Mazloun, S., Taylor, K. E., & Biswas, N. (2018). Soybean peroxidase-catalyzed treatment of azo dyes with or without Fe<sup>o</sup> pretreatment. *Water Environ. Res.*, 90(8), 675–684. <https://doi.org/10.2175/106143017X15131012153149>
- Cui, M., Ono, M., Kimura, H., Ueda, M., Nakamoto, Y., Togashi, K., Okamoto, Y., Ihara, M., Takahashi, R., Liu, B., Saji, H. (2012). Novel 18 F-labeled benzoxazole derivatives as potential positron emission tomography probes for imaging of Cerebral  $\beta$ -Amyloid Plaques in alzheimer's disease. *J. Med. Chem.*, 55, 9136–9145. <https://doi.org/10.1021/jm300251n>
- de Andrade Gonçalves, P., dos Santos Junior, M. C., do Sacramento Sousa, C., Góes-Neto, A., Luz, E. D. M. N., Damaceno, V. O., Niella, A. R. R. Filho, J. M. B., de Assis, S. A. (2019). Study of sodium 3-hydroxycoumarin as inhibitors in vitro, in vivo and in silico of *Moniliophthora perniciosa* fungus. *Eur. J. Plant Pathol.*, 153, 15–27. <https://doi.org/https://doi.org/10.1007/s10658-018-1536-2> Study
- Demmer, C. S., & Bunch, L. (2015). Benzoxazoles and oxazolopyridines in medicinal chemistry studies. *Eur. J. Med. Chem.*, 97, 778–785. <https://doi.org/10.1016/j.ejmech.2014.11.064>
- Deng, X., Chai, X., Wei, C., & Fu, L. (2011). Rapid determination of quinoline and 2-hydroxyquinoline in quinoline biodegradation process by tri-wavelength UV/Vis spectroscopy. *Analytical Sciences*, 27(5), 493–497. <https://doi.org/10.2116/analsci.27.493>
- Detsi, A., Kontogiorgis, C., & Hadjipavlou-litina, D. (2017). Coumarin derivatives: an updated patent review. *EOTP*, 27(11), 1201–1226. <https://doi.org/10.1080/13543776.2017.1360284>
- Ding, H., Wu, Y., Zou, B., Lou, Q., Zhang, W., Zhong, J., Lu, L., Dai, G. (2016). Simultaneous removal and degradation characteristics of sulfonamide , tetracycline , and quinolone antibiotics by laccase-mediated oxidation coupled with soil adsorption. *J. Hazard. Mater.*, 307, 350–358. <https://doi.org/10.1016/j.jhazmat.2015.12.062>
- Dunwell, D. W., Evans, D., & Hicks, T. A. (1975). Synthesis and anti-inflammatory activity of some 2-heteroaryl-a-methyl-5-benzoxazoleacetic acids. *J. Med. Chem.*, 18(11), 1158–1159. <https://doi.org/10.1021/jm00245a026>
- Feldmannova, M., Hilscherova, K., Marsalek, B., & Blaha, L. (2006). Effects of N-Heterocyclic polyaromatic hydrocarbons on survival, reproduction, and biochemical parameters in *Daphnia magna*. *Environ. Toxicol.*, 425–431. <https://doi.org/10.1002/tox>

- Feng, W., Taylor, K. E., Biswas, N., & Bewtra, J. K. (2013). Soybean peroxidase trapped in product precipitate during phenol polymerization retains activity and may be recycled. *J. Chem. Technol. Biotechnol.*, 88(8), 1429–1435. <https://doi.org/10.1002/jctb.4075>
- Flock, C., Bassi, A., & Gijzen, M. (1999). Removal of aqueous phenol and 2-chlorophenol with purified soybean peroxidase and raw soybean hulls. *J. Chem. Technol. Biotechnol.*, 74, 303–309.
- Gacche, R. N., & Jadhav, S. G. (2012). Antioxidant activities and cytotoxicity of selected coumarin derivatives: preliminary results of a structure-activity relationship study using computational tools. *J. Exp. Clin. Med.*, 4(3), 165–169. <https://doi.org/10.1016/j.jecm.2012.04.007>
- Geng, Z., Rao, K. J., Bassi, A. S., Gijzen, M., & Krishnamoorthy, N. (2001). Investigation of biocatalytic properties of soybean seed hull peroxidase. *Catal.*, 64, 233–238. [https://doi.org/https://doi.org/10.1016/S0920-5861\(00\)00527-7](https://doi.org/https://doi.org/10.1016/S0920-5861(00)00527-7)
- Gomtsyan, A. (2012). Heterocycles in drug and drug discovery. *Chem. Heterocycl. Compd.*, 48(1), 7–10. <https://doi.org/10.1007/s10593-012-0960-z>
- Harmange, J., Weiss, M. M., Germain, J., Polverino, A. J., Borg, G., Bready, J., Chen, D., Choquette, D., Coxon, A., DeMelfi, T., DiPietro, L., Doerr, N., Estrada, J., Flynn, J., Graceffa, R. F., Harriman, S. P., Kaufman, S., La, D. S., Long, A., Martin, M. W., Neervannan, S., Patel, V. F., Potashman, M., Regal, K., Roveto, P. M., Scharg, M. L., Starnes, C., Tasker, A., Teffera, Y., Wang, L., White, R. D., Whittington, A., Zanon, R. (2008). Naphthamides as novel and potent vascular endothelial growth factor receptor tyrosine kinase inhibitors: design, synthesis, and evaluation. *J. Med. Chem.*, 51, 1649–1667.
- Henriksen, A., Mirza, O., Indiani, C., Teilum, K., Smulevich, G., Welinder, K. G., & Gajhede, M. (2001). Structure of soybean seed coat peroxidase: A plant peroxidase with unusual stability and haem-apoprotein interactions. *Protein Sci.*, 10, 108–115. <https://doi.org/10.1110/ps.37301.108>
- Hiwarkar, A. D., Srivastava, V. C., & Mall, I. D. (2015). Comparative studies on adsorptive removal of indole by granular activated carbon and bagasse fly ash. *Environ. Prog. Sustain. Energy*, 35(3), 809–814. <https://doi.org/10.1002/ep>
- Hohmann, C., Schneider, K., Bruntner, C., Irran, E., Nicholson, G., Bull, A. T., Jones, A. L., Brown, R., Stach, J. E. M., Goodfellow, M., Winfried, B., Krämer, M., Imhoff, J. F., Süßmuth, R. D., Fiedler, H. (2009). Caboxamycin, a new antibiotic of the benzoxazole family produced by the deep-sea strain *Streptomyces* sp. NTK 937. *J. Antibiot.*, 62(48), 99–104. <https://doi.org/10.1038/ja.2008.24>
- Hsu, Y. M., Harner, T., Li, H., & Fellin, P. (2015). PAH measurements in air in the Athabasca oil sands region. *Environ. Sci. Technol.*, 49(9), 5584–5592. <https://doi.org/10.1021/acs.est.5b00178>

- Jun, L. Y., Yon, L. S., Mubarak, N. M., Bing, C. H., Pan, S., Danquah, M. K., Abdullah, E. C., Khalid, M. (2019). An overview of immobilized enzyme technologies for dye and phenolic removal from wastewater. *J. Environ. Chem. Eng.*, 7(2), 102961. <https://doi.org/10.1016/j.jece.2019.102961>
- Jyothi, M., & Merugu, R. (2013). Antibacterial and antifungal activity of some newly substituted benzoxazoles. *Int. J. Chem. Tech. Res.*, 5(5), 2425–2428.
- Kamal, A., Reddy, K. S., Khan, M. N. A., Shetti, R. V. C. R. N. C., Ramaiah, M. J., Pushpavalli, S. N. C. V. L., Srinivas, C., Pal-Bhadra, M., Chourasia, M., Sastry Narahari, G., Juvekar, A., Zingde, S., Barkume, M., (2010). Synthesis, DNA-binding ability and anticancer activity of benzothiazole /benzoxazole – pyrrolo [2,1-c][ 1, 4] benzodiazepine conjugates. *Bioorg. Med. Chem.*, 18(13), 4747–4761. <https://doi.org/10.1016/j.bmc.2010.05.007>
- Kamal, J. K. A., & Behere, D. V. (2003). Activity, stability and conformational flexibility of seed coat soybean peroxidase. *J. Inorg. Biochem.*, 94, 236–242. [https://doi.org/https://doi.org/10.1016/S0162-0134\(03\)00004-7](https://doi.org/https://doi.org/10.1016/S0162-0134(03)00004-7)
- Karam, J., & Nicell, J. A. (1997). Potential applications of enzymes in waste treatment. *J. Chem. Technol. Biotechnol.*, 50, 141–153.
- Khatik, G. L., Dube, N., Pal, A., & Nair, V. A. (2011). Highly efficient one-pot synthesis of 2-aminobenzoxazoles using triflic acid as a cyclodesulfurizing reagent. *Synth. Commun.*, 41, 2631–2639. <https://doi.org/10.1080/00397911.2010.515337>
- Kim, H. Y., Kim, T., Cha, S. M., & Yu, S. (2017). Degradation of sulfamethoxazole by ionizing radiation: Identification and characterization of radiolytic products. *Chem. Eng. J.*, 313, 556–566. <https://doi.org/10.1016/j.cej.2016.12.080>
- Klibanov, A.M., Alberti, B. N., Morris, E. D., & Felshin, L. M. (1980). Enzymatic removal of toxic phenols and anilines from waste waters. *J. Appl. Biochem.*, 2(5), 414–421.
- Klibanov, A. M., Tu, T.-M., & Scott, K. P. (1983). Peroxidase-Catalyzed Removal of Phenols from Coal-Conversion Waste Waters. *Science*, 221(4607), 259–261.
- Kong, L., Kadokami, K., Wang, S., Duong, H. T., & Chau, H. T. C. (2015). Monitoring of 1300 organic micro-pollutants in surface waters from Tianjin, North China. *Chemosphere*, 122, 125–130. <https://doi.org/10.1016/j.chemosphere.2014.11.025>
- Kosjek, T., Perko, S., Zupanc, M., Zanoški Hren, M., Landeka Dragičević, T., Žigon, D., Kompare, B., Heath, E. (2012). Environmental occurrence, fate and transformation of benzodiazepines in water treatment. *Water Res.*, 46(2), 355–368. <https://doi.org/10.1016/j.watres.2011.10.056>
- Lafi, W. K., Shannak, B., Al-Shannag, M., Al-Anber, Z., & Al-Hasan, M. (2009). Treatment of olive mill wastewater by combined advanced oxidation and biodegradation. *Sep. Purif. Technol.*, 70, 141–146.



<https://doi.org/10.1016/j.seppur.2009.09.008>

- Leyva, E., Montalvo, C., Moctezuma, E., & Leyva, S. (2008). Photocatalytic degradation of pyridine in water solution using ZnO as an alternative catalyst to TiO<sub>2</sub>. *J. Ceram. Process Res.*, 9(5), 455–462.
- Lin, Q., & Jianlong, W. (2010). Biodegradation characteristics of quinoline by *Pseudomonas putida*. *Bioresource Technology*, 101(19), 7683–7686. <https://doi.org/10.1016/j.biortech.2010.05.026>
- Liu, Y. S., Ying, G. G., Shareef, A., & Kookana, R. S. (2012). Occurrence and removal of benzotriazoles and ultraviolet filters in a municipal wastewater treatment plant. *Environ. Pollut.*, 165, 225–232. <https://doi.org/10.1016/j.envpol.2011.10.009>
- Manzano, C. A., Marvin, C., Muir, D., Harner, T., Martin, J., & Zhang, Y. (2017). Heterocyclic aromatics in petroleum coke, snow, lake sediments and air samples from the Athabasca oil sands region. *Environ. Sci. Technol.*, 51(10), 5445–5453. <https://doi.org/10.1021/acs.est.7b01345>
- Martini, J., Orge, C. A., Faria, J. L., & Pereira, M. F. R. (2018). Sulfamethoxazole degradation by combination of advanced oxidation processes. *J. Environ. Chem. Eng.*, 6, 4054–4060. <https://doi.org/10.1016/j.jece.2018.05.047>
- Martins, P., Jesus, J., Santos, S., Raposo, L. R., Roma-Rodrigues, C., Baptista, P. V., & Fernandes, A. R. (2015). Heterocyclic anticancer compounds: Recent advances and the paradigm shift towards the use of nanomedicine's tool Box. *Molecules*, 20(9), 16852–16891. <https://doi.org/10.3390/molecules200916852>
- Maruthamuthu, Rajam, S., P, C. R. S., G, B. D. A., & Ranjith, R. (2016). The chemistry and biological significance of imidazole, benzimidazole, benzoxazole, tetrazole and quinazolinone nucleus. *J. Chem. Pharm. Res.*, 8(5), 505–526.
- Mashhadi, N. (2019). Oxidative polymerization of heterocyclic aromatics using soybean peroxidase for treatment of wastewater. PhD dissertation, University of Windsor, Ontario, Canada
- Mashhadi, N., Taylor, K. E., Biswas, N., Meister, P., & Gauld, J. W. (2019a). Oligomerization of 3-substituted quinolines by catalytic activity of soybean peroxidase as a wastewater treatment . Product formation and computational studies. *Chem. Eng. J.*, 364, 340–348. <https://doi.org/10.1016/j.cej.2019.01.184>
- Mashhadi, N., Taylor, K. E., Jimenez, N., Varghese, S. T., Levi, Y., Lonergan, C., Lebeau, e., Lamé, M., Lard, E., Biswas, N., (2019b). Removal of selected pharmaceuticals and personal care products from wastewater using soybean peroxidase. *J. Environ. Manage.*, 63(3), 408–415. <https://doi.org/10.1007/s00267-018-01132-9>
- McNaught, A. D., & Wilkinson, A. (2014). *IUPAC Compendium of Chemical Terminology- the Gold Book* (2.3.3). <https://doi.org/10.1002/9783527626854.ch7>

- Miao, X. S., Bishay, F., Chen, M., & Metcalfe, C. D. (2004). Occurrence of antimicrobials in the final effluents of wastewater treatment plants in Canada. *Environ. Sci. Technol.*, 38(13), 3533–3541. <https://doi.org/10.1021/es030653q>
- Morsi, R., Bilal, M., Iqbal, M. N., & Ashraf, S. S. (2020). Laccases and peroxidases: The smart, greener and futuristic biocatalytic tools to mitigate recalcitrant emerging pollutants. *Sci. Total Environ.*, 714, 136572. <https://doi.org/10.1016/j.scitotenv.2020.136572>
- Mukherjee, D. (2019). Treatment of aqueous arylamine contaminants by enzyme-catalyzed oxidative polymerization. PhD dissertation, University of Windsor, Ontario, Canada
- Mukherjee, D., Taylor, K. E., & Biswas, N. (2018). Soybean peroxidase-induced treatment of dye-derived arylamines in water. *Water Air Soil Pollut.*, 8, 229–283. <https://doi.org/10.1007/s11270-018-3936-5>
- Mulla, S. I., Hu, A., Sun, Q., Li, J., Ashfaq, M., & Yu, C. (2018). Biodegradation of sulfamethoxazole in bacteria from three different origins. *J. Environ. Manage.*, 206, 93–102. <https://doi.org/10.1016/j.jenvman.2017.10.029>
- Ncanana, S., & Burton, S. (2007). Oxidation of 8-hydroxyquinoline catalyzed by laccase from *Trametes pubescens* yields an antioxidant aromatic polymer. *J. Mol. Catal. B-Enzym.*, 44, 66–71. <https://doi.org/10.1016/j.molcatb.2006.09.005>
- Nguyen, L. N., Hai, F. I., Price, W. E., Kang, J., Leusch, F. D. L., Roddick, F., Merwe, J. P., Magram, S. F., Nghiem, L. D. (2015). Degradation of a broad spectrum of trace organic contaminants by an enzymatic membrane reactor : Complementary role of membrane retention and enzymatic degradation. *Int. Biodeterior. Biodegradation.*, 99, 115–122. <https://doi.org/10.1016/j.ibiod.2014.12.004>
- Noguera-Oviedo, K., & Aga, D. S. (2016). Lessons learned from more than two decades of research on emerging contaminants in the environment. *J. Hazard. Mater.*, 316, 242–251. <https://doi.org/10.1016/j.jhazmat.2016.04.058>
- Nowak, P. M., Wozniakiewicz, M., Piwowarska, M., & Koscielniak, P. (2016). Determination of acid dissociation constant of 20 coumarin derivatives by capillary electrophoresis using the amine capillary and two different methodologies. *J. Chromatogr.*, 1446, 149–157. <https://doi.org/10.1016/j.chroma.2016.03.084>
- Padoley, K. V., Mudliar, S. N., & Pandey, R. A. (2008). Heterocyclic nitrogenous pollutants in the environment and their treatment options - An overview. *Bioresour. Technol.*, 99(10), 4029–4043. <https://doi.org/10.1016/j.biortech.2007.01.047>
- Pandey, V. P., Awasthi, M., Singh, S., Tiwari, S., & Dwivedi, U. N. (2017). A comprehensive review on function and application of plant peroxidases. *Biochem Anal Biochem*, 6(1), 1–16. <https://doi.org/10.4172/2161-1009.1000308>
- Parsiavash, L., Saboora, A., & Moosavi Nejad, S. Z. (2015). Investigating on the stability

- of peroxidase extracted from soybean (glycine max var. williams) and effects of Na<sup>+</sup> and K<sup>+</sup> ions on its activity. *J. Cell Mol. Res.*, 7(2), 94–101.  
<https://doi.org/https://doi.org/10.22067/jcmr.v7i2.43716>
- Patapas, J., Al-Ansari, M. M., Taylor, K. E., Bewtra, J. K., & Biswas, N. (2007). Removal of dinitrotoluenes from water via reduction with iron and peroxidase-catalyzed oxidative polymerization: A comparison between *Arthromyces ramosus* peroxidase and soybean peroxidase. *Chemosphere*, 67, 1485–1491.  
<https://doi.org/10.1016/j.chemosphere.2006.12.040>
- Paul, S., Bhattacharyya, P., & Das, A. R. (2011). One-pot synthesis of dihydropyrano [2,3- c] chromenes via a three component coupling of aromatic aldehydes, malononitrile, and 3-hydroxycoumarin catalyzed by nano-structured ZnO in water: a green protocol. *Tetrahedron Lett.*, 52(36), 4636–4641.  
<https://doi.org/10.1016/j.tetlet.2011.06.101>
- Potashman, M. H., Bready, J., Coxon, A., Demelfi, T. M., Dipietro, L., Doerr, N., Elbaum, D., Estrada, j., Gallant, P., Germain, J., Gu, Y., Harmanage, J. C., Kaufman, S. A., Kendall, r., Kim, J. L., Kumar, G. N., Long, A. M., Neervannan, S., Patel, V. F., Polverino, A., Rose, P. Plas, S., Whittington, D., Zanon, R., Zhao, H. (2007). Design, synthesis, and evaluation of orally active benzimidazoles and benzoxazoles as vascular endothelial growth factor-2 receptor tyrosine kinase inhibitors. *J. Med. Chem.*, 50, 4351–4373. <https://doi.org/10.1021/jm070034i>
- Reineke, A. K., Göen, T., Preiss, A., & Hollender, J. (2007). Quinoline and derivatives at a tar oil contaminated site: Hydroxylated products as indicator for natural attenuation? *Environ. Sci. Technol.*, 41(15), 5314–5322.  
<https://doi.org/10.1021/es070405k>
- Richardson, S. D., & Ternes, T. A. (2018). Water Analysis: Emerging Contaminants and Current Issues. *Analytical Chemistry*, 90(1), 398–428.  
<https://doi.org/10.1021/acs.analchem.7b04577>
- Rivera-Utrilla, J., Sánchez-Polo, M., Ferro-García, M. Á., Prados-Joya, G., & Ocampo-Pérez, R. (2013). Pharmaceuticals as emerging contaminants and their removal from water. A review. *Chemosphere*, 93(7), 1268–1287.  
<https://doi.org/10.1016/j.chemosphere.2013.07.059>
- Rosal, R., Rodríguez, A., Perdigón-Melón, J. A., Petre, A., García-Calvo, E., Gómez, M. J., Aguera, a., Fernández-Alba, A. R. (2010). Occurrence of emerging pollutants in urban wastewater and their removal through biological treatment followed by ozonation. *Water Res.*, 44(2), 578–588. <https://doi.org/10.1016/j.watres.2009.07.004>
- Ryan, B. J., Carolan, N., & Ofagain, C. (2006). Horseradish and soybean peroxidases: comparable tools for alternative niches ? *Trends Biotechnol.*, 24(8), 355–363.  
<https://doi.org/10.1016/j.tibtech.2006.06.007>
- Salam, L. B., Ilori, M. O., & Amund, O. O. (2017). Properties, environmental fate and biodegradation of carbazole. *3 Biotech*, 7(2), 1–14. <https://doi.org/10.1007/s13205->

- Schlich, M., Fornasier, M., Nieddu, M., Sinico, C., Murgia, S., & Rescigno, A. (2018). 3-hydroxycoumarin loaded vesicles for recombinant human tyrosinase inhibition in topical applications. *Colloids Surf. B*, 171, 675–681. <https://doi.org/10.1016/j.colsurfb.2018.08.008>
- Schuster, J. K., Harner, T., Su, K., Mihele, C., & Eng, A. (2015). First results from the oil sands passive air monitoring network for polycyclic aromatic compounds. *Environ Sci Technol*, 49(5), 2991–2998. <https://doi.org/10.1021/es505684e>
- Seenaiiah, D., Rekha, T., Padmaja, A., & Padmavathi, V. (2017). Synthesis and antimicrobial activity of pyrimidinyl bis (benzazoles). *Med. Chem. Res.*, 26, 431–441. <https://doi.org/10.1007/s00044-016-1758-9>
- Shen, Q., Shao, J., Peng, Q., Zhang, W., Ma, L., Chan, A. S. C., & Gu, L. (2010). Hydroxycoumarin derivatives: novel and potent  $\alpha$ -glucosidase inhibitors. *J. Med. Chem.*, 53, 8252–8259. <https://doi.org/10.1021/jm100757r>
- Shi, J., Han, Y., Xu, C., & Han, H. (2019). Anaerobic bioaugmentation hydrolysis of selected nitrogen heterocyclic compound in coal gasification wastewater. *Bioresour. Technol.*, 278, 223–230. <https://doi.org/10.1016/j.biortech.2018.12.113>
- Siemers, A. K., Palm, W. U., Faubel, C., Mänz, J. S., Steffen, D., & Ruck, W. (2017). Sources of nitrogen heterocyclic PAHs (N-HETs) along a riverine course. *Sci. Total Environ.*, 590–591, 69–79. <https://doi.org/10.1016/j.scitotenv.2017.03.036>
- Singh, S., Veeraswamy, G., Bhattarai, D., Goo, J., & Lee, K. (2015). Recent advances in the development of pharmacologically active compounds that contain a benzoxazole scaffold. *Asian J. Org. Chem.*, 4, 1338–1361. <https://doi.org/10.1002/ajoc.201500235>
- Slachtova, V., & Brulikova, L. (2018). Benzoxazole derivatives as promising antitubercular agents. *ChemistrySelect*, 3, 4653–4662. <https://doi.org/10.1002/slct.201800631>
- Šlachtova, V., Chasak, J., & Brulikova, L. (2019). Synthesis of various 2 - aminobenzoxazoles: the study of cyclization and smiles rearrangement. *ACS*, 4, 19314–19323. <https://doi.org/10.1021/acsomega.9b02702>
- Sommer, P. S. M., Almeida, R. C., Schneider, K., Beil, W., Süßmuth, R. D., & Fiedler, H. (2008). Nataxazole, a new benzoxazole derivative with antitumor activity produced by streptomyces sp. Tü 6176. *J. Antibiot.*, 61(11), 683–686.
- Souza, B. M., Marinho, B. A., Moreira, F. C., Dezotti, M. W. C., Boaventura, R. A. R., & Vilar, V. J. P. (2017). Photo-Fenton oxidation of 3-amino-5-methylisoxazole: a by-product from biological breakdown of some pharmaceutical compounds. *Environ. Sci. Pollut. Res.*, 24, 6195–6204. <https://doi.org/10.1007/s11356-015-5690-1>
- Stasinakis, A. S., Thomaidis, N. S., Arvaniti, O. S., Asimakopoulos, A. G., Samaras, V.

- G., Ajibola, A., ... Lekkas, T. D. (2013). Contribution of primary and secondary treatment on the removal of benzothiazoles, benzotriazoles, endocrine disruptors, pharmaceuticals and perfluorinated compounds in a sewage treatment plant. *Sci. Total Environ.*, 463–464, 1067–1075.  
<https://doi.org/10.1016/j.scitotenv.2013.06.087>
- Steevensz, A., Al-Ansari, M. M., Taylor, K. E., Bewtra, J. K., & Biswas, N. (2009). Comparison of soybean peroxidase with laccase in the removal of phenol from synthetic and refinery wastewater samples. *J Chem. Technol. Biotechnol.*, 84, 761–769. <https://doi.org/10.1002/jctb.2109>
- Steevensz, A., Cordova Villegas, L. G., Feng, W., Biswas, N., & Taylor, K. E. (2014b). Soybean peroxidase for industrial wastewater treatment : a mini review. *Environ. Eng. Sci.*, 9(3), 181–186. <https://doi.org/10.1680/jees.13.00013>
- Steevensz, A., Madur, S., Al-ansari, M. M., Taylor, K. E., Bewtra, J. K., & Biswas, N. (2013). A simple lab-scale extraction of soybean hull peroxidase shows wide variation among cultivars. *Ind. Crops. Prod.*, 48, 13–18.  
<https://doi.org/10.1016/j.indcrop.2013.03.030>
- Steevensz, A., Madur, S., Feng, W., Taylor, K. E., Bewtra, J. K., & Biswas, N. (2014a). Crude soybean hull peroxidase treatment of phenol in synthetic and real wastewater : Enzyme economy enhanced by Triton X-100. *Enzyme Microb. Technol.*, 55, 65–71.  
<https://doi.org/10.1016/j.enzmictec.2013.12.005>
- Sysak, A., & Obminska-Mrukowics, B. (2017). Isoxazole ring as a useful scaffold in a search for new therapeutic agents. *Eur. J. Med. Chem.*, 137, 292–309.  
<https://doi.org/10.1016/j.ejmech.2017.06.002>
- Urrea, D. A. M., Haure, P. M., Einschlag, F. S. G., & Contreras, E. M. (2018). Horseradish peroxidase-mediated decolourization of Orange II : modelling hydrogen peroxide utilization efficiency at different pH values. *Environ. Sci .Pollut. Res.*, 25, 19989–20002. <https://doi.org/https://doi.org/10.1007/s11356-018-2134-8>
- Valderrama, B., Ayala, M., & Vazquez-duhalt, R. (2002). Suicide inactivation of peroxidases and the challenge of engineering more robust enzymes. *Chem. Biol.*, 9(02), 555–565. [https://doi.org/https://doi.org/10.1016/s1074-5521\(02\)00149-7](https://doi.org/https://doi.org/10.1016/s1074-5521(02)00149-7)
- Vitaku, E., Smith, D. T., & Njardarson, J. T. (2014). Analysis of the structural diversity, substitution patterns, and frequency of nitrogen heterocycles among U.S. FDA approved pharmaceuticals. *J. Med. Chem.*, 57(24), 10257–10274.  
<https://doi.org/10.1021/jm501100b>
- Wang, Lei, Asimakopoulos, A. G., & Kannan, K. (2015). Accumulation of 19 environmental phenolic and xenobiotic heterocyclic aromatic compounds in human adipose tissue. *J. Environ. Int.*, 78, 45–50.  
<https://doi.org/10.1016/j.envint.2015.02.015>
- Wang, Lei, Zhang, J., Sun, H., & Zhou, Q. (2016). Widespread occurrence of

- benzotriazoles and benzothiazoles in tap water: influencing factors and contribution to human exposure. *Environ. Sci. Technol.*, 50(5), 2709–2717.  
<https://doi.org/10.1021/acs.est.5b06093>
- Wang, Lu, Liu, Y., Ma, J., & Zhao, F. (2016). Rapid degradation of sulphamethoxazole and the further transformation of 3-amino-5-methylisoxazole in a microbial fuel cell. *Water Res.*, 88, 322–328. <https://doi.org/10.1016/j.watres.2015.10.030>
- Wang, Y., Xu, H., Feng, L., Shen, X., Wang, C., Huo, X., Tian, X., Ning, j., Zhang, B., Sun, C., Deng, S. (2019). Oxidative coupling of coumarins catalyzed by laccase. *Int. J. Biol. Macromol.*, 135, 1028–1033. <https://doi.org/10.1016/j.ijbiomac.2019.05.215>
- Zhang, X. (2019). *Enzymatic treatment of selected pesticides in aqueous system*. M.Sc thesis, University of Windsor, Ontratio, Canada.
- Zhang, Z., Zhou, L., Zhao, S., Deng, H., & Deng, Q. (2006). 3-Hydroxycoumarin as a new matrix for matrix-assisted laser desorption/ionization time-of-flight mass spectrometry of DNA. *J. Am Soc. Mass Spectrom.*, 17, 1665–1668.  
<https://doi.org/10.1016/j.jasms.2006.07.010>

## APPENDICES

### *Appendix A. Preparation of SBP and catalase stock solutions*

#### **SBP stock solution**

Distilled water (100 mL) was added to 1.4 g of solid powder of crude SBP. The mixture was stirred overnight using magnetic stirrers. This mixture was then centrifuged at 4000 rpm for 20-25 minutes and the supernatant was separated and stored at 4 °C for future use.

#### **Catalase stock solution**

Solid bovine liver catalase (0.5 g) was dissolved in 100 mL of distilled water (99500 U/mL in this stock). The solution was stirred for around 3 hours using a magnetic stirrer and stirrer plate and then stored at 4 °C for future use.

### *Appendix B. SBP activity assay*

To measure the activity of soybean peroxidase, a colorimetric assay was used prior to each set of experiment. The initial rate of formation of a pink chromophore at 510 nm was measured by a built-in kinetic rate calculation function in the UV-Vis spectrometer. UV-Vis spectrometer was set on kinetic mode, 30 second run time with 5 second cycle time and zero-order reaction rate.

#### **Reagents to prepare 50 mL solution:**

1. 0.025 g of 4-aminoantipyrine (4-AAP)
2. 5 mL of 10X concentrated phenol solution (100 mM phenol in 0.5 M monobasic/dibasic sodium phosphate  $pH = 7.4$ )

- 100  $\mu\text{L}$  of freshly prepared 100 mM  $\text{H}_2\text{O}_2$
- The contents were made up to 47.5 mL with distilled water

#### Test procedure in 1 mL cuvette:

- Blank: The spectrometer was blanked with 950  $\mu\text{L}$  of freshly prepared assay reagent mixed with 50  $\mu\text{L}$  distilled water.
- Sample: 950  $\mu\text{L}$  reagent was mixed quickly with 50  $\mu\text{L}$  of diluted SBP solution, and the rate of color formation at 510 nm was monitored.

#### Data calculations:

$$\text{SBP activity in cuvette (U/mL)} = \frac{\text{initial rate} \left( \frac{\text{AU}}{\text{S}} \right) \times \left( \frac{60 \text{ S}}{1 \text{ Min}} \right) \times (\text{dilution in the cuvette})}{6 \text{ mM}^{-1} \times \text{cm}^{-1}} = \text{initial rate} \times 200$$

- Initial rate  $= \frac{\Delta A_{510}}{\Delta t} = \frac{\Delta A_{510}}{\text{S}}$
- $\Delta C = \frac{A}{\epsilon l}$ , where,  $\epsilon = 6.0 \text{ mM}^{-1} \text{cm}^{-1}$  and path length ( $l$ ) = 1.0 cm
- Reaction takes place in 1.0 mL cuvette so:  

$$\frac{\text{mM}}{\text{min}} \times 1.0 \text{ mL} = 1.0 \frac{\mu\text{mol}}{\text{min}} = 1.0 \text{ U}$$
- Activity of SBP sample = SBP activity in cuvette (U/mL) SBP  $\times$  dilution factor

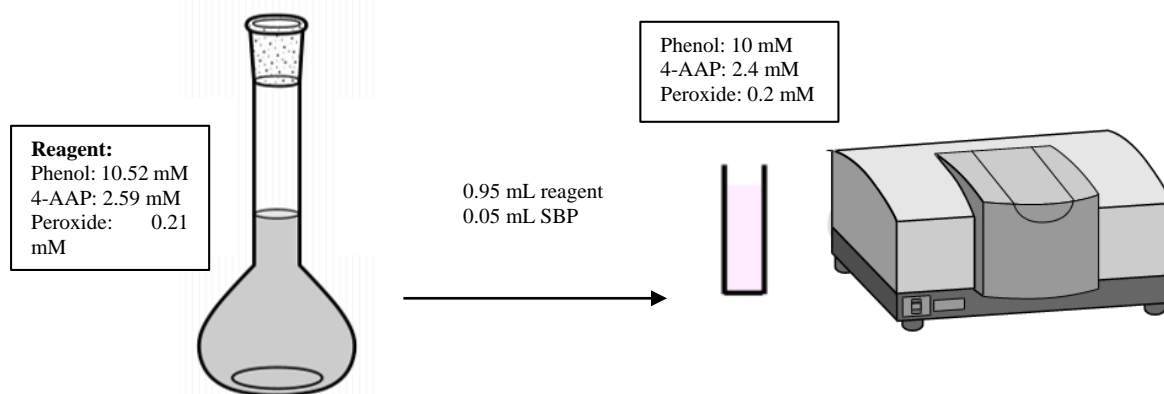


Figure B-1 SBP activity procedure

#### Appendix C. Residual SBP activity assay

To measure the remaining activity of SBP in the reaction mixture after the enzymatic treatment, residual SBP activity assay was used. The principles of residual SBP



activity are the same as regular SBP activity assay. However, for low SBP activity after reaction, concentrated reagent may be needed. For instance, to prepare 2 - fold more concentrated reagent, the same amount of 10 X phenol, 4-AAP and hydrogen peroxide mentioned in Appendix B are added and made up to 25 mL with distilled water. In order to keep the final concentration of each component in the cuvette constant, the ratio of reagent to enzyme was reformulated:

**For 2X concentrated reagent:**

0.5 mL of freshly prepared reagent is mixed with 0.5 mL SBP sample, so SPB activity in cuvette (U/mL) =

$$\frac{\text{initial rate} \left( \frac{\text{AU}}{\text{S}} \right) \times \left( \frac{60 \text{ S}}{1 \text{ Min}} \right) \times (\text{dilution in the cuvette})}{6 \text{ mM}^{-1} \times \text{cm}^{-1}} = \text{initial rate} \times 20$$

**For 4X concentrated reagent:**

0.25 mL of freshly prepared reagent is mixed with 0.75 mL SBP sample, so SPB activity in cuvette (U/mL) =

$$\frac{\text{initial rate} \left( \frac{\text{AU}}{\text{S}} \right) \times \left( \frac{60 \text{ S}}{1 \text{ Min}} \right) \times (\text{dilution in the cuvette})}{6 \text{ mM}^{-1} \times \text{cm}^{-1}} = \text{initial rate} \times 13.3$$

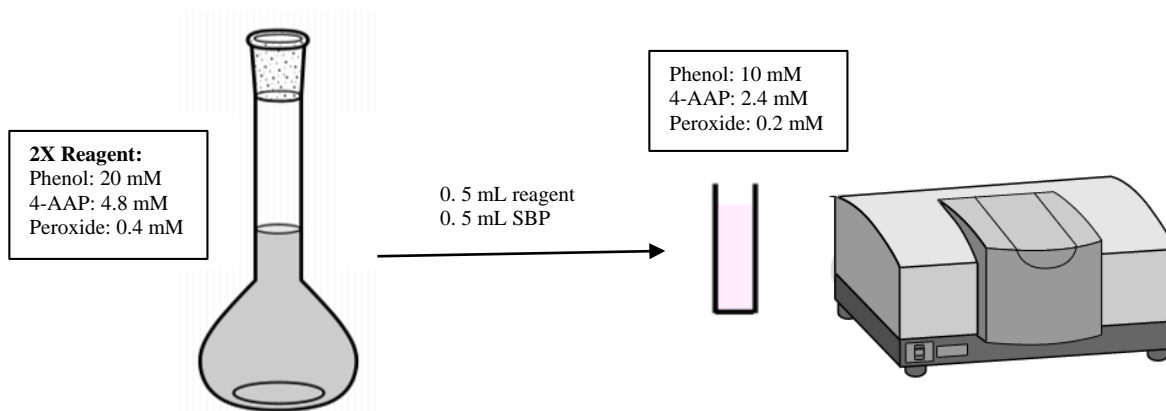


Figure C-1 SBP residual activity procedure for 2X concentrated reagent

**Appendix D. Residual hydrogen peroxide assay**

To determine the residual hydrogen peroxide after the enzymatic treatment, a colorimetric assay was conducted. A reagent consisting of phenol, 4-AAP and Novo ARP enzyme was added to the sample. Through the reaction of ARP with peroxide, phenolic radicals were formed, coupled with 4-AAP and produced a chromophore with  $\lambda_{\text{max}} = 510$  nm. The absorbance was checked with UV-Vis spectrophotometer after 18 minutes and concentration of residual hydrogen peroxide was measured using the predominated calibration curve.

If the enzymatic treatment of the substrate generated color in the mixture, color correction was needed for this colorimetric assay. The spectrophotometer was blanked with water by adding 200  $\mu\text{L}$  of water to 800  $\mu\text{L}$  of the filtered sample, mixed, and the absorbance was then measured at 510 nm. Later on, the measured absorbance was subtracted from the absorbance monitored in colorimetric assay and was plugged into the calibration curve to find the corresponding concentration of residual hydrogen peroxide.

**Reagents to prepare 20 mL solution:**

1. 10 mL of 10X concentrated phenol solution (100 mM phenol in 0.5 M monobasic/dibasic sodium phosphate pH = 7.4)
2. 0.051 grams of 4-aminoantipyrine (4-AAP)
3. 250  $\mu\text{L}$  of Novo ARP enzyme (concentrate)
4. The contents were made up to 20 mL with distilled water

**Test procedure:**

1. Blank: The spectrometer was blanked with 200  $\mu\text{L}$  of prepared reagent mixed with 800  $\mu\text{L}$  distilled water.
2. Sample: 800  $\mu\text{L}$  of filtered sample from the batch reactors was mixed with 200  $\mu\text{L}$  of prepared reagent and the absorbance was measured at 510 nm after 18 min color development period.
3. Calibration curve: various dilutions of hydrogen peroxide (0.1 to 1.0 mM) were made from 100 mM freshly prepared stock solution; 800  $\mu\text{L}$  of each diluted hydrogen peroxide sample was added to 200  $\mu\text{L}$  of above mentioned

reagent and the absorbance was monitored at 510 nm after 18 min. The calibration curve for hydrogen peroxide is shown in figure D-1 and all data points are the average of triplicate values.

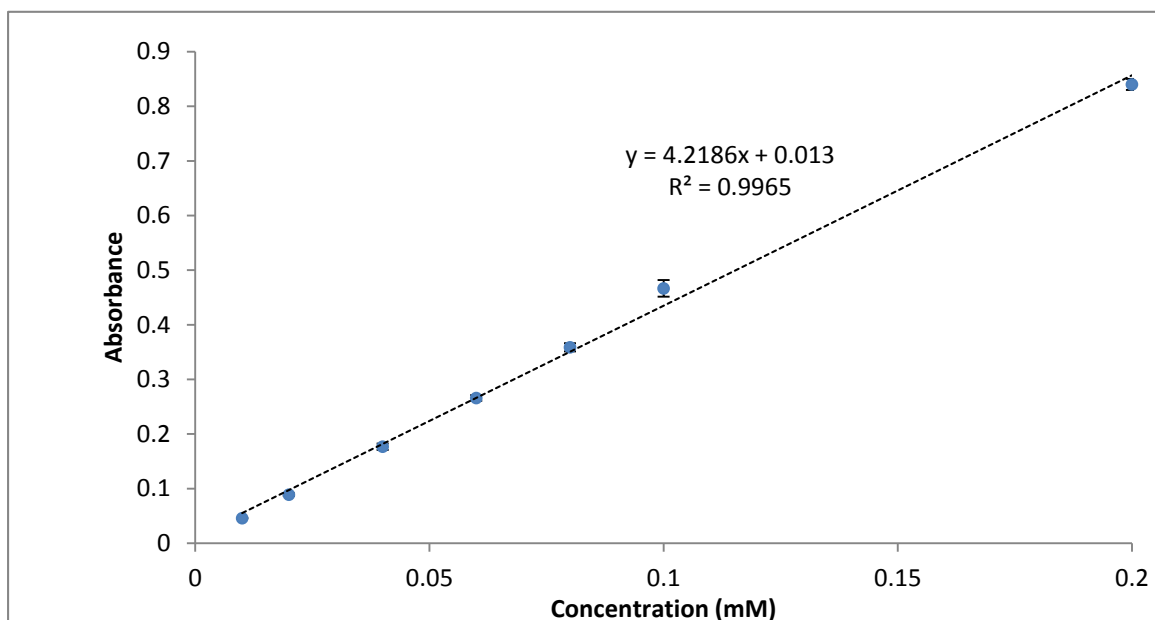


Figure D-1 Hydrogen peroxide calibration curve

#### ***Appendix E. HPLC Calibration curves***

The standard curves for the substrates were created using results from the HPLC analyses. For 3-HC, different concentrations of the substrate were made up in 40 mM buffer. The pH range was varied from 3.6 to 9.0 using acetic acid-sodium acetate buffer for pH range 3.6-5.6, phosphate buffer for pH range 6.0-8.0 and tris(hydroxymethyl)-aminomethane-HCl for pH range 8.0-9.2. Table 3-1 summarizes the HPLC conditions for 3-HC standard curves.

For 2-ABO, since it showed the same absorbance in water and various buffers (10 mM- pH from 4.0-8.0), only one calibration curve was created. The pH range finding using UV-Vis was performed previously (data not shown here). Table 3-2 summarizes the HPLC conditions for 2-ABO standard curves.

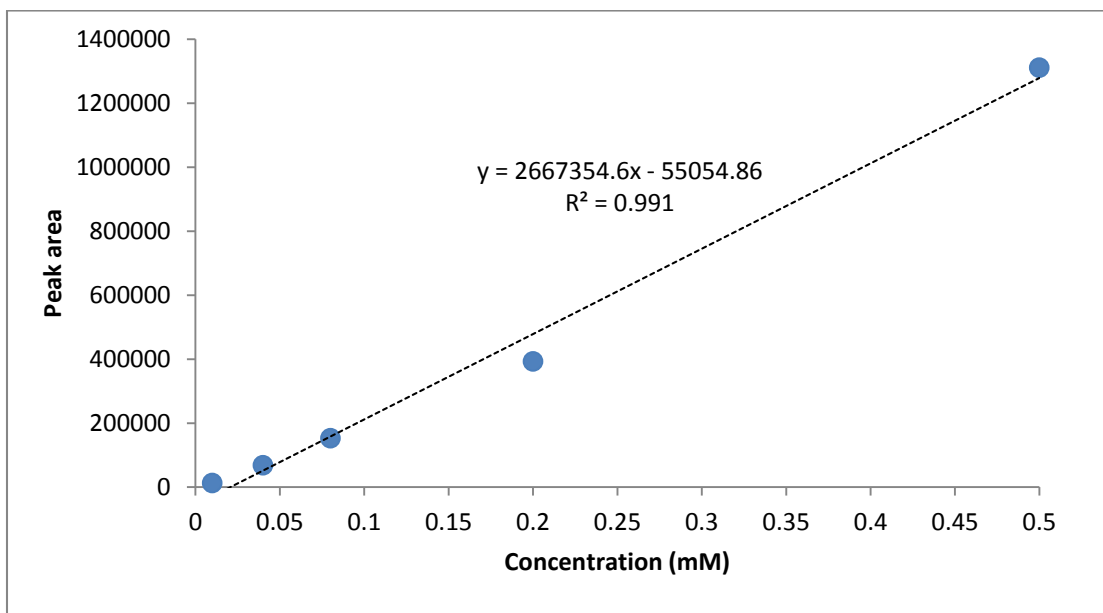


Figure E-1, 3-HC standard curve in pH 3.6 at 312 nm

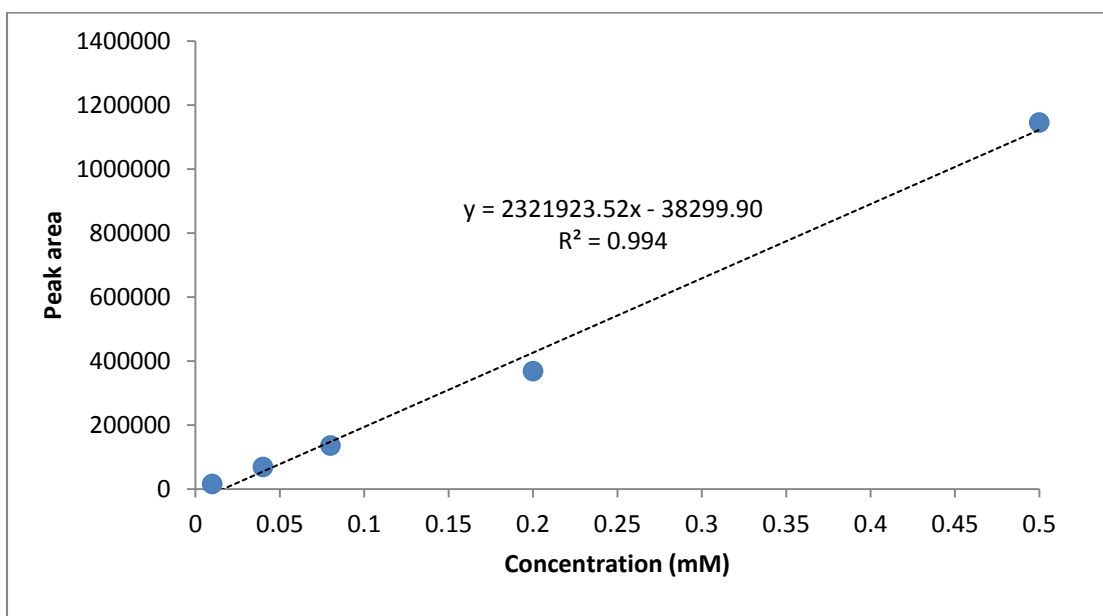


Figure E-2, 3-HC standard curve in pH 4.0 at 312 nm

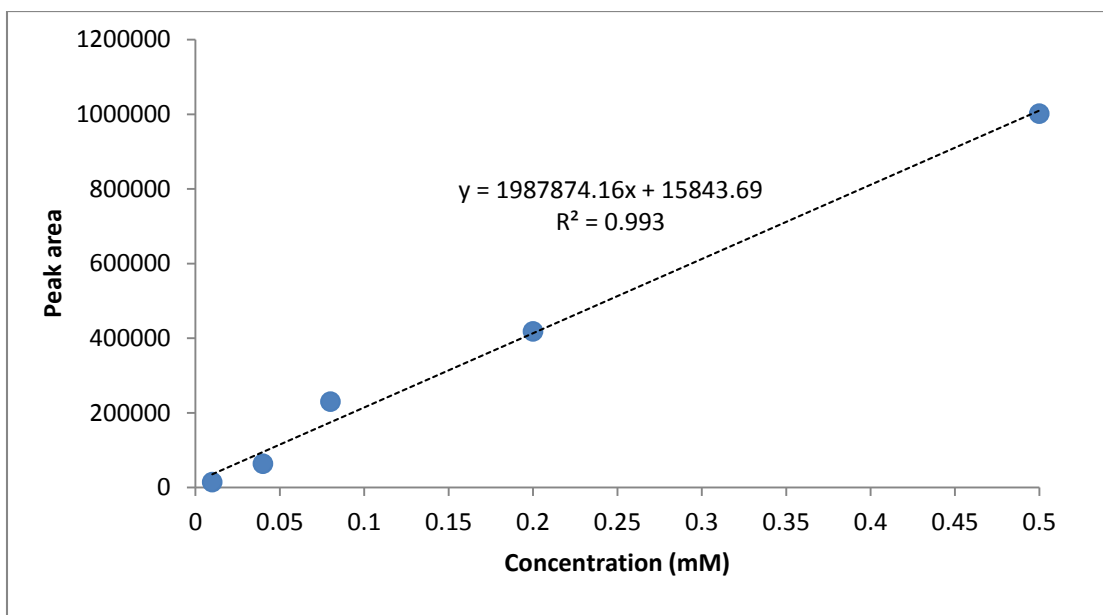


Figure E-3, 3-HC standard curve in pH 4.6 at 312 nm

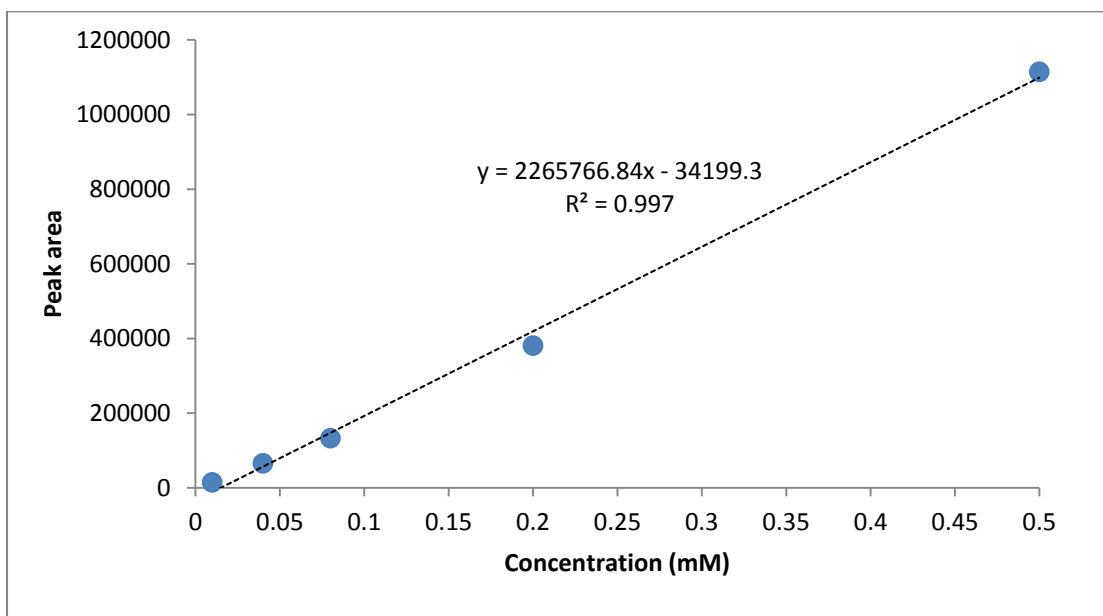


Figure E-4, 3-HC standard curve in pH 5.0 at 312 nm

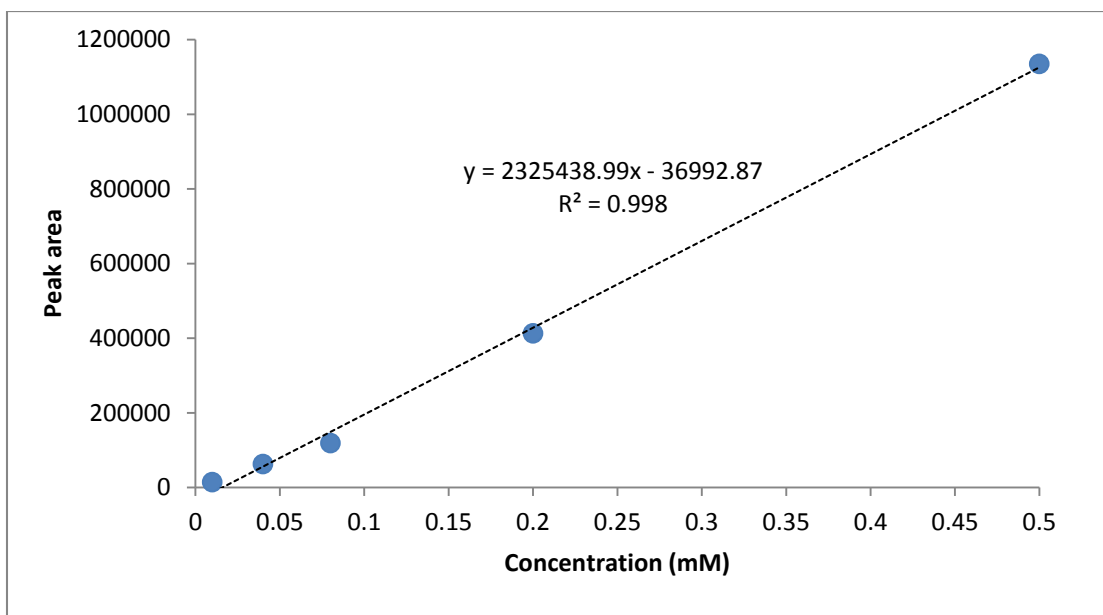


Figure E-5, 3-HC standard curve in pH 5.6 at 312 nm

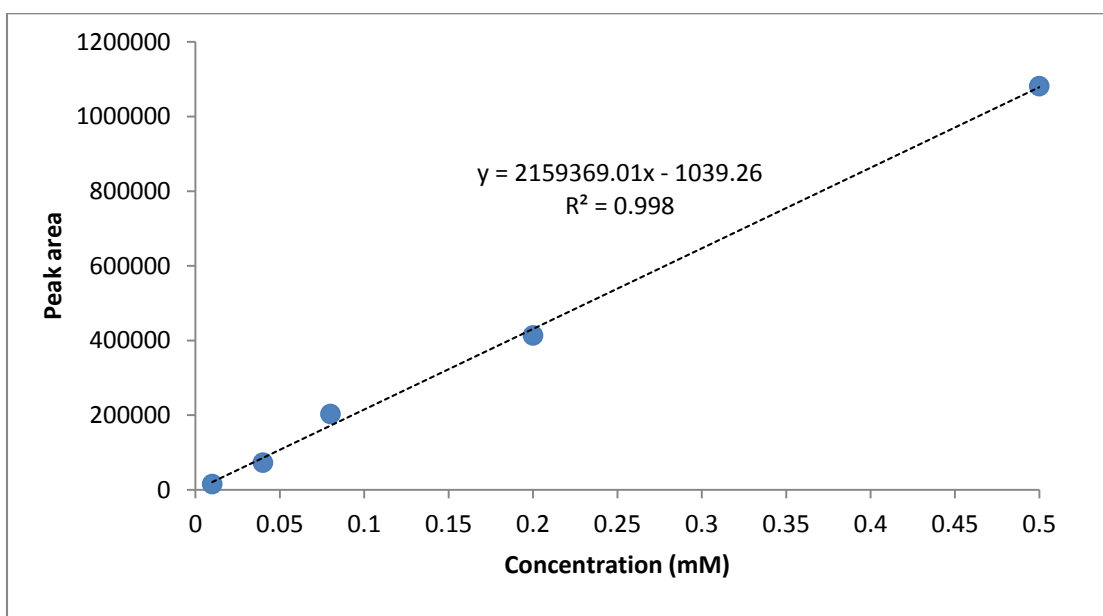


Figure E-6, 3-HC standard curve in pH 6.0 at 312 nm

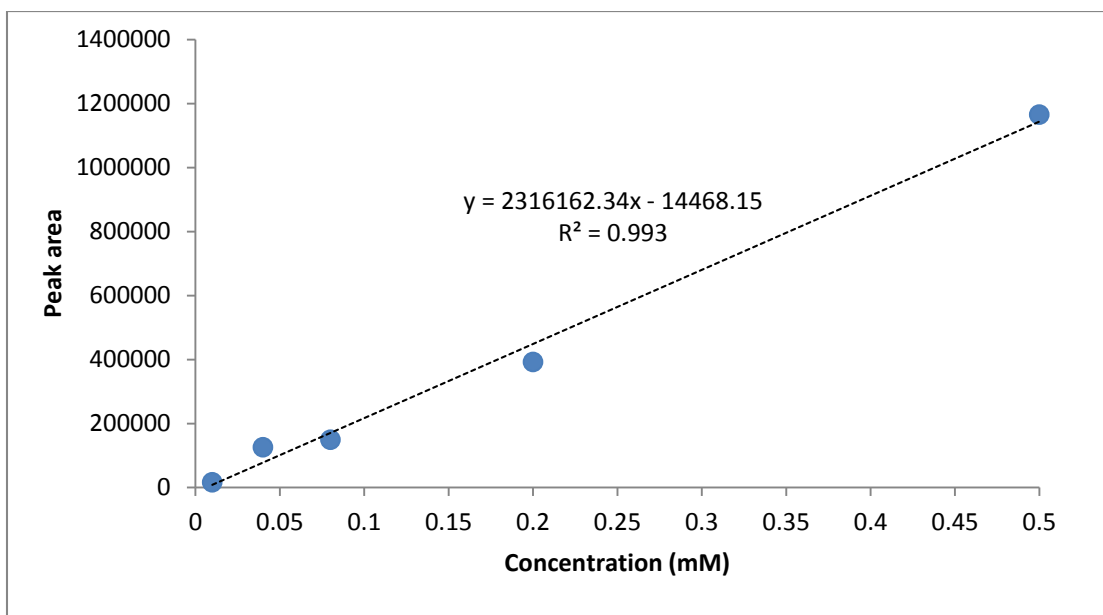


Figure E-7, 3-HC standard curve in pH 6.5 at 312 nm

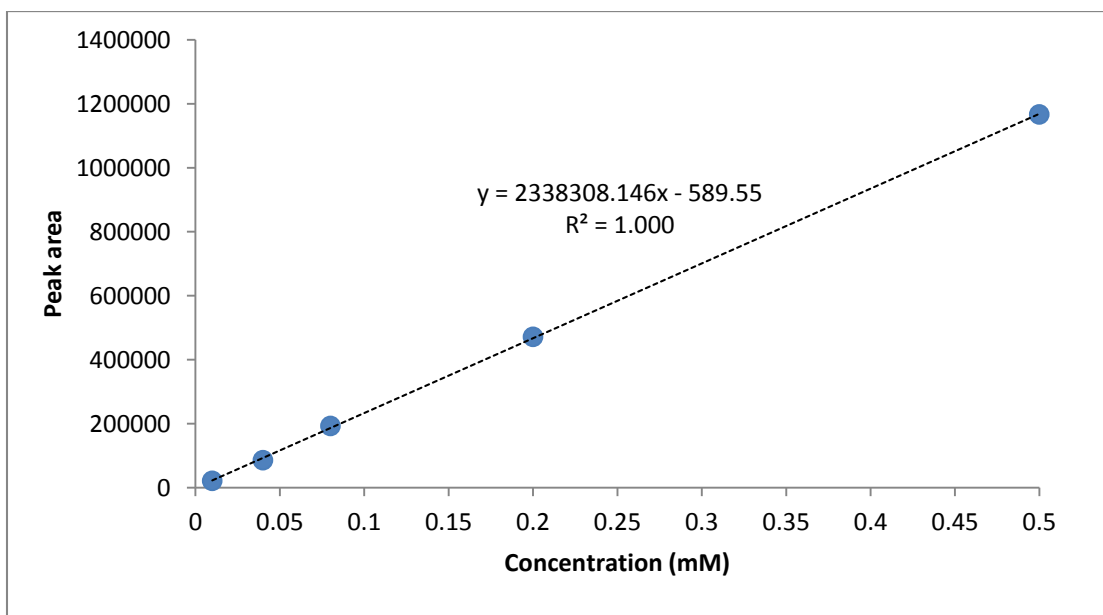


Figure E-8, 3-HC standard curve in pH 7.0 at 312 nm

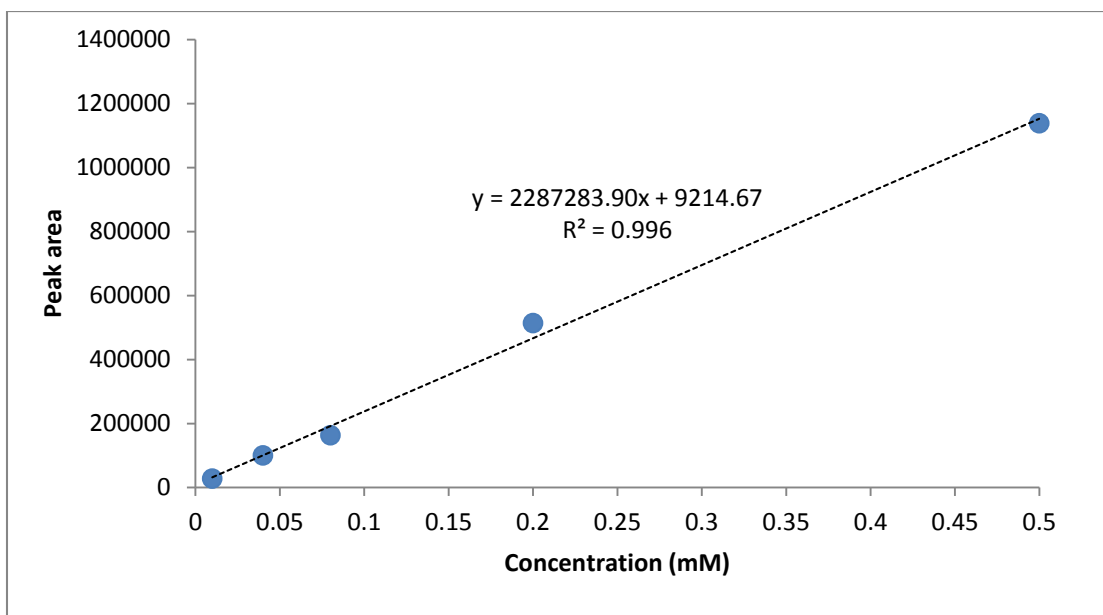


Figure E-9, 3-HC standard curve in pH 7.5 at 312 nm

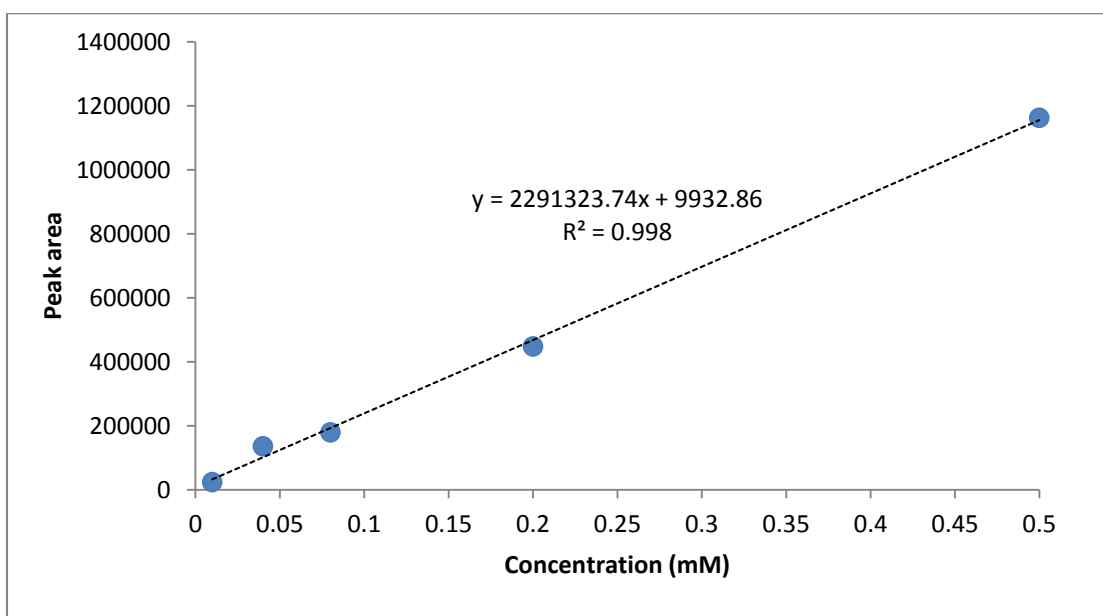


Figure E-10, 3-HC standard curve in pH 8.0 (phosphate buffer) at 312 nm



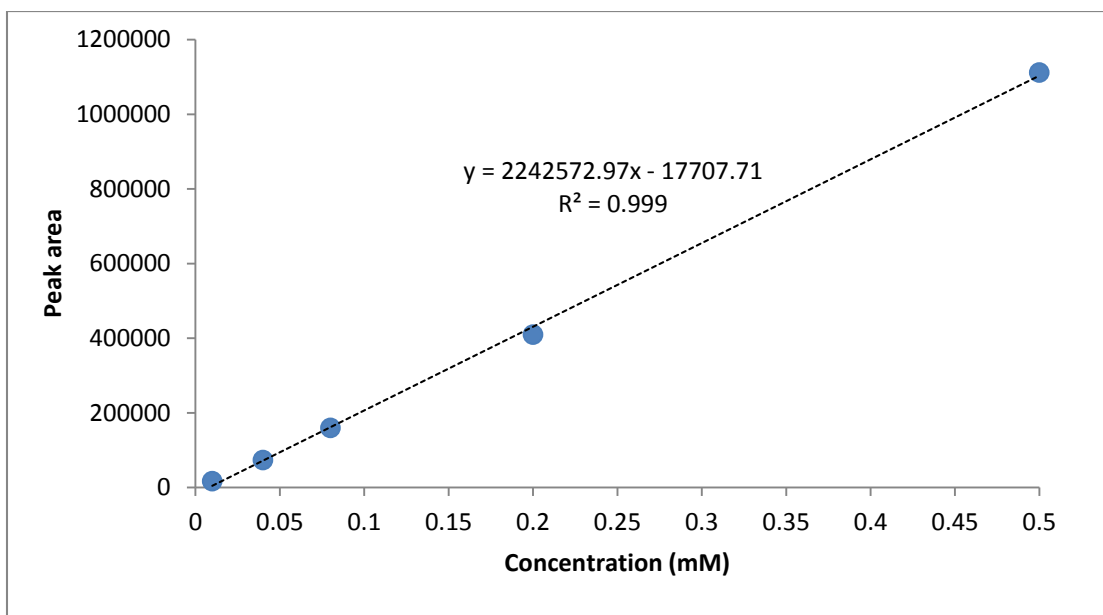


Figure E-11, 3-HC standard curve in pH 8.0 (tris-HCL buffer) at 312 nm

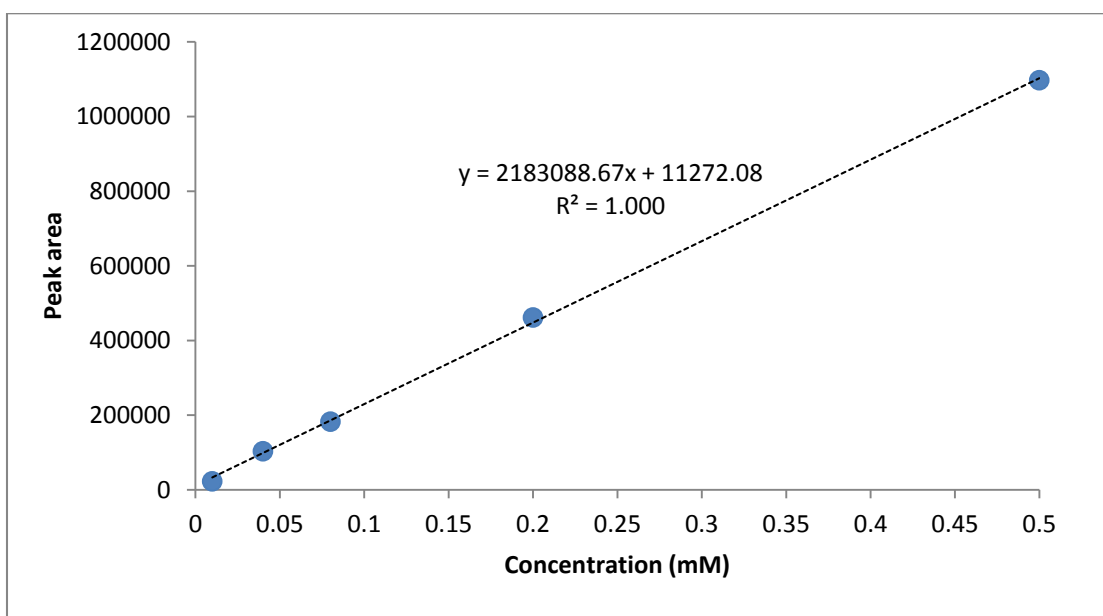


Figure E-12, 3-HC standard curve in pH 8.6 at 312 nm

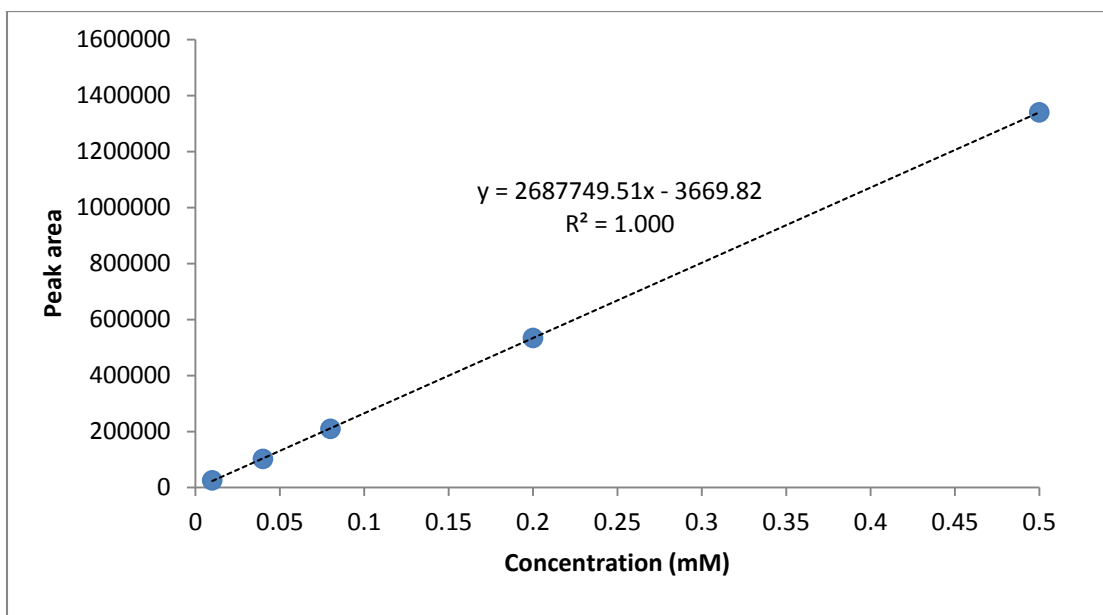


Figure E-13, 3-HC standard curve in pH 9.0 at 312 nm

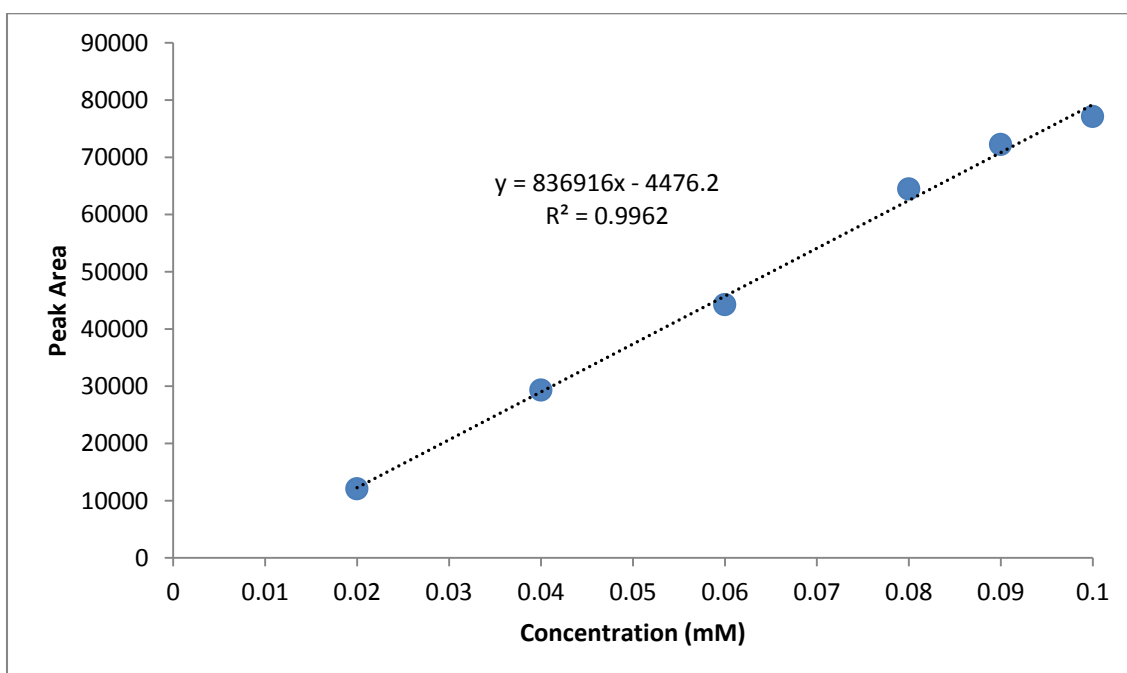
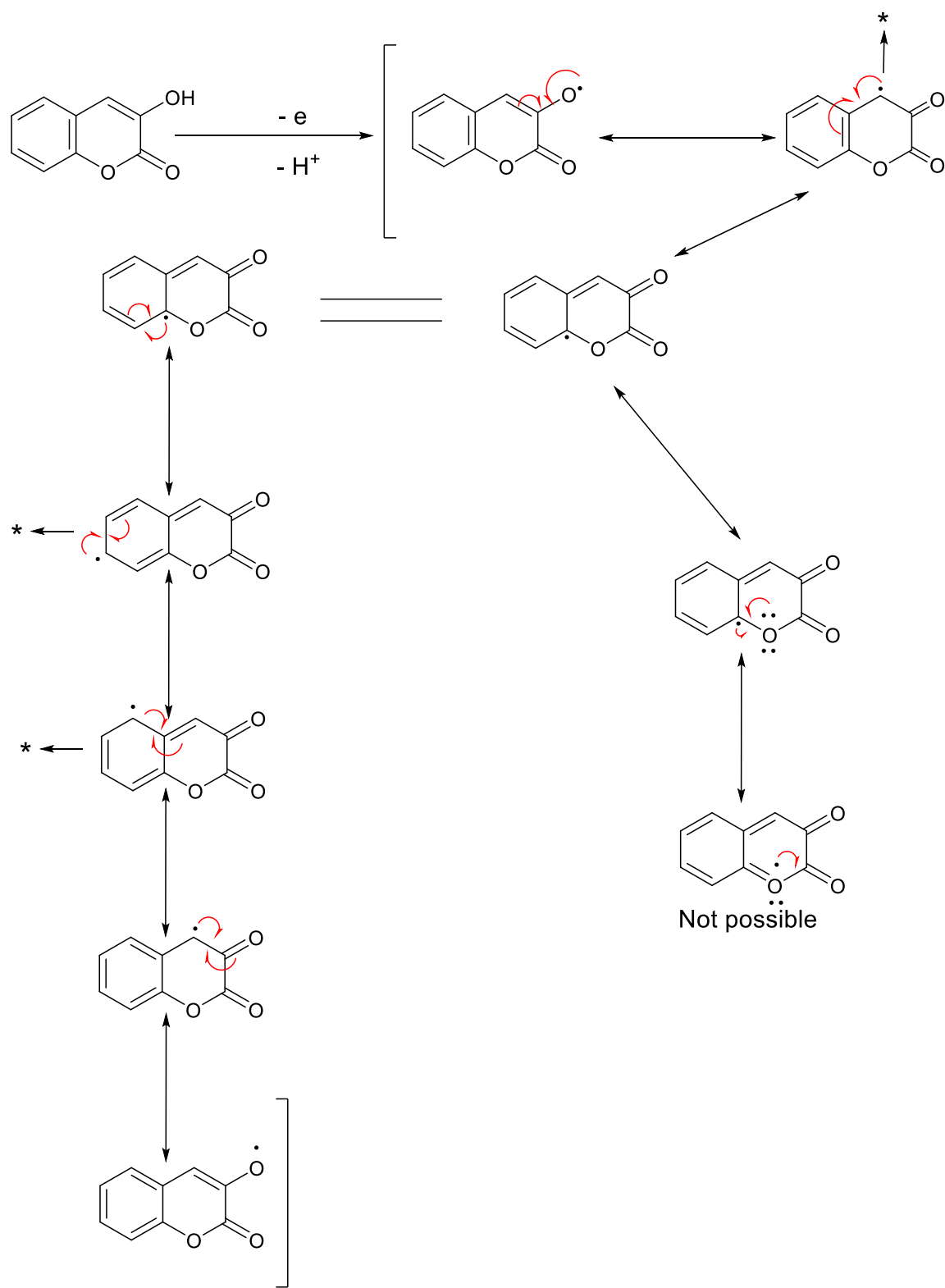


Figure E-14, 2-ABO standard curve in water at 237 nm

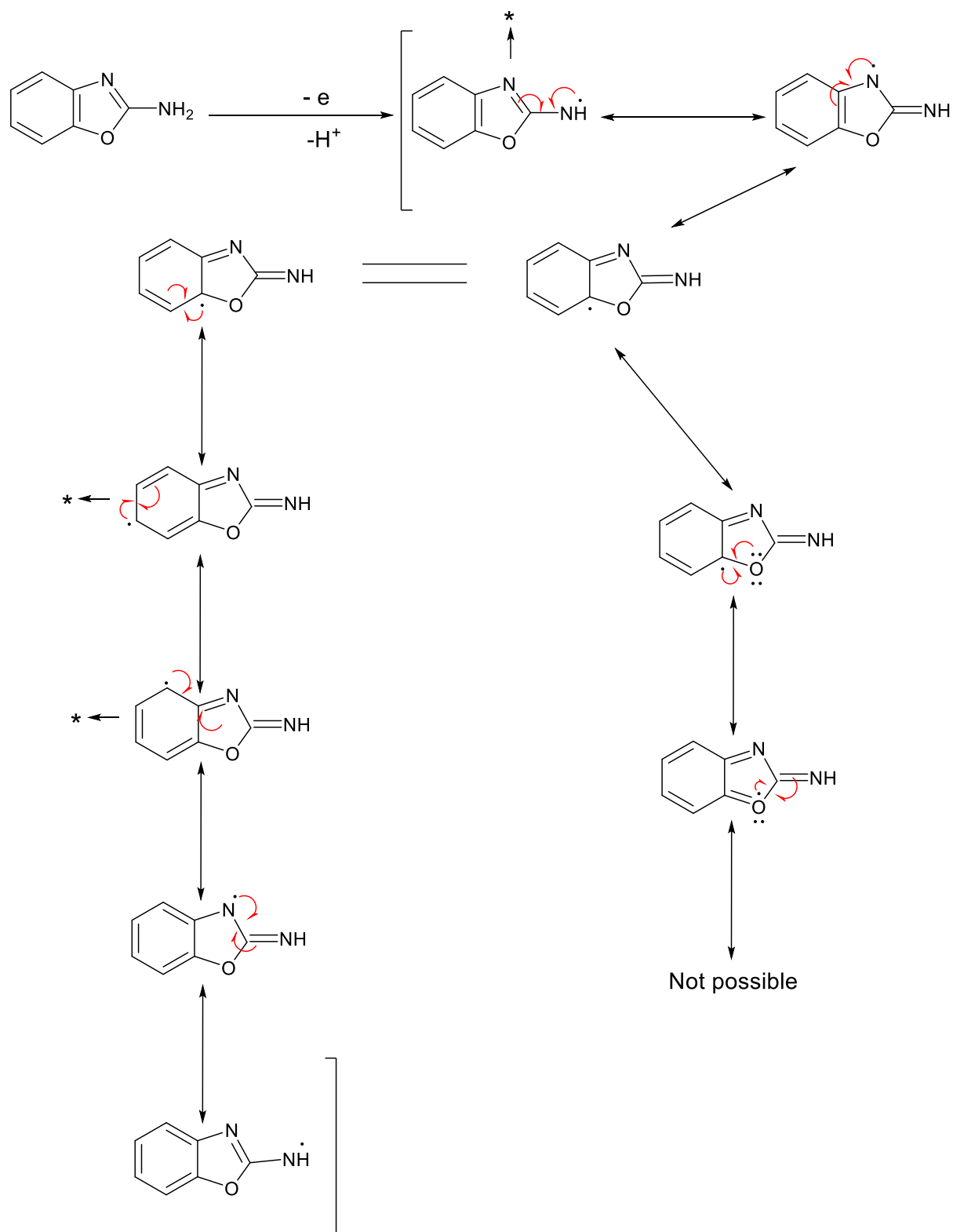
*Appendix F. Electron delocalization of 3-HC*



\* Possible coupling and re-aromatization



*Appendix G. Electron delocalization of 2-ABO*



\* Possible coupling and re-aromatization

## VITA AUCTORIS

NAME: Negin Ziaayee Bideh

PLACE OF BIRTH: Yazd, Iran

YEAR OF BIRTH: 1989

EDUCATION: Farzanegan High School, Yazd, Iran, 2007

University of Amirkabir, B.Sc., Tehran, Iran, 2012

University of Windsor, M.Sc., Windsor, ON, 2020